NASA CR-72774
MTI-70TR59

FLEXIBLE ROTOR BALANCING BY THE EXACT POINT-SPEED INFLUENCE COEFFICIENT METHOD

By

Juergen M. Tessarzik

MECHANICAL TECHNOLOGY INCORPORATED

Prepared for

NATIONAL AERONAUTICS AND SPACE ADMINISTRATION

NASA--Lewis Research Center

Contract NAS3-13473

W. J. Anderson – Chief, Bearings Branch

NASA CR-72774
MTI-70TR59

FINAL REPORT

Flexible Rotor Balancing by the Exact Point-Speed Influence Coefficient Method

By

Juergen M. Tessarzik

Prepared Under Contract NAS 3-13473

Mechanical Technology Incorporated
968 Albany-Shaker Road
Latham, New York 12110

Technical Management

William J. Anderson, Chief, Bearings Branch

Lewis Research Center

Cleveland, Ohio

NATIONAL AERONAUTICS AND SPACE ADMINISTRATION

FOREWORD

The investigation reported herein was performed by Mechanical Technology Incorporated in fulfillment of Contract NAS 3-13473 for the National Aeronautics and Space Administration, Lewis Research Center, Cleveland, Ohio. Mr. William J. Anderson was the NASA Project Manager.

The computer program used to calculate the correction weights for the Exact Point-Speed Influence Coefficient Balancing Method, and the analysis upon which the program is based, were written by Dr. Jorgen Lund, Consultant to MTI.

The experimental data reported herein was acquired with the assistance of Mr. Walter Spodnewski, Senior Technician. The computer calculations were conducted by Mrs. F. Gillham.

ABSTRACT

A test program was conducted to confirm experimentally the validity of the Exact Point-Speed Influence Coefficient Method for balancing rotating machinery, and to assess the practical aspects of applying the method to flexible rotors.

Testing was performed with a machine having a 41-inch (104 cm) long, 126-pound (57 kg) rotor. The rotor was operated over a speed range encompassing three rotor-bearing system critical speeds: two "rigid body" criticals and one flexural critical. Rotor damping at the flexural critical was very low due to the journal bearings being located at the nodal points of the shaft.

The balancing method was evaluated for three different conditions of initial rotor unbalance. The method was found to be effective and practical. Safe (and slow) passage through all the critical speeds was obtained after a reasonable number of balancing runs. Success of the balancing method was, in large part, due to the accuracy of the instrumentation system used to obtain phase angle measurements during the balancing procedure.

TABLE OF CONTENTS

TABLE OF CONTENTS (Cont.)

LIST OF FIGURES

LIST OF FIGURES (continued)

LIST OF TABLES

SUMMARY

A test program has been conducted to obtain an initial assessment of the "realworld" effectiveness of the Exact Point-Speed Influence Coefficient Balancing Method for balancing flexible rotors. This balancing method, including a digital computer program for calculating balance correction weights, was analytically verified during a previous NASA contract effort. The objectives of the herein reported test program were to experimentally confirm the validity of the balancing method, and to assess the practical aspects of applying the method to actual flexible-rotor machines.

The test program was performed with a machine having a 41-inch (104 cm) long, 126-pound (57 kg) rotor, which was supported by two self-acting fluid-film pivoted pad journal bearings. The rotor had a three-mass configuration: one mass being centrally located between bearings; the remaining two masses being overhung at each end of the rotor.

The rotor was operated at speeds up to 16 500 rpm. Three rotor-bearing system critical speeds were encountered within this speed range. The first two critical speeds were essentially "rigid body" criticals; the third critical, which occurred at about 11,000 rpm, was the first flexurel critical of the rotor. Rotor damping at the flexural critical was very low due to the journal bearings being located at the nodal points of the rotor. The test machine thus provided an excellent (severe) challenge for evaluation of the balancing method.

Three conditions of initial rotor unbalance were investigated:

I. Rotor with residual unbalance (unbalance remaining after low-speed, rigid-body balancing on a commercial balancing machine);

II. Rotor with substantial unbalance added along the rotor in an in-line out-of-phase configuration (single axial plane, weights all on same side of shaft centerline); See Figure 34.

III. Rotor with substantial unbalance added along the rotor in an in-line out-of-phase configuration (single axial plane, weights on overhung masses on same side of shaft centerline but opposite from weights on central mass); See Figure 39.

For the second and third initial unbalance conditions, satisfactory rotor balance was obtained for operation up to 80 percent of the third critical speed after the first balancing run. (For the residual unbalance condition, operation up to 80 percent of the third critical was possible prior to the first balancing run). Rotor operation through the third critical speed was achieved with a total of two balancing runs for Unbalance Condition I, while a total of three balancing runs were required for Unbalance Condition III. Although operation through the third critical was not demonstrated for Unbalance Condition II, the test data indicated that such operation would hav been achieved after six, or possibly seven, balancing runs.

The results of this investigation definitely confirm the validity of the Exact Point-Speed Influence Coefficient Balancing Method. It also appears that the method is reasonably effective from a practical standpoint.* The condition of strong in-line, in-phase unbalance (Unbalance Condition II) was the most difficult condition with respect to achieving rotor operation through the flexural critical.

The success of this balancing method is strongly dependent upon the accuracy of the phase angle measurements taken during the balancing procedure. An instrumentation set-up for obtaining satisfactory phase angle measurements was demonstrated.

It is also apparent that expeditious use of the balancing method, with respect to selection of balancing planes and speeds, is greatly enhanced by having some a priori knowledge of the critical speed response characteristics of the rotor being balanced.

Further evaluation of the effectiveness of the Exact Point-Speed Influence Coefficient Balancing Method appears warranted, particularly with respect to rotors which must operate through several flexural critical speeds.

*To some extent, a conclusion about the effectiveness of the balancing method must be a relative assessment. In this regard, a final assessment of effectiveness must await the availability of "effectiveness data" relative to other flexible rotor balancing methods.

INTRODUCTION

One of the axioms of machinery design is achievement of high operational performance. "Higher performance" is usually characterized by one or more of the following goals:

1. Higher power (transmitted or generated)
2. Reduced size and weight
3. Increased power (transmitted or generated) per pound of machinery weight (hp/lb)
4. Reduced specific fuel consumption (lb/hp-hr)
5. Higher efficiency
6. Higher reliability.

An important class of machinery to which these goals are applied, and to which the herein reported investigation was specifically directed, is that in which the principal kinematic motion is simple rotation of a shaft, or a system of shafts. For this class of machinery, shaft speed and shaft size are almost always intimately associated with achievement of the "higher performance" goals.

With increasing frequency, design engineers are finding that the interactions between higher performance goals and shaft speed and size are resulting in machinery designs that require the rotating shaft assembly to operate in its flexural (bending) regime. That is, shaft speeds and size are such that the flexibility of the rotating assembly may significantly influence the dynamic behavior of the assembly over some, or most, of the required operating speed range. In other words, the shaft assembly cannot be presumed to behave as a rigid body throughout the required speed range.

One of the major problems that has retarded development of "flexible rotor" machinery is the problem of balancing the shaft assembly for acceptable mechanical operation throughout the required operating speed range.* Whereas commercial

*The word "balancing", as used in this report, means reducing the distributed mass eccentricity along the length of a shaft to the point where the synchronous whirl orbits of the shaft, resulting from the mass eccentricity, are reduced to acceptable values throughout the operating speed range.

balancing equipment is readily available to perform "rigid rotor" balancing for either production-line or for one-of-a-kind requirements, such equipment does not exist for "flexible rotor" balancing. This, in large part, is due to the fact that the basic technology of "flexible rotor" balancing is still in the early stages of formulation and evaluation. "Rigid rotor" balancing technology, on the other hand, is well established [1, 2, 3].*

The fact that the technology for "flexible rotor" balancing is not well established does not mean that "flexible rotor" machinery is not being built. There are, today, large steam turbines in central power plants which run (at constant speed) between their second and third flexural critical speeds. However, attainment and maintenance of satisfactory rotor balance is a critical problem. Balancing of these rotors is usually accomplished by first performing "rigid rotor" (low speed) balancing, followed by "flexible rotor" (design speed) balancing based on empirical techniques which have evolved from years of prior experience with this type of machinery [4].

There are other types of machinery which could definitely achieve higher performance goals if the shafts could be reliably and economically balanced for operation in the "flexible" regime. For example, it has been shown that significant weight, cost and maintenance savings can be achieved in helicopter power transmission systems if the main rotor drive shafts could be supported by only two bearings [5]. However, this would require that the shafts be capable of operating smoothly through six to eight flexural critical speeds, a capability which has not yet been satisfactorily achieved, due, primarily, to the balancing problem. The field of advanced aircraft gas turbines is rapidly moving into the "flexible rotor" regime, and encountering significant problems in the process [5,7]. Likewise, turbopumps, superchargers, and large industrial compressors are entering the "flexible rotor" regime as a result of the constant quest for higher performance [8].

In recognition of the increasing need for rotating machinery which can operate satisfactorily in the "flexible rotor" regime, the National Aeronautics and Space Administration (NASA) has embarked upon a program to develop and evaluate the

* Numbers in brackets designate similarly numbered references listed on page 41 .

technology of "flexible rotor" balancing.* This report describes the results of the second investigation performed within the program area. In the first investigation, a relatively simple "flexible rotor" balancing method was analytically evaluated [10]. The method is based upon linear influence-coefficient deflection theory, and has been named the "Exact Point-Speed Influence Coefficient Balancing Method". The results of the initial analytical evaluation of this method were sufficiently promising to warrant an experimental evaluation of the method. This report describes the results of the first experimental evaluation.

The Exact Point-Speed Influence Coefficient Balancing Method places very few restrictions upon the kinds of rotor-bearing systems to which it is applicable. The rotor may be rigid or flexible, the bearings damped or undamped. The test machine used for the herein described investigation contained a "three-mass" rotor supported by self-acting tilting-pad journal bearings. The bearings were lubricated by a low-viscosity fluid to purposely minimize shaft damping (Dow Corning 200 Fluid; 0.65 centistokes at $77^{\circ}F$ ($25^{\circ}C$)). The rotor was operated through its first three rotor-bearing system critical speeds. The first two criticals were essentially "rigid body" criticals. The third critical speed (the first "flexural" critical) was particularly sensitive to shaft unbalance since the journal bearings were located essentially at the nodes of the response mode. Consequently, the bearings did not contribute any effective damping at the third critical speed. For all practical purposes, the third critical of the test rotor was undamped, and hence presented an excellent (severe) initial test of the Exact Point-Speed Influence Coefficient Balancing Method.

*The "flexible rotor regime" is usually considered to be the range of shaft speeds above 70 percent of the first "flexural" critical speed of the shaft. However, it should be recognized that the first "flexural" critical speed is not necessarily the first critical speed of the shaft system. Shaft critical speeds should always be computed taking into account the stiffness characteristics of the bearing system. It frequently happens that the first two rotor-bearing system critical speeds are "rigid body" criticals. In this case, the third rotor-bearing system critical speed becomes the "first" flexural critical. (A discussion of rotor-bearing system critical speeds is given in [9].)

THEORY OF EXACT POINT-SPEED INFLUENCE COEFFICIENT BALANCING METHOD

The general rotor shown in Figure 1 may be considered, for purposes of discussion, as a number of discrete masses, each dz in thickness. Each incremental mass is located at eccentricity $\bar{w}$ from the rotor elastic axis, where $\bar{w}$ is a vector function of distance along the rotor, and may thus be written $\bar{w}(z)$. The rotor residual unbalance distribution is shown in Figure 1 in the plane of the paper, but it should be remembered thoughout this discussion that the distribution is, in general, three-dimensional. The net unbalance for each axial element of the rotor may, if desired, be resolved into a single resultant unbalance moment vector $\bar{U}_p$. This quantity may be expressed in the form

$$\bar{U}_p = \rho_p A_p \int_0^{\ell_p} \bar{w}_p(z)\, dz, \qquad (1)$$

where $\bar{U}_p$ has units of mass x length, and is referred to as the unbalance moment of the shaft element. Here, ρ_p is the weight density of the rotor material in the "p^{th}" element, of which there are n such elements. A_p is the cross-sectional area, and $\bar{w}_p(z)$ is the (three-dimensional) mass eccentricity vector function. In Figure 1, the indicated integration is performed from the left side of the element ($z = 0$) to the right side ($z = \ell_p$).

The actual distribution of residual unbalance in a rotor is initially unknown, but it may be determined by examination of rotor vibration amplitudes and/or dynamic forces which are transmitted to the bearing supports and thence to the ground. A method for determining this unbalance distribution is discussed in this portion of the report. This information serves as the basic input to the balancing computer program. Knowledge of the effective residual unbalance moments $\bar{U}_p$ at specified locations allows the addition of correction weights to nullify the residuals at critical points along the rotor.

Information on the dynamic properties and behavior of a rotor in its bearings is of great importance in selecting both the number and the most effective

locations of balancing planes. For instance, a rotor known to be operating in its rigid-body regime requires, in general, only two balancing planes. A flexible rotor, on the other hand, requires three or more balancing planes. The exact number of planes depends upon the unbalance-excited mode shapes assumed by the rotor. The mode shapes in turn are influenced by the critical speeds which lie within or close to the operating speed range of the rotor. A general rule is not yet available for determining the minimum number of planes necessary for balancing a flexible rotor. Consequently, some a priori knowledge of the unbalance response characteristics of a rotor is of great assistance in selecting the number and location of balancing planes. Final selection of the balancing planes is usually a compromise based upon practical factors, such as accessibility, associated with the rotor design.

Consider the rotor shown in Figure 1 to be mounted in flexible supports. Any number of supports may be specified,* and these supports may contain any combination of mass, flexibility, and damping. It is required that rotor amplitudes and phase angles be measured at each axial location, and at each rotor speed, where low (theoretically zero) amplitude is ultimately desired as a result of the balancing process.

Consider next a coordinate system ξ,η which is fastened to and rotates with the rotor at speed ω. The rotating unbalance moments, U_p, fixed in the ξ,η coordinate system, cause rotor displacements which rotate with respect to the fixed x, y coordinate system as shown in Figure 2. In this figure, the quantities w_c and w_s are the ξ and η components respectively, of rotor amplitude, measured in the rotating coordinate system. At any point "j" along the rotor axis, rotating displacements w_c and w_s may be converted to the stationary coordinates by the relationship:

$$x_j = w_{c_j} \cos \omega t - w_{s_j} \sin \omega t \qquad (2)$$

$$y_j = w_{c_j} \sin \omega t + w_{s_j} \cos \omega t.$$

* The present computer program is limited to 24 supports by the dimension statements.

The rotor amplitude in the rotating coordinate system may be expressed in complex notation as follows:

$$\overline{w}_{R_j} = w_{c_j} + iw_{s_j} = w_{R_j} e^{i\phi_j}. \tag{3}$$

Also,

$$\overline{w}_{F_j} = x_j + i\, y_j = w_{F_j} e^{i(\omega t + \phi_j)} \tag{4}$$

where $i = \sqrt{-1}$, and where w_{F_j} is the rotor amplitude expressed in the fixed coordinate system. The quantities w_{R_j} and w_{F_j} are of course equal.

Figure 3 shows the rotor in the rotating ξ, η coordinate system. The actual distributed unbalance is approximated by n discrete unbalance moments distributed along the shaft.

Vibration amplitudes and unbalance moments may be related by means of influence coefficients "α" in the following matrix equation:

$$\{w_R\} = [\alpha] \cdot \{U_p\} \tag{5}$$

The α_{jp} are the linear coefficients which relate deflection at location j due to unbalance moment at location p. It will now be assumed the number of balancing planes, into which both trial weights and final correction weights will be placed, is equal to the number of unbalance moments, "n".

As shown by Equation 3, the displacement quantities w_R are complex, and for any plane p:

$$\alpha_{jp} = \alpha_{c,jp} + i\, \alpha_{s,jp}. \tag{6}$$

The unbalance moments U_p may also be resolved into their components:

$$U_p = U_{c,p} + i\, U_{s,p} \tag{7}$$

where subscripts "c" and "s" denote the real and imaginary components, respectively.

The order of $[\alpha]$ will be v by n, where v is the total number of displacement elements in the w_R column matrix and n, as previously defined, is the number of balancing planes. The number of displacement elements in turn is given by

$$v = mN \tag{8}$$

where

m = number of stations along the rotor at which displacements are measured, and

N = number of balancing speeds at which m measurements are taken.

There are thus $v = mN$ rows and n columns in the general $[\alpha]$ matrix. As will be discussed later, this matrix must be inverted for solution of Equation 5. The $[\alpha]$ matrix must therefore be a square matrix. That is, v must equal n. Cases where this may not be the case are briefly discussed below.

The foregoing matrix equation may be written in long form as follows, where the number of the balancing speed is indicated by a superscript.

$$
\begin{Bmatrix} w_1^{(1)} \\ w_2^{(1)} \\ \cdot \\ w_m^{(1)} \\ \cdot \\ \cdot \\ \cdot \\ w_1^{(2)} \\ w_2^{(2)} \\ \cdot \\ w_m^{(2)} \\ \cdot \\ \cdot \\ \cdot \\ w_1^{(N)} \\ w_2^{(N)} \\ \cdot \\ w_m^{(N)} \end{Bmatrix} = \begin{bmatrix} \alpha_{11}^{(1)} & \alpha_{12}^{(1)} & \cdots & \alpha_{1n}^{(1)} \\ \alpha_{21}^{(1)} & \alpha_{22}^{(1)} & \cdots & \alpha_{2n}^{(1)} \\ \cdot & \cdot & \cdots & \cdot \\ \alpha_{m1}^{(1)} & \alpha_{m2}^{(1)} & \cdots & \alpha_{mn}^{(1)} \\ \cdot & \cdot & \cdots & \cdot \\ \cdot & \cdot & \cdots & \cdot \\ \cdot & \cdot & \cdots & \cdot \\ \alpha_{11}^{(2)} & \alpha_{12}^{(2)} & \cdots & \alpha_{1n}^{(2)} \\ \alpha_{21}^{(2)} & \alpha_{22}^{(2)} & \cdots & \alpha_{2n}^{(2)} \\ \cdot & \cdot & \cdots & \cdot \\ \alpha_{m1}^{(2)} & \alpha_{m2}^{(2)} & \cdots & \alpha_{mn}^{(2)} \\ \cdot & \cdot & \cdots & \cdot \\ \cdot & \cdot & \cdots & \cdot \\ \cdot & \cdot & \cdots & \cdot \\ \alpha_{11}^{(N)} & \alpha_{12}^{(N)} & \cdots & \alpha_{1n}^{(N)} \\ \alpha_{21}^{(N)} & \alpha_{22}^{(N)} & \cdots & \alpha_{2n}^{(N)} \\ \cdot & \cdot & \cdots & \cdot \\ \alpha_{m1}^{(N)} & \alpha_{m2} & \cdots & \alpha_{mn}^{(N)} \end{bmatrix} \cdot \begin{Bmatrix} U_1 \\ U_2 \\ \\ U_3 \\ \cdot \\ \cdot \\ \cdot \\ \cdot \\ \cdot \\ \cdot \\ \cdot \\ \cdot \\ U_{n-1} \\ \\ U_n \end{Bmatrix} \qquad (9)
$$

In Equation (9), the subscripts on the elements of the displacement vector {w} denote measurement locations along the rotor, these being the locations at which low vibration amplitudes are desired. It should be recalled that the capability of obtaining low vibration amplitudes at certain specified points on the rotor for selected speeds is the source of the name of the "Exact Point-Speed Flexible Rotor Balancing Method." The subscripts on the U vector indicate balancing planes in which trial weights are to be located during the balancing process and in which final correction weights will be placed.

The balancing procedure involves solution of the foregoing equation for U_1, U_2, ..., U_n, which are the components of residual unbalance in the "n" balancing planes. The process involves measurement of amplitudes and phase angles, calculation of the influence coefficients "α", and finally inversion of the α matrix for solution of the U quantities.

In order to illustrate the foregoing mathematical technique, two measurement locations A and B will be selected. As the first step in determining the α-matrix, the rotor is run in the as-received condition (residual unbalance) at speed ω_1. At locations A and B, the (complex) rotor vibration amplitudes w_{AO} and w_{BO} and corresponding phase angles are recorded. These amplitudes are related to residual unbalance by the equation,

$$\begin{Bmatrix} w_{Ao}^{(1)} \\ w_{Bo}^{(1)} \end{Bmatrix} = \begin{bmatrix} \alpha_{A1}^{(1)} & \alpha_{A2}^{(1)} & \cdots & \alpha_{An}^{(1)} \\ \alpha_{B1}^{(1)} & \alpha_{B2}^{(1)} & \cdots & \alpha_{Bn}^{(1)} \end{bmatrix} \begin{Bmatrix} U_1 \\ U_2 \\ \cdot \\ \cdot \\ \cdot \\ U_n \end{Bmatrix} \qquad (10)$$

Next, a trial unbalance moment, T, is inserted in balance plane 1, at angle $\emptyset$, measured from an axial reference plane. The angle $\emptyset$ is usually made equal to zero for convenience. Again the rotor is run at speed ω_1 and amplitudes $w_{A1}^{(1)}$ and $w_{B1}^{(1)}$ and corresponding phase angles are recorded, thereby defining,

$$\begin{Bmatrix} w_{A1}^{(1)} \\ w_{B1}^{(1)} \end{Bmatrix}_{\omega_1} = \begin{bmatrix} \alpha_{A1}^{(1)} & \alpha_{A2}^{(1)} \cdots & \alpha_{An}^{(1)} \\ \alpha_{B1}^{(1)} & \alpha_{B2}^{(1)} \cdots & \alpha_{Bn}^{(1)} \end{bmatrix} \begin{Bmatrix} U_1 + T \\ U_2 \\ \vdots \\ U_n \end{Bmatrix} \qquad (11)$$

Subtracting Equation (10) from Equation (11) gives,

$$\alpha_{A1}^{(1)} = \frac{w_{A1}^{(1)} - w_{Ao}^{(1)}}{T}$$

$$\alpha_{B1}^{(1)} = \frac{w_{B1}^{(1)} - w_{Bo}^{(1)}}{T} \qquad (12)$$

Thus, two of the influence coefficients in Equation (9) have been obtained. Next, the trial unbalance moment is inserted in balancing plane 2 ($U_2 + T$), and the above procedure is repeated, yielding,

$$\alpha_{A2}^{(1)} = \frac{w_{A2}^{(1)} - w_{Ao}^{(1)}}{T}$$

$$\alpha_{B2}^{(1)} = \frac{w_{B2}^{(1)} - w_{Bo}^{(1)}}{T} \qquad (13)$$

All of the coefficients may be similarly determined. In general, for balancing plane "p",

$$\alpha_{Ap}^{(1)} = \frac{w_{Ap}^{(1)} - w_{Ao}^{(1)}}{T}$$

$$\alpha_{Bp}^{(1)} = \frac{w_{Bp}^{(1)} - w_{Ao}^{(1)}}{T} \qquad (14)$$

where $1 \leq p \leq n$ and T is in balancing plane "p". It should be noted that T may be different for each plane if desired. Thus, the first two rows of the α-matrix of Equation (9) are defined. Now a second balancing speed ω_2 is selected and the above procedure is repeated. This yields the influence coefficients of the second two rows of Equation (9):

$$\alpha_{Ap}^{(2)} = \frac{w_{Ap}^{(2)} - w_{Ao}^{(2)}}{T} \tag{15}$$

$$\alpha_{Bp}^{(2)} = \frac{w_{Bp}^{(2)} - w_{Bo}^{(2)}}{T} \quad .$$

This procedure must be repeated $N = (\frac{n}{2})$ times for n-even and $N = (\frac{n+1}{2})$ times for n-odd, where n is the number of balancing planes. In general, the following equation must yield a whole number:

$$N = \frac{n}{m} \tag{16}$$

where

N = number of balancing speeds,

n = number of balancing planes, and

m = number of measurement locations.

When N as computed above is not a whole number it must be increased to the next larger integer. Alternatively, n or m, or both, may be changed such that N becomes an integer. When this latter course is chosen, all of the measured amplitude and phase angle data (obtained at the m locations for N speeds) is used for solution of Equation (9). For the former condition (N increased to the next larger integer), all of the acquired data is not required for solution of Equation (9). For example, consider the case in which four balancing planes are used for exact point-speed balancing at three measurement locations. Here, $N = \frac{4}{3}$. Two balancing speeds are thus required (N is increased to the next largest integer). But this yields six (m x N = 6) sets of amplitude and phase information. Since the α-matrix must be square (4 x 4), two rows must be deleted. Two sets of data at the second speed may thus be ignored. Other combinations are of course possible.

It is apparent from Equation (9), and from the preceding discussion, that various combinations of balancing speeds and measurement stations may be used in the

balancing process, depending upon the number of balancing planes dictated by the unbalance response characteristics of the rotor. For instance, with two balancing planes, balancing may be performed for low amplitudes at two important rotor locations at one speed. Alternatively, balancing at one important location at each of two speeds is possible. With three balancing planes, several combinations are possible, such as balancing at one location at each of three speeds. Equally possible is balancing at two locations at one speed and one location at a second speed. The combinations expand rapidly as the number of balancing planes is increased to four, five, or more planes.

In the foregoing procedure, the w-vector and the α-matrix were defined numerically. Inverting the α-matrix and forming the product $\{w\} \cdot [\alpha]^{-1}$ allows the "effective" unbalance U vector to be obtained. The selection of "n" balancing planes results in an analytical consolidation of the distributed unbalance into n effective "local" values located at the balance planes. For this reason, it is essential to specify an adequate number of balance planes to represent the unbalances causing the rotor to deflect in a particular manner. Each individual complex unbalance, U_p, is thus the effect of the general rotor unbalance at the corresponding balance plane p. Placing an equivalent but opposite unbalance $(-U_p)$ at station p nullifies the effective residual unbalance at p. When such equivalent unbalances are placed in all selected balancing planes, the residual unbalance is nullified throughout the entire rotor, and the rotor is balanced.

The balancing computer program documented in [10] carries out the above operations automatically, accepting measured displacement and phase angles as input in keeping with the procedure outlined. Program output consists of a number of specified balance corrections, which are related to the stated angular reference position ($\emptyset = 0$) on the rotor by calculated phase angles. It should be recalled that the program will not balance a rotor where any physical condition is violated, e.g., one balancing plane is always inadequate where an axial distribution of unbalance exists. Specific examples of balancing effectiveness upon the number of balancing planes used are shown in Figure 4.

An improved version of the reference [10] computer program was used for the balancing tests documented in this report. The improved program contains four optional features for increased experimental accuracy and convenience. These features are as follows:

1) A provision to read instrumentation calibration factors for amplitude and phase angle measurements directly into the program. This feature eliminates the need for manual conversion of instrumentation output voltages into displacement and phase angle units.

2) A provision to include phase angle off-set. Such a feature allows for a non-zero angle between the reference axial plane and the axial plane(s) containing the trial weight holes. Thus, the calculated angular locations for the balancing correction weights are relative to the actual trial weight holes in each plane, decreasing chances for error.

3) A provision for specifying shaft out-of-roundness at the measuring locations. Substraction of the synchronous harmonic of shaft out-of-roundness from displacement transducer signals at the measuring stations may well make the difference between a rotor that can be successfully balanced and one that cannot. Such a correction becomes increasingly important as the ratio of shaft out-of-roundness to unbalance displacement amplitude increases. This feature was not investigated in the course of the experiments described in this report, because the out-of-roundness of the test shaft was a small fraction of the observed orbit amplitudes.

4) Provisions for trial weight runs with the trial weight placed first in one (specified) radial position in each trial weight plane, and then placed 180 degrees opposite from the original position in the same axial plane. Trial weight runs with the weight placed first in one location and then 180 degrees away can result in increases in experimental accuracy. This is because the averaging of two amplitude vectors obtained by separate and opposing trial weight placements acts to reduce the experimental error. (Most of the experimental results documented in this report were obtained by means of this technique.)

FLEXIBLE ROTOR BALANCING TEST APPARATUS

The basic mechanical apparatus used for the herein described balancing tests had previously been designed and built for turbulent journal bearing tests and for rotor unbalance response measurements. The system was specifically designed to accentuate rotor unbalance, thus providing an excellent vehicle for experimental rotor balancing tests.

Test Rotor Configuration

The test rotor shown in Figure 5 was 41-inches (104 cm) long and had a nominal bearing diameter of 2.500 (63.5 mm) inches. The rotor (2)* was basically symmetrical about its mid-point and had a three-mass configuration with the two end masses (3) overhung from each of the journal bearings. The center span between bearings was 25 inches (63.5 cm).

The center mass, 6 inches (152.4 mm) in diameter by 6 inches (152.4 mm) long, was integral with the shaft. The detachable end masses (3), also 6 inches (152.4 mm) in diameter but only 3 inches (76.2 mm) long, were shrunk onto the shaft and secured by locknuts (33). The weight of the center mass, exclusive of the 2.5-inch (63.5 mm) diameter shaft section, was 36 pounds (16.3 kg); that of each end mass, 19 pounds (8.6 kg). Total rotor weight was 126 pounds (57 kg). Rotor material was nitrided Nitralloy 135 (modified).

The test rotor was equipped with a row of axial, tapped holes (34,35) on each side of each mass. The tapped holes, 15 degrees apart, were on a 2.625-inch (66.7 mm) radius from the center of the shaft. The holes were No. 10-32 in size, except for two opposing 3/8-16 holes in each set which were used for trial weight placement. The large and the small holes were in-line in all three rotor masses.

One of the end disks was equipped on its outer diameter with a narrow (1/4-inch; 6.3 mm) reflective foil which extended for 180 degrees between the two large size tapped holes. The other half of the circumference of the disk was painted dull black. The circumferential mid-point position on the reflective strip was

* In this section numbers in parentheses refer to detail part numbers in Figure 5.

the reference point on the rotor from which the angles for maximum dynamic displacement at the other rotor stations were measured (phase angles).

The reflective segment extended (in the direction of shaft rotation) between the two large trial weight holes. These holes were arbitrarily marked zero degrees and 180 degrees, as shown in Figure 7. Consequently, the reference point (the mid-point of the reflective strip) actually led the zero degree position marked on the disk by 90 degrees. Therefore, 90 degrees had to be added to all phase angle measurements, which was equivalent to making the reference position and the zero degree position on the rotor coincident. (The same result could have been obtained by rotating the reflective strip on the disk, until it covered the arc 90-0-270 degrees). The test rig setup is shown in Figure 6, and the relationship among the reference mark, the trial weight locations, and the angular markings on the rotor is shown in Figure 7.

Test Rotor Support Bearings

The test rotor was radially supported by two identical tilting-pad type journal bearings, shown in Figures 8 and 9. Each of the bearings consisted of four radially rigid pads (6)*, with each pad extending over an 80 degree arc and with a pivot position of 44 degrees (55 percent) from the leading edge. The pivot configuration was that of a fixed sphere (integral with the pivot (8)) in contact with a cylindrical surface. The ball-in-cylinder pivot geometry allowed the pad to tilt in both the pitch and roll directions. Thus, it permitted the pads to track both translatory and conical shaft motions. The latter capability is particularly appreciated in a test machine, because it allows the experimenter greater latitude in setting the maximum permissible orbits without fear of contact between the shaft and the edges of the pads.

Pad length in the axial direction was 2.5 inches (63.5 mm) and the radial clearance between each pad (at the pivot location) and the shaft was 0.00187 inch (0.0475 mm). (Calculated journal bearing fluid-film radial stiffness as a function of rotor speed is presented and discussed below). Horizontal and vertical radial stiffnesses are identical for the bearings which were oriented in the load-between-pivots configuration.

*In this section, numbers in parentheses refer to detail part numbers in Figure 8.

The lubricating fluid for the journal bearings was Dow Corning 200, with a kinematic viscosity of 0.65 cs at 77 degrees F (25 degrees C). The bearings were operated in a flooded condition, with a temperature rise held to 10 degrees F (5.5 degrees C) maximum.

Axial positioning of the test rotor was provided by two externally pressurized air thrust bearings located on both sides of the rotor center mass. Locations of the thrust bearings are indicated in Figure 5 and in Section B-B of Figure 8.

Mechanical Features of the Apparatus

The test machine (Figure 5) was mounted on a structural steel base weighing approximately 3,200 pounds (1455 kg). The base was isolated from the floor by rubber pads. (These details of the base assembly are mentioned here only for reasons of documentation. There is no inherent requirement of the exact Point-Speed Balancing Method relative to the type of machinery base used.) Bolted to the top plate of the base was an aluminum jig plate (20)* to which were fastened the individual housings (9 and 11) for the journal and thrust bearings respectively, and the proximity probe holders (4) which held capacitance probes (31) used to measure motions of the end masses (3). Also mounted to the same plate was the electric drive motor (30).

The journal bearing housings (3) were equipped with seal rings (5) on both sides. Each of these rings had a clearance seal adjacent to the bearing housing with an outboard annular scavenging cavity. Outside the scavenging cavity was a labyrinth seal to restrict entry of air into the cavity. Bearing fluid leaking into the cavity wa pumped back into the sump by two separate, electrically-driven pumps. A positive-displacement pump driven by an air motor forced the bearing fluid through a water cooled heat exchanger and back into the journal bearing housings. Journal bearing supply pressure was controlled to ensure a flooded condition. Journal bearing temperature was measured by thermocouples welded to the back of the two lower pads in each bearing.

The drive motor (30) was a 30-hp, 30,000-rpm, 600-hz, 600-volt electric motor, powered from a variable frequency generator set. The test rotor was coupled to the drive motor by a crowned spline coupling (14,15,16). The teeth on the shaft part of the coupling (15) were crowned so that the coupling could accommodate up to a 0.030-inch (0.782 mm) radial misalignment between the axes of the motor and the test shaft without shaft restraint.

*In this section numbers in parentheses refer to detail part numbers in Figure 5.

Instrumentation

The instrumentation required for the balancing operation may be separated into two groups according to function:

a) instrumentation for machine control
b) instrumentation for acquisition of balancing data.

Machine control instrumentation consisted of pressure gages indicating thrust bearing air supply pressure, journal bearing fluid supply pressure, drive motor bearing air-mist lubrication pressure, thermocouples indicating journal bearing pad and bearing fluid temperature, and a speed counter for shaft rotational speed. To insure safe rotor operation under heavy unbalance loads, vertical and horizontal capacitance-type proximity probes were installed in three locations along the rotor axis for orbit indications. These orbits were monitored during test runs through oscilloscope observation.

A total of five signals were used for acquisition of the data needed for rotor balancing. Vertical rotor displacements were measured with capacitanct-type proximity probes and Wayne Kerr amplifiers at four locations along the rotor axis. The locations of the proximity probes along the rotor axis are shown in Figure 10.

A schematic of the complete data acquisition system as it was used for the flexible rotor balancing tests described in this report is shown in Figure 11.

The selection of the vertical plane instead of the horizontal plane for displacement measurements was an arbitrary decision. At this time, no rule is available for specifying a priori the required number of measuring stations along the axis of the rotor for balancing by the method investigated. In fact, this topic was one of the items under study. The computer program allows the substitution of data obtained at different speeds for data obtained at different rotor locations, provided that the product of the number of measuring stations and the rotational speeds at which trial weight data are taken is equal to the number of balancing planes in which correction weights are to be added. For this test, four measurement stations were used. The data from each station was always recorded so that different combinations of speeds and measuring stations could be selected, as desired, for computations of correction weight values.

The fifth signal required for the balancing operation (commonly referred to as the reference signal) was used to relate a fixed angular position on the rotor (the equivalent of the commonly used 'mark') to the angular position at which maximum dynamic displacement occurred at each of the four measurement stations. This angular relationship, called phase-angle, was obtained as follows: Half of the circumference of one of the end masses was covered with a reflective foil and the other half painted dull black. Each time the reflective arc passed under an optical proximity sensor (MTI Fotonic sensor, Model KD-38) a constant but adjustable voltage was generated. This square-wave signal was then converted to a sine wave in a band-pass tracking filter (Vibration Instrument Company, Tracking Analyzer 235 DS). The phase relationship between the converted reference signal and each of the displacement signals (analyzed one at a time) was measured in a phase meter (Model 933A, also made by Vibration Instrument Company).

The tracking analyzer (VIC 235 DS) was a dual channel model. In one channel, the reference signal was converted to a sine wave, while in the other channel, one of the four data signals was filtered to remove all frequency components other than the first harmonic corresponding to shaft rotational speed. The tracking (frequency) signal for the Tracking Analyzer was provided by the square wave phase-angle reference signal.

Amplitude read-out was obtained directly from the Tracking Analyzer, which provided an output level meter from 0.003 to 10 volts rms full scale, adjustable in seven steps.

Phase angle read-out was visually obtained from the digital phase-angle display provided by the phase meter.

The data acquisition system, as described above, is sufficient to conduct flexible rotor balancing. However, depending upon the mechanical characteristics of the rotor system, it may be important, and at the same time difficult, to obtain amplitude data for all four probes at exactly the same rotational speed. It is important to obtain the data at exactly the same speed if either the amplitude or the phase angle is highly sensitive to small changes in the nominal value of the data-taking speed, as for example, near an undamped shaft critical speed. On the other hand, particular rotor drive controls, temperature effects, and

damping may make it difficult to hold rotor speed constant long enough to take all required readings.

The requirement of nearly simultaneous readings was met for the test machine through use of an available seven channel tape recorder. Five phase-tied channels were used for the four displacement signals and the reference signal, while two direct reading channels were used for data identification (voice and rotational speed). By playing back the magnetic tape four times and switching from one displacement signal to the next, data was obtained at nearly identical rotational speeds.

General Analysis of the Rotor-Bearing System

Some knowledge of the dynamic response characteristics of a particular rotor to be balanced can be very valuable with respect to selection of both balancing planes and measurement stations. Critical speed calculations, and associated undamped mode shapes, will identify the number of criticals within or close to the operating speed range of the rotor, as well as the degree of "flexibility" of the rotor over the speed range. The mode shape plots can greatly assist in the selection of balance planes, both number and location.

As a matter of practical preparation for the balancing process, the locations of the proximity probes along the rotor axis should be at other than the shaft nodal points as they occur in the vicinity of the balancing speeds. Should the probes be at or near the nodal points, the low amplitude readings obtained may be a source of error in the calculation.

For the test rotor-bearing system, the following calculations were performed:

a) Journal bearing stiffnesses, both horizontal and vertical, as a function of rotational speed (Curve A, Figure 12).

b) Rotor critical speeds as a function of bearing stiffness (Curves B, C, D, Figure 12).

c) Rotor undamped mode shapes at the calculated critical speeds for vertical bearing stiffnesses of 10^5 lb/in (1.75×10^7 n/m) for each bearing (Figure 13).

The critical speeds of the test rotor-bearing system were obtained from Figure 12 at the points where the bearing stiffness curve (A) intersects the rotor critical speed curves. The first and second rotor critical speeds are so close together as to be nearly indistinguishable. They are basically rigid-body resonances and are predicted to occur around 7000 rpm.

The third critical speed is predicted for the vicinity of 11,000 rpm with both nodal points located within the length of the journal bearings (see Figure 13). This critical contains, of course, significant shaft bending.

As a supplement to the theoretical analysis, exploratory test machine runs were conducted. For these runs, covering the speed range between 3000 and 10,500 rpm, rotor amplitude and phase angle plots were made. These plots indicated a speed range between 7000 and 7500 rpm where rotor amplitudes, as well as phase angles, showed a very noticeable and rapid fluctuation, apparently caused by the presence and close proximity of the first two rigid-body critical speeds. Rotor amplitudes increased very rapidly at speeds above 10,300 rpm, thus identifying the approach to the third critical speed. A smaller, but always finite and nearly constant, rotor amplitude peak at 10,210 rpm was tentatively identified as a housing resonance. The phase angle plots obtained concurrently with the rotor amplitude data were found to contain interesting and valuable data. They showed that phase angle fluctuated by different amounts over the rotor speed range, and also that the phase angle fluctuations were not the same at the four rotor stations at which they were measured. Inspection of the phase angle plots permitted selection of balancing speeds at those points where the phase angle readings were steadiest. Phase angles obtained for the residual rotor unbalance condition are not shown in this report. However, a set (for the four rotor measuring stations) of phase angle plots covering the entire speed range up to 16,500 rpm, and therefore, including the third critical speed at 10,960 rpm, are included as Figures 14 through 17 for the rotor in its balanced condition at the conclusion of Test Case I. The corresponding amplitude plots for Stations 1, 2, and 4 are shown in Figures 18 through 20.

TEST RESULTS

Test Case I - Rotor With Residual Unbalance

The first application of the Exact Point-Speed Influence Coefficient Balancing Method to the test machine was aimed at reducing the original, residual unbalance as it prevailed after slow-speed dynamic balancing prior to assembly of the rotor in its bearings. The test situation was very realistic, because no a priori knowledge existed about the residual unbalance distribution in the rotor. Even though the rotor was well balanced by current standards, the first exploratory run of the test machine revealed that passage through the third critical speed (where essentially undamped rotor bending occurred) could not be attempted without endangering the instrumentation probes and possibly the test machine as well. Rotor orbits exceeding 0.010 inch (0.254 mm) in diameter were inadvertently produced during the exploratory run, before it was realized that rotor excursions increased extremely rapidly in the immediate vicinity of the third critical speed. In subsequent runs, rotor speeds were generally not allowed to increase beyond the point where orbits reached approximately 0.006 inch (0.152 mm) in diameter.

Initial Rotor Condition

The initial vertical rotor amplitudes for the speed range from 3,000 to 10,450 rpm are recorded as curves 'A' in Figures 21 through 24, which present amplitude data for probe locations 1, 2, 3, and 4, respectively, as shown in Figure 10. These curves, which were plotted "on-line" during actual tests, indicate that an acceptable level of dynamic balance was maintained up to 10,000 rpm as a result of the initial, slow speed balancing performed on a commercial balancing machine. The initial rotor amplitudes measured at the four measuring stations along the rotor axis were recorded in this form to permit an assessment of amplitude reductions as a result of the subsequent balancing effort. Subsequent results are shown as Curves B, C, etc. in these and later figures. The availability of these amplitude graphs and their complimentary phase angle plots also contributes to the success of the balancing process itself. In certain frequency ranges, rotor amplitudes and phase angles may fluctuate greatly as a result of small variations in speed.

Experimental accuracy can be increased through selection of balancing speeds at which both amplitudes and phase angles are well behaved.

Sequence of Balancing Runs

The computer program for exact point-speed balancing of flexible rotors allows for several alternatives and options in the balancing process. The chart in Figure 25 provides a record of the selected alternatives and options, and all sequential steps taken in the process of balancing the rotor having only residual unbalance. The first trial weight run with the rotor in its original condition was followed by balancing calculation No. 1, and then by a check-out run with the calculated correction weights installed in the rotor. The resultant amplitudes of the improved rotor are recorded as Curves B in Figures 26 through 29. Balancing calculation No. 1 was based upon trial weight data obtained at two rotor stations (2 and 4, see Figure 10) and at two balancing speeds (6060 and 10,450 rpm). Trial weight placement was performed in all four rotor balancing planes.

The results based upon this initial calculation were not considered satisfactory in that large amplitudes remained near the third critical speed. Therefore, a new calculation of correction weights was made (Calculation No. 2), and the first set of correction weights was discarded. The second calculation was based upon the same data obtained from the initial trial weight run, but included additional readings from measuring stations 1 and 2. Only one rotor speed (10,450 rpm) was utilized for balancing.

The balance correction weights calculated in computer run No. 2 proved to be too large for the tapped holes provided in the center disk of the rotor. It was noted however, that the correction weights calculated for the two sides of the center disk were of nearly equal magnitude and approximately 180 degrees out-of-phase. Since the net centrifugal correction force from these weights appeared to be small, a new correction weight calculation (No. 3) was made based on three balancing planes (rather than four), using three probe readings only. In this calculation only one correction plane (instead of two) was specified for the center disk.

The reduction in rotor amplitudes obtained by using the correction weights given by Calculation No. 3 was encouraging. The reduced amplitudes are compared to the original amplitudes in Figures 21 through 24, (Curves C and A respectively). A new trial weight balancing run was, therefore, made with this first set of three-plane correction weights left in the rotor. For improved accuracy, the new trial weight readings were obtained with the trial weight first placed in the zero-degree position and then also in the 180-degree position in each correction plane. Based upon experience gained in the first two balancing attempts, several trial combinations of probe readings and speeds were used for calculations of balance correction weights. Calculation No. 10, which was for four rotor planes and one speed, was selected for correction weight installation.

A consecutive numbering of the balancing calculations performed during the entire test series was maintained. Those calculations that are not listed in Figures 25, 34 or 39 were check runs on either the computer program, the effect of balance plane selection, the effect of trial weight placement, or were discarded because of errors in data processing.

The results of balancing calculation No. 10 were highly successful, permitting sustained operation of the test machine at the third critical speed for the first time. During the first run through the third critical speed, rotor peak amplitudes of approximately 0.0035 inch (0.089 mm) were recorded (Curve D, Figures 21 through 24). During this run, the rotor was held for approximately three minutes at and near the critical speed, a circumstance which may have contributed to the observation of larger amplitudes at the critical than were noted on subsequent occasions, when the rotor tended to either back off the third critical or pass right through it. In all subsequent test runs through the third critical speed with the rotor in this particular balance condition, peak amplitudes could not be made to exceed one-half to two-thirds of those shown in Figures 21 through 24. A similar experience was noted near the conclusion of Test Case III. There again, larger rotor amplitudes were observed the first time the rotor passed through the third critical speed with the newly computed correction weights installed. Subsequent runs through the critical with the same correction weights always resulted in smaller resonant amplitudes.

Trial weight balancing runs (No. 3) were again conducted with the rotor in its best as-balanced condition. The trial weights were again placed in the zero-degree and 180-degree positions in each of three balancing planes. Reversion to three plane balancing at this point was deemed necessary, because the amplitude signals at the probe station nearest the bearing were considered to be too small to be read accurately. The amplitude curves of the well balanced rotor, shown by Curves D in Figures 21 through 24, have extremely steep slopes at the approach to the third critical speed. Since it became nearly impossible to hold the rotor at constant speed just below the third critical speed and still obtain amplitude readings large enough to be meaningful, an attempt was made to take readings (trial weight data) directly at the peak of the amplitude curves at the third critical speed.

Several balancing calculations utilizing the results of trial weight run No. 3 were made. Calculation No. 15 represented the last attempt to improve the residual unbalance condition of the test rotor still further. The calculations were based upon trial weight data taken exactly at the critical speed. Even though only very small correction weights were calculated, which appeared to be of the right order of magnitude, no improvement in the rotor amplitude occurred when these weights were placed in their calculated angular positions. In fact, the peak amplitudes at the third critical became somewhat higher. The lack of success in this final balancing attempt is attributed to the very rapidly changing phase angle at the peak rotor amplitude, and to the inability of the current test set-up to hold rotor speed constant long enough to permit simultaneous reading of amplitude and phase angle.

Test Results For Rotor With Residual Unbalance - Test Case I

Rotor balance improvement is usually defined in terms of either rotor amplitude or bearing force reduction within the rotor operating speed range.

The test rotor for the herein described balancing experiments was designed to operate over the speed range of 0-24000 rpm. However, the rotor was purposely designed with nearly zero bearing damping at the third critical speed, which is

just below 11,000 rpm. In any currently practical application, this rotor would not be expected to operate at or above the third critical speed. If common commercial balancing standards were applied, the test rotor would be limited to an operating speed of approximately 80 percent of the third critical speed, or 9,000 rpm.

In order to present a meaningful comparison of the balance improvement as a result of application of the Exact Point-Speed Balancing Method to the test rotor, tabulated rotor amplitudes at four rotor stations are presented for three operating speeds (6,000, 9,000, and 10,960 rpm) for the initial unbalance condition, and after the two successive balancing runs (Calculations No. 3 and No. 10) which brought the rotor into its best balance condition.

Table I gives a listing of these values for Test Case I. The values in Table I were extracted from Figures 21 through 24, where rotor amplitudes are plotted as continuous functions of speed. Also shown in Table I are the calculated percentages in rotor amplitude reduction based upon each of the successive balancing runs, and also upon all runs together (total reduction).

Inspection of the tabulated results indicates that amplitude reductions along the rotor axis were not uniform. In fact, near the bearing stations where amplitudes were quite small to begin with, an increase in amplitude was registered for the best balanced condition. The probable reason for this seemingly anomalous result can be understood upon consideration of the objective and starting point for this test case. Because of the relatively low initial unbalance, further amplitude reductions were not mandatory at speeds below the third critical speed. Instead, the objective was to reduce rotor unbalance until passage through the third critical speed became possible. Therefore, all selected balancing speeds were in the immediate vicinity of the third critical speed, where all resulting amplitudes are considerably lower than the initial amplitudes. In addition, the steady-state peak rotor amplitude at the critical speed was reduced from very large (unmeasured) values to those listed in Table I. For the rotor in general, (i.e., considering all measurement stations in total), a slow but steady reduction in average amplitude for all stations combined is seen for each successive balancing run at each tabulated speed. Balance improvements are most pronounced at the balancing locations at exactly the balancing speed, while

Table I

BALANCE IMPROVEMENT - TEST CASE I

ROTOR WITH RESIDUAL UNBALANCE

PEAK - TO - PEAK ROTOR AMPLITUDES										
ROTOR SPEED (RPM)	PROBE STATION (SEE FIGURE 10)	BEFORE BALANCING		AFTER 1ST. BALANCING RUN (CALCULATION NO. 3)		% REDUCTION DUE TO 1ST. BALANCING RUN	AFTER 2ND. BALANCING RUN (CALCULATION NO. 10)		% REDUCTION DUE TO 2ND BALANCING RUN	TOTAL % REDUCTION
		micro in.	micron	micro in.	micron		micro in.	micron		
6,000	1	200	5.08	50	1.27	75.0	35	0.89	30.0	82.5
	2	325	8.26	210	5.33	35.4	250	6.35	(19.0)	23.1
	3	75	1.91	180	4.57	(140.0)[2]	180	4.57	0.	(140.0)
	4	185	4.70	235	5.97	(27.0)	180	4.57	23.4	2.7
9,000	1	110	2.79	85	2.16	22.7	20	0.51	76.5	82.0
	2	365	9.27	175	4.45	52.0	235	5.97	(35.6)	35.6
	3	100	2.54	225	5.72	(125.0)	175	4.45	22.2	(75.0)
	4	180	4.57	180	4.57	0.	125	3.18	30.6	30.5
10,960[1]	1	Greater than		Greater than		--	3700	93.98	--	--
	2	5000	127.0	5000	127.0	--	2900	73.66	--	--
	3	(See Note 3)		(See Note 3)		--	1800	45.72	--	--
	4	"	"	"	"	--	3300	83.82	--	--

1. Third critical speed of test rig (1st flexural critical).
2. Increase in amplitude.
3. 5000 microinches was the maximum amplitude permitted in the test rig. Because of this limitation, the test rig was not actually run up to 10,960 rpm until after the 2nd balancing run.

increased amplitudes may occur at other speeds and other rotor locations. The very first attempt at balancing of the rotor with residual unbalance is an example of this. There it was attempted to balance the rotor at two speeds (6060 and 10,450 rpm) but with proximity probes located only in the center and at the right end of the rotor. After the balancing corrections had been made, the rotor amplitude at the left end was much larger than before, at least up to the higher balancing speed (see Figures 26 through 29, Curve B).

Test Case II - Rotor With In-Line, In-Phase Unbalance

Initial Rotor Condition

For the second balancing test case, the rotor was intentionally unbalanced. Substantial weights were attached to the rotor at equal radii in four separate planes at identical angular positions. At both overhung end masses, the unbalance weights were attached on the side of the disk facing the journal bearing. Balance correction weights were applied to the outboard side of the end disk, and, for some correction runs, at only one of the two sides of the center mass. This case was thus designed to test the realistic situation in which balancing planes and unbalance locations do not coincide.

Four unbalanced masses of 0.343 oz-inch (24.6 gr-cm) each were added to the rotor in its best balanced condition at the conclusion of Test Case I. The angular location of the unbalance weights was at 10 degrees. (See Figure 7 for angular rotor locations.) Rotor amplitudes resulting from this unbalance addition are shown in Figures 30 through 33, Curves A.

The amplitude curves (together with phase angle measurements which are not shown) indicate the rotor to be orbiting in what is essentially a cylindrical mode (with some rotor bending) in the frequency range between 5,000 and 10,000 rpm. The average amplitude in this range corresponds fairly closely to the displacement of the rotor gravity axis from the rotor axis of rotation due to the addition of the total unbalance of 1.372 oz-inch (98.4 gm-cm).

Sequence of Balancing Runs

The balancing runs for Test Case II were perfor d in the sequence shown in Figure 34. Attempts to balance the rotor in four planes were unsuccessful on two occasions (balancing calculations No. 16 and No.22) because the calculated weights at each end of the center mass were too large to be accommodated in the tapped holes provided for them. (The weights were 180-degrees apart, similar to the positioning encountered in Calculation No. 2, in Test Case I). Three-plane balancing was required in order to obtain the first testable set of correction weights. The resulting improvement is shown by Curves B, Figure 30 through 33. The next set of correction weights was obtained from four-plane balancing which led to the improved rotor condition indicated by Curves C, Figures 30 through 33. This balancing run reduced rotor amplitudes at station 4 and 1. but caused increases at other rotor stations, (see Table II - Second Balancing Run).

A rather interesting situation developed during the following trial weight run No. 3. At the selected balancing speed of 10,800 rpm, a large phase angle variation ($\pm$ 30^{o}) was encountered for the dynamic amplitude at the center disk location. This situation, which only occurred when the rotor was run without trial weights, was observed even though the amplitude readings were neither small nor rapidly fluctuating, thus providing an exception to previous observations. The attempt to utilize the trial weight data for calculation of correction weights for three balancing planes only, and with the bearing location as the third measuring station, was not successful. Vector plots of amplitudes and phase angles indicated that the calculated correction weights would not yield any improvement, and no weights were made. Subsequent trial weight runs were successfully implimented at a reduced speed of 10,700 rpm, thus indicating that even relatively small changes in balancing speed in close vicinity to a critical speed, may cause significant changes in the behavior of the phase angle.

Test Results For Rotor With In-Line, In-Phase Unbalance - Test Case II

The second test case differs substantially from the first in that a relatively large initial unbalance was added to the rotor in Case II. At high unbalance conditions, rotor amplitudes and phase angles are more constant with time, which apparently leads to a very rapid initial unbalance reduction. For the first

balancing run of the second test case, the reductions in amplitude at 3,000 and 9,000 rpm ranged between 81 and 88 percent.

After two additional balancing runs, the total amplitude reduction ranged between 80 and 94.5 percent. The numerical results for the improved rotor balance in Test Case II are shown in Table II. Graphical plots of the reduced rotor amplitudes are shown in Figures 30 through 33 (Curves D).

Table II does not contain any values for reduced rotor amplitudes at the third critical speed (10,960 rpm). This is due to the suspension of balancing efforts at the point where rotor dynamic behavior was similar to that noted at the start of Test Case I (residual unbalance). The amount of additional effort required to improve the rotor in Test Case II so that it would meet the criterion for running at and through the third critical speed may be estimated by comparing the average rotor amplitude after each of the balancing runs in Test Case I and Test Case II. Table II-b shows those values extracted from Tables I and II.

TABLE II-b

AVERAGE ROTOR AMPLITUDES (MICRO-INCHES) BEFORE AND AFTER BALANCING CORRECTION RUNS IN TEST CASES I AND II

	Test Case II				Test Case I		
Rotor Speed (rpm)	Original Condition	Correction Runs I	II	III	Original Condition	Correction Runs I	II
6000	1695	249	274	229	196	169	161
9000	1865	254	310	229	189	166	139

It may be concluded from the foregoing data that at least three or four more balancing runs would have beer required to attain the level of balance necessary to pass through the third critical speed with this particular rotor.

Test Case III - Rotor With In-Line, Out-Of-Phase Unbalance

Initial Rotor Condition

For the third and final test case investigated, the intentionally-added unbalance weights in the rotor were shifted to create an entirely different unbalance situation.

Table II

BALANCE IMPROVEMENTS - TEST CASE II

ROTOR WITH IN-LINE, IN-PHASE UNBALANCE

PEAK - TO - PEAK ROTOR AMPLITUDES												
ROTOR SPEED (RPM)	PROBE STATION (SEE FIGURE 10)	BEFORE BALANCING		AFTER 1ST. BALANCING RUN (CALCULATION NO. 18)		% REDUCTION DUE TO 1ST. BALANCING RUN	AFTER 2ND. BALANCING RUN (CALCULATION NO. 20)		% REDUCTION DUE TO 2ND. BALANCING RUN	AFTER 3RD. BALANCING RUN (CALCULATION NO. 23)		% REDUCTION AFTER 3RD. BALANCING RUN	TOTAL % REDUCTION
		micro in.	micron	micro in.	micron		micro in.	micron		micro in.	micron		
6000	1	1450	36.83	260	6.60	82.1	230	5.84	11.5	75	1.91	67.4	94.8
	2	1450	36.83	200	5.08	86.3	280	7.11	(40.0)*	280	7.11	0	80.7
	3	1800	45.72	210	5.33	88.3	335	8.51	(59.5)*	335	8.51	0	81.4
	4	2080	52.83	325	8.26	84.4	250	6.35	23.1	225	5.72	10.0	89.2
9000	1	1700	43.18	190	4.83	88.8	350	8.89	(84.2)*	100	2.54	71.4	94.1
	2	1700	43.18	200	5.08	88.2	350	8.89	(75.0)*	300	7.62	14.3	82.4
	3	2000	50.80	375	9.53	81.3	430	10.92	(14.7)*	405	10.29	5.8	79.8
	4	2060	52.32	250	6.35	87.9	110	2.79	56.0	110	2.79	0	94.7

* INCREASE IN AMPLITUDE

MTI-9488

After removal of all correction weights applied in the course of the second test case, the unbalance weights attached to each end disk for Test Case II were moved by 180 degrees. Since all weights were of equal magnitude and at equal distances from the rotor axis, each of the weights attached to one end disk balanced statically one of the two weights located at the center disk. Moreover, the weights at the end disks and the weights at the center disk were also located symmetrically about the rotor mid point, thus balancing each other dynamically. This kind of unbalance arrangement is totally unresponsive to any attempt at balancing in a conventional (rigid rotor) balancing machine. In fact, the occurrence of this type of unbalance is the predominant reason why rotors behave flexibly and are thus required to operate away from their flexible-shaft critical speed.

The unbalance combination selected for this final test case is again not an unrealistic one. A typical example for this type of unbalance in practical applications may be visualized by assuming that the end disks were keyed to the test rotor with one key each (in-line, in-phase) and that the two sides of the rotor center mass were specified as balancing planes. This appears as a reasonable specification whenever the end disks are representative of light wheels or gears which require no balancing. While the resulting rigid body balance may be satisfactory, the bending of the rotor caused by the keyway unbalance at the end wheels may be excessive near the shaft bending critical speeds.

Test rotor amplitudes for the initial rotor condition resulting from the addition of in-line, out-of-phase unbalanced masses of 0.686 oz-in (49.2 gm-cm) on each side of the rotor axis of rotation are shown as curves A in Figures 35 through 38. Rapidly increasing rotor orbits prohibited test machine operation at speeds above 9000 rpm.

Sequence of Balancing Runs

The sequence of balancing runs comprising Test Case III is shown in Figure 39.

Partly as a result of increasing experience, this last test case was conducted with fewer unrewarding trials. For all three correction runs, the same three

probe locations and balancing planes were used. For additional information, four-plane corrections were also calculated for each run. For the first two such four-plane calculations (No. 24 and No. 26), the computed correction weights again turned out to be much too large for the tapped holes provided in the center disk. However, for the last calculation, weights were obtained of a magnitude comparable to those calculated for three-plane correction. The selection of the correction weights from calculation No. 28 (three-plane correction) over those from calculation No. 29 (four-plane correction) for the final correction was arbitrary.

Test Results for Rotor With In-Line, Out-of-Phase Unbalance - Test Case III

The balancing effort applied to the test rotor with in-line, out-of-phase unbalance proved to be very successful. Values of initial and improved rotor amplitudes, as well as the corresponding percentages, are shown in Table III. Continuous plots of rotor amplitudes versus speed for Test Case III are shown in Figures 35 through 38, where curves A represent the initial rotor condition before balancing, and curves B, C, and D show the reduced rotor amplitudes resulting from the first, second, and third successive balancing runs, respectively. The first correction run reduced rotor amplitudes at 9000 rpm rotor speed by nearly 94 percent. The following two correction runs reduced amplitudes by another 1.6 and 1.1 percent of the initial unbalance respectively.

While the last two reductions were significant, insofar as they put the rotor in a balanced condition which permitted passage through the third critical speed, the really significant amplitude reduction obviously occurred at the very first balancing trial. This achievement contrasts with the result of the final balancing in the previous Test Case II, where the initial reduction amounted to only 86.3 percent at 9000 rpm. While the difference of about 8 percent does not seem large, it nevertheless becomes significant because it appears that subsequent balancing runs reduce rotor amplitudes only by small percentages when measured against the initial rotor amplitudes.

The consequence of this fact is well demonstrated by the different balance conditions achieved in Test Cases II and III. The rotor passed the third critical speed after the third balancing run in Test Case III, while it was estimated that

Table III

BALANCE IMPROVEMENT - TEST CASE III

ROTOR WITH IN-LINE, OUT-OF-PHASE UNBALANCE

		PEAK-TO-PEAK ROTOR AMPLITUDES										
ROTOR SPEED (RPM)	PROBE STATION	BEFORE BALANCING		AFTER 1ST. BALANCING RUN (CALCULATION NO. 25)		% REDUCTION DUE TO 1ST. BALANCING RUN	AFTER 2ND. BALANCING RUN (CALCULATION NO. 27)		% REDUCTION DUE TO 2ND. BALANCING RUN	AFTER 3RD. BALANCING RUN (CALCULATION NO. 28)		% REDUCTION DUE TO 3RD. BALANCING RUN	TOTAL % REDUCTION
		micro in.	micron	micro in.	micron		micro in.	micron		micro in.	micron		
6000	1	810	20.57	250	6.35	69.1	100	2.54	60.0	185	4.70	(85.0)	77.2
	2	425	10.80	75	1.91	82.4	75	1.91	0.	100	2.54	33.3	76.5
	3	625	15.88	220	5.59	64.8	175	4.45	20.5	110	2.79	37.1	82.4
	4	420	10.67	190	4.83	54.8	250	6.35	(31.6)[2]	85	2.16	66.0	79.8
9000	1	2730	69.34	125	3.18	95.4	75	1.91	40.0	230	5.84	(206.7)	91.6
	2	2510	63.75	150	3.81	94.0	40	1.02	73.3	100	2.54	(150.0)	96.0
	3	2530	64.26	250	6.35	90.1	180	4.57	28.0	85	2.16	52.8	96.6
	4	2810	71.37	125	3.18	95.6	185	4.70	48.0	70	1.78	62.2	97.5
10,960[1]	1	Greater than		Greater than			Greater than		-	2125	53.98	-	-
	2	5000	127.0	5000	127.0		5000	27.0	-	2075	52.71	-	-
	3	(See Note 3)		(See Note 3)			(See Note 3)		-	1400	35.56	-	-
	4	"	"	"	"		"	"	-	3100	78.74	-	-

1. Third critical speed of test rig (1st flexural critical).
2. Increase in amplitude.
3. 5000 microinches was the maximum amplitude permitted in the test rig. Because of this limitation, the test rig was not actually run up to 10,960 rpm until after the 2nd balancing run.

at least 3 or 4 additional balancing runs (for a total of six or seven) would have been required to reduce rotor amplitudes to comparable levels in Test Case II.

The reason for the much more drastic initial reduction in rotor amplitude in Test Case III seems to lie in the different initial unbalance configurations that were applied to the test rotor in Test Cases II and III. The predominantly static unbalance in Test Case II seems to have caused very unsteady rotor operation, with considerable fluctuations in both rotor amplitude and phase angle for very small changes in rotor speed. (See Figures 30 through 33, Curves A). In the vicinity of the balancing speed, the bent rotor in Test Case III showed practically no amplitude or phase-angle variations, as evidenced by Curves A, in Figures 35 through 38. The explanation for the smooth rotor operation in the latter situation may well lie in the journal bearings. For the bent-shaft case, rotor whirl amplitudes in the bearings were small because the bearings were located very nearly at the nodal points. In Test Case II, the large static unbalance caused the rotor to whirl in its bearings with amplitudes between one-half to two-thirds of the bearing clearance.

A summary of rotor amplitudes, as they existed before balancing and after each of the two or three consecutive balancing runs for each test case, is shown in Table IV. Amplitudes have been averaged for all four rotor stations and the percentage reductions shown are the cummulative results of one, two, or three consecutive balancing runs applied to each test case.

Table IV

SUMMARY OF BALANCE IMPROVEMENT

TEST CASE	ROTOR SPEED (RPM)	BEFORE BALANCING		AFTER 1ST. BALANCING RUN		% REDUCTION DUE TO FIRST BALANCING RUN	AFTER 2ND.* BALANCING RUN		% REDUCTION DUE TO FIRST AND SECOND BALANCING RUNS *	AFTER 3RD.* BALANCING RUN		TOTAL % REDUCTION
		micro in.	micron	micro in.	micron		micro in.	micron		micro in.	micron	
		AVERAGE PEAK-TO-PEAK ROTOR AMPLITUDES (FOUR ROTOR STATIONS COMBINED)										
I	6000	196	4.98	169	4.29	14.0	161	4.10	4.4	-	-	17.8
	9000	189	4.79	166	4.22	11.9	139	3.52	16.5	-	-	26.5
IV	6000	1695	43.05	249	6.32	85.3	274	6.95	83.8	229	5.81	86.5
	9000	1865	47.37	254	6.45	86.4	310	7.87	83.4	229	5.81	87.7
III	6000	570	14.48	184	4.67	67.8	150	3.81	73.7	120	3.05	78.9
	9000	2645	67.18	163	4.13	93.9	120	3.05	95.5	121	3.08	95.4

* Balancing runs 1 through 3 were consecutive for each test case, with new balance correction weights added for each new run.

CONCLUSIONS

The experimental program documented in this report has shown that a flexible rotor supported in journal bearings having very low damping capability can be systemacically balanced for operation close to and through its third critical speed (first flexural critical). The test apparatus is felt to have provided a severe test of the theoretical balancing procedure.

The Exact Point-Speed Influence Coefficient Balancing Method, which was used to calculate the balance correction weights for the test rotor, has been shown to be capable of effectively reducing large rotor unbalances. One unbalance correction run is usually sufficient to obtain smooth rotor operation up to 80 percent of the first flexural critical speed of the rotor. To obtain safe (and slow) operation through the first flexural critical, two to five additional unbalance correction runs may be required, depending upon the initial condition of rotor unbalance. For two of the three initial unbalance conditions investigated, passage through the first flexural critical speed was achieved with a total of three correction runs. For the remaining initial unbalance condition (in-line in-phase unbalance), the test data indicated that six or seven correction runs would have been required to permit passage through the third critical. This particular unbalance condition was the one which most strongly excited the "rigid body" critical speeds of the rotor, and which produced the largest synchronous whirl orbits within the bearings. There is some indication that large amplitude bearing orbits may interact with the rotor dynamics in such a way as to cause fluctuations in the amplitude and phase angle data used for calculation of the unbalance correction weights. Such fluctuations can be a source of error in the computed corrections.

The instrumentation system selected and assembled for the experiments reported herein has proven itself reliable, easy to operate, and of adequate accuracy. Inherent mechanical rotor-bearing system characteristics, rather than instrumentation sensitivity or accuracy, appeared to be the factor which limited the amount of balancing improvement which could be achieved in each run.

The reported experimental investigation has given every indication that the Exact Point-Speed Influence Coefficient Balancing Method is a reasonably effective

method, at least over a speed range encompassing the fundamental "flexural" critical speed of a rotor. Expeditious use of the balancing method can be greatly enhanced by having an a priori knowledge of the dynamic response characteristics of the rotor to be balanced. Such knowledge can be obtained using rotor-bearing system critical speed computer programs which are readily available.

RECOMMENDATIONS

It is recommended that further evaluation of the Exact Point-Speed Influence Coefficient Balancing Method be obtained by subjecting the method to a wider range of test conditions. This can be done in several meaningful ways. For instance, several additional initial unbalance configurations can be tested using the present test-rotor configuration. One unbalance configuration might consist of a single unbalance weight placed at one end of the rotor, which would tend to induce conical rotor motions. A second configuration might consist of unbalance weights of different magnitudes, located in different angular positions in three or four axial rotor planes, so as to force the rotor into a corkscrew mode of vibration. These two cases represent departures from the in-line unbalance conditions considered to date.

A further test of the Exact Point-Speed method would be an investigation of its effectiveness on a different test-rotor configuration. For example, removal of one of the end masses of the test rotor will alter drastically the dynamic behavior of the system. Bearing loads and bearing dynamic properties will be changed, resulting in different amplitudes of vibration at all points on the rotor.

An important step in evaluation of the Exact Point-Speed Balancing Method (or any balancing method) must be application of the method to rotor systems which operate over a speed range encompassing several (perhaps up to four) flexural critical speeds. Based on experience with and performance of the Exact Point-Speed method to date, it appears that high priority for a truly supercritical test evaluation is warranted.

Experimental evaluation of the computer program option for automatic subtraction of shaft out-of-roundness at the measuring stations should be conducted as part of any further investigation into the practical usefulness of computer-assisted flexible rotor balancing.

LIST OF REFERENCES

1. Muster, D., "Balancing of Rotating Machinery, Part I: Theory of Balancing", Shock and Vibration Handbook (edited by Harris, C.M. and Crede, C.E.), Vol. 3, McGraw-Hill Book Co., New York, 1961, pp. 39-1 to 39-22.

2. Senger, W.I., "Balancing of Rotating Machinery, Part II: Practice of Balancing", Shock and Vibration Handbook (edited by Harris, C.M. and Crede, C.E.), Vol. 3, McGraw-Hill Book Co., New York, 1961, pp. 39-23 to 39-41.

3. Den Hartog, J.P., Mechanical Vibrations, 4th Edit., McGraw-Hill Book Co., New York, 1956, pp.232-243.

4. Lindsey, J.R., "Significant Developments in Methods for Balancing High-Speed Rotors", ASME Paper No. 69-Vibr-53, presented at the 2nd Vibrations Conference, March 30, 1968.

5. Prause, R.H., Meacham, H.C., and Voorhees, J.E., "The Design and Evaluation of a Supercritical-Speed Helicopter Power-Transmission Shaft", Transactions of the ASME, Vol. 89, Series B, No. 4, Nov. 1967, pp. 719-728.

6. Gunter, E.J., "Influence of Flexibly Mounted Rolling Element Bearings on Rotor Response, Part 1 - Linear Analysis", Transactions of the ASME, Vol. 92, Series F, No. 1, January 1970, pp. 59-75 (the Introduction and the References given in this paper will give the reader a good overview of the problems associated with flexible rotor critical speeds in high-performance engines).

7. Curwen, P.W., "Feasibility of Gas Bearings for Small High-Performance Aircraft Gas Turbines", Mechanical Technology Inc.; USAAVLABS Technical Report 68-87, U.S. Army Aviation Materiel Laboratories, Fort Eustis, Va., March 1969. (This report illustrates the very flexible nature of the LP-spool in advanced two-spool aircraft gas turbines).

8. Sternlicht, B., and Lewis, P., "Vibration Problems With High-Speed Turbomachinery", Transactions of the ASME, Vol. 90, Series B, No. 1, Feb. 1968, pp. 174-186.

9. Rieger, N.F., "Rotor-Bearing Dynamics Design Technology, Part I: State-of-the-Art", Mechanical Technology Inc.; Technical Report AFAPL-TR-65-45, Part I, Air Force Aero Propulsion Laboratory, Wright-Patterson Air Force Base, Ohio, May 1965, Chapter 4.

10. Rieger, N.F., "Computer Program for Balancing of Flexible Rotors"; Mechanical Technology Incorporated, Technical Report 67TR68, prepared for NASA-Lewis Research Center under Contract NAS 3-10926, September 15, 1967.

APPENDIX A

TEST PLAN FOR BALANCING TESTS

I. Purpose of Tests

To obtain experimental verification of the effectiveness of the computer program for balancing of flexible rotors as reported under NASA Contract NAS 3-10926. The scope of the tests described herein shall be in accordance with the statement of work contained in Contract NAS 3-13473.

II. Test Equipment

A. Rotor-bearing system as refurbished for these tests under contract NAS 3-13473.

B. Electronic instrumentation system consisting of capacitance probes (7) with Wayne-Kerr amplifiers for rotor amplitude detection, an MTI Fotonic Sensor for reference signal generation, and an electromagnetic speed pick-up with Hewlett-Packard counter for rotor speed measurements. A dual channel tracking analyzer and a phase meter (235 DS and 933 A, respectively, by Vibration Instrument Company) are to be used for amplitude and phase angle measurements.

III. Test Procedure

The test procedure shall be in accordance with the description of a typical test cycle as described in Appendix C, "Balancing Procedure." Specific test cases shall be as follows:

A. Test Case I shall consist of the original, residual rotor unbalance as it prevails after low-speed dynamic balancing prior to assembly of the rotor in its bearings.

B. Test Case II shall consist of the rotor in its best-balanced condition (at the conclusion of Test Case I) with four additional unbalance weights of equal magnitude located in a single axial plane on the same side of the rotor. These weights shall be of sufficient size to produce significant orbit sizes, and shall be located such that not all of them are in planes selected for balancing.

C. Test Case III shall consist of the rotor in its best-balanced condition (at the conclusion of Test Case I) with four additional unbalance weights of equal magnitude added in a single axial plane. The unbalance weights shall be placed at the 12 o'clock position in planes one and four and in the 6 o'clock position in planes two and three. The unbalance weights shall be of sufficient size to produce significant orbit sizes, and shall be located such that not all of them are in planes selected for balancing.

For all three test cases, the rotor amplitudes shall be plotted as functions of rotor speed prior to beginning of the balancing process and after conclusion of each balancing cycle.

Rotor amplitudes of 0.00150-inch peak-to-peak are considered to be too small for accurate phase angle measurement with the present test equipment. Rotor amplitudes of 0.000200-inch peak-to-peak will, therefore, be considered as a satisfactory lower limit for balancing improvements. At the system critical speeds, or at speeds corresponding to other rotor disturbances, the journal bearing clearance (0.0035 inch) shall be considered as an upper limit to rotor vibration amplitude.

For all test cases, the selection of the number of balancing planes, the number of data acquisition planes, and the number of balancing speeds shall be recorded. Any other options in the balancing program exercised in the course of the experimental test runs shall also be recorded.

APPENDIX B

CALIBRATION PROCEDURE

The following probes and instruments were subjected to calibration checks prior to test data acquisition:

a) proximity sensors (4)
b) Wayne-Kerr amplifiers for above sensors (4)
c) Tracking Analyzer (Model 235DS - Vibration Instrument Company)
d) Phase Meter (Model 933A - Vibration Instrument Company)
e) X-Y plotter.

The proximity sensors were calibrated in a bench fixture consisting of a probe hold-down clamp and a flat steel disk mounted on a micrometer stem. Beginning with an initial position where the sensor tip is in close contact with the steel disk, the micrometer was used to move the disk away from the probe. The incremental changes in output voltage indicated by a Wayne-Kerr amplifier connected to the sensor were recorded as a function of micrometer travel. The relationship of distance between sensor tip and steel surface versus output voltage was plotted and a "best-fit" straight line drawn through the data points. Typically, a capacitance-type sensor with a range of 0.010 inch (1 volt output for a probe-to-surface distance of 0.010 inch) may have maximum deviation of approximately 2 percent from the linear straight line near the ends of the specified distance range.

The linearized voltage-distance relationship was determined for each probe and subsequently utilized as input constants for the Exact Point-Speed Balancing Computer Program.

The following four calibration values were determined for the probes:

Probe No.	Calibration Constant (Mils/Vrms)
1	30.2
2	29.7
3	30.7
4	31.4

The Wayne-Kerr amplifiers were calibrated prior to the experiments by the manufacturers representative (MTI). A daily check of these meters required only a bias adjustment to reset the meter output to one volt.

The Tracking Analyzer (235 DS) was received as a new and calibrated piece of equipment just prior to the balancing tests. Daily bias adjustments were made for the amplitude read-out and for the phase angle between the two channels. The phase adjustment was accomplished by feeding a common oscillator signal to both channels and comparing the phase angle of the output signals in the phase meter. The bias was adjusted, as required, to bring the phase difference to zero.

The Phase Meter (933 A) was adjusted for zero phase distortion between reference input and signal input with the same signal fed into both inputs. The adjustment of the phase meter preceded, of course, the phase adjustment of the Tracking Analyzer.

A valuable check on the proper interpretation of the polarity and magnitude of the phase angle indicated by the phase meter was obtained by displaying the appropriate output signals from the Tracking Analyzer on an oscilloscope screen. In this manner phase angles may be determined for checking purposes within 5 degrees of the values indicated by the phase meter.

The X-Y plotter was calibrated in frequency for all amplitudes by using an oscillator to drive the tracking analyzer. During regular data plotting operations, amplitudes were continually spot-checked by readings and corresponding hand notations from the analyzer amplitude meter.

No estimate is available on the overall dynamic accuracy of the instrumentation system used in this experiment. However, certain limitations in the instrumentation were recognized. For instance, the Phase Meter has a stated minimum signal input requirement of 2.5 millivolts rms. This corresponds to approximately 0.000075-inch peak-to-peak rotor amplitude, when measured with capacitance probes having a 0.010-inch linear range. If rotors with less initial amplitude due to unbalance are to be balanced, either shorter range probes or pre-amplifiers would have to be used.

The filter bandwidth selected in the Tracking Analyzer will also affect the accuracy of the phase angle measurement, although only slightly. In general, a decreasing filter bandwidth and decreasing signal amplitude will cause a slight deterioration in the phase angle measurement accuracy. At the 50 cycle bandwidth setting (which was used for all experiments) the maximum phase angle deviation did not exceed 1^{o}. For the 5 cycle bandwidth setting, deviations of +0.5 to -3.0 degrees have been recorded for the input voltage range of 100 to 2.5 millivolts rms.

APPENDIX C

BALANCING PROCEDURE

The procedure for conducting a balancing test run was as follows:

1) The unbalanced test rotor was slowly, but continuously run up in speed until rotor deflections reached values which were not to be exceeded for safety or operational reasons. For the test rotor, the maximum allowable deflection had been arbitrarily set as 0.0035 to 0.005 inch (0.089 to 0.127 mm) peak-to-peak. For several locations on the rotor, vertical amplitudes were recorded on magnetic tape for the complete run.

2) Rotor amplitudes and phase angles as functions of rotor speed were plotted from magnetic tape by an X-Y plotter. From these plots, suitable balancing speeds were selected.

3) A suitable trial weight was placed at the reference location on the rotor in the first balancing plane. The rotor was then run up in speed to the first pre-selected balancing speed. At that speed, vertical rotor amplitudes were recorded on tape. If the rotor was to be balanced at two speeds, it was then brought to the second pre-selected balancing speed and again the vertical rotor amplitudes were recorded on magnetic tape.

4) The above process (described in (3)) was then repeated with the trial weight placed in each of the remaining balancing planes.

5) Steps (3) and (4) were then repeated with the trial weight placed 180^{o} from the previous locations, but in the same axial planes.

6) From magnetic tape, amplitudes and phase angle readings were obtained from the Tracking Analyzer (235 DS) and the Phase Meter (933 A) respectively.

7) The tabulated data was read into the computer (time sharing terminal) for correction weight calculations.

8) Steel set screws were filed to match the calculated correction weights, and located at the proper angles in the pre-drilled holes in the rotor disks.

9) With the correction weights in place, steps (1) and (2) were repeated. Through comparison of the original and the balanced rotor amplitudes, the effectiveness of the balancing effort was determined.

The whole procedure was then repeated until satisfactory rotor balance was obtained.

APPENDIX D

TYPICAL BALANCING DATA FOR A SELECTED CASE

Date of Test: 7-14-70

Trial Weight Run: Test Case III, Run 3

Rotor Balancing Speed: 10800 ± 10 rpm

Measuring Station	Rotor Amplitude (mV rms)	Phase Angle	Trial Weight oz-in	Trial Weight Location
1	.028	+ 108	None	
2	.025	- 72	None	
3	.020	- 79	None	
4	.022	+ 108 ± 6	None	
1	.190	+ 86	.0723	Plane 1 at 0°
2	.160	- 92	.0723	
3	.100	- 93	.0723	
4	.170	+ 87	.0723	
1	.120	- 101	.0723	Plane 1 at 180°
2	.120	+ 77	.0723	
3	.065	+ 75	.0723	
4	.160	- 98	.0723	
1	.100	- 104	.0723	Plane 2 at 0°
2	.090	+ 67	.0723	
3	.044	+ 61	.0723	
4	.100	- 103	.0723	
1	.100	+ 86	.0723	Plane 2 at 180°
2	.100	- 98	.0723	
3	.070	- 98	.0723	
4	.120	+ 89	.0723	
1	.086	- 103	.0723	Plane 3 at 0°
2	.090	+ 66	.0723	
3	.040	+ 63	.0723	
4	.092	- 102	.0723	
1	.120	+ 85	.0723	Plane 3 at 180°
2	.110	- 98	.0723	
3	.068	- 97	.0723	
4	.120	+ 84	.0723	

Measuring Station	Rotor Amplitude (mV rms)	Phase Angle	Trial Weight oz-in	Trial Weight Location
1	.160	+ 81	.0723	Plane 4 at 0°
2	.150	- 96	.0723	
3	.096	- 94	.0723	
4	.160	+ 82	.0723	
1	.140	- 100	.0723	Plane 4 at 180°
2	.120	+ 73	.0723	
3	.068	+ 74	.0723	
4	.130	- 105	.0723	

APPENDIX E

CALCULATED CORRECTION WEIGHTS FOR TEST BALANCING RUNS

Test Case	Calculation No.	Balancing Plane	Correction Weight oz-in	Correction Weight gm-cm	Correction Weight Angle (Degrees)
I	2	1	.1630	11.7375	1.3
		2	.6265	45.1136	196.5
		3	.6435	46.3378	15.5
		4	.1130	8.1370	202.1
	3	1	.0385	2.7723	57.9
		2	.0455	3.2764	350.4
		4	.0456	3.2836	335.9
	10	1	.0120	0.8641	252.8
		2	.0144	1.0369	21.5
		3	.0244	1.7570	212.3
		4	.0141	1.0153	184.8
	15	1	.0013	0.0936	245.8
		2	.0173	1.2458	47.8
		4	.0038	0.2736	7.1
II	16	1	.0496	3.5716	206.3
		2	1.8859	135.8017	190.0
		3	1.2431	89.5144	9.8
		4	.4008	28.8612	176.3
	18	1	.2402	17.2966	184.2
		3	.6816	49.0813	187.6
		4	.2075	14.6538	185.2
	20	1	.0370	2.6643	241.2
		2	.1481	10.6645	246.3
		3	.0704	5.0694	125.4
		4	.1107	7.9714	225.8
	21	1	.0754	5.4295	149.4
		3	.0976	7.0281	132.2
		4	.0468	3.3700	68.5
	22	1	.1410	10.1533	337.6
		2	.8360	60.1995	185.3
		3	.8751	63.0151	4.8
		4	.1484	10.6861	135.1

Test Case	Calculation No.	Balancing Plane	Correction Weight oz-in	Correction Weight gm-cm	Correction Weight Angle (Degrees)
	23	1	.0368	2.6499	190.8
		3	.0385	2.7723	238.7
		4	.0297	2.1387	31.1
III	24	1	.1213	8.7374	211.5
		2	.7542	54.3092	227.8
		3	1.2732	91.6819	32.2
		4	.3440	34.7711	187.2
	25	1	.2125	15.3019	204.6
		3	.5576	40.1522	7.1
		4	.2794	20.1193	184.8
	26	1	.0184	1.3250	276.5
		2	.3616	26.0385	219.3
		3	.3400	24.4831	48.5
		4	.0546	3.9317	199.1
	27	1	.0461	3.3196	219.0
		3	.0275	1.9802	152.3
		4	.0213	1.5338	323.2
	28	1	.0178	1.2818	353.7
		3	.0085	.6121	150.1
		4	.0355	2.5563	183.6
	29	1	.0385	2.7723	348.9
		2	.0471	3.3916	2.6
		3	.0484	3.4852	166.9
		4	.0534	3.8453	171.2

NOMENCLATURE

A,B	Specified rotor locations	
A_p	Rotor cross-sectional area	$in.^2$
N	Number of balancing speeds	
T	Trial unbalance moment	oz.-in.
U_p	Unbalance moment in plane p	oz.-in.
i	$\sqrt{-1}$	
ℓ_p	Length of rotor element	in.
m	Number of measurement stations	
n	Number of balancing planes	
p	Balancing plane	
t	Time	sec.
v	Number of displacement readings	
$\overline{w}$	Unbalance eccentricity	in.
w_c	Cosine component of rotor amplitude in rotating coordinates	in.
w_s	Sine component of rotor amplitude in rotating coordinates	in.
w_F	Rotor amplitude in fixed coordinates	in.
w_R	Rotor amplitude in rotating coordinates	in.
x,y	Fixed coordinate system axes	
z	Distance along rotor	in.
α_{jp}	Influence coefficients	
ξ,η	Rotating coordinate system axes	
ρ_p	Rotor weight density	$lb/in.^3$
ω	Rotor angular velocity	rad/sec.

FIGURES

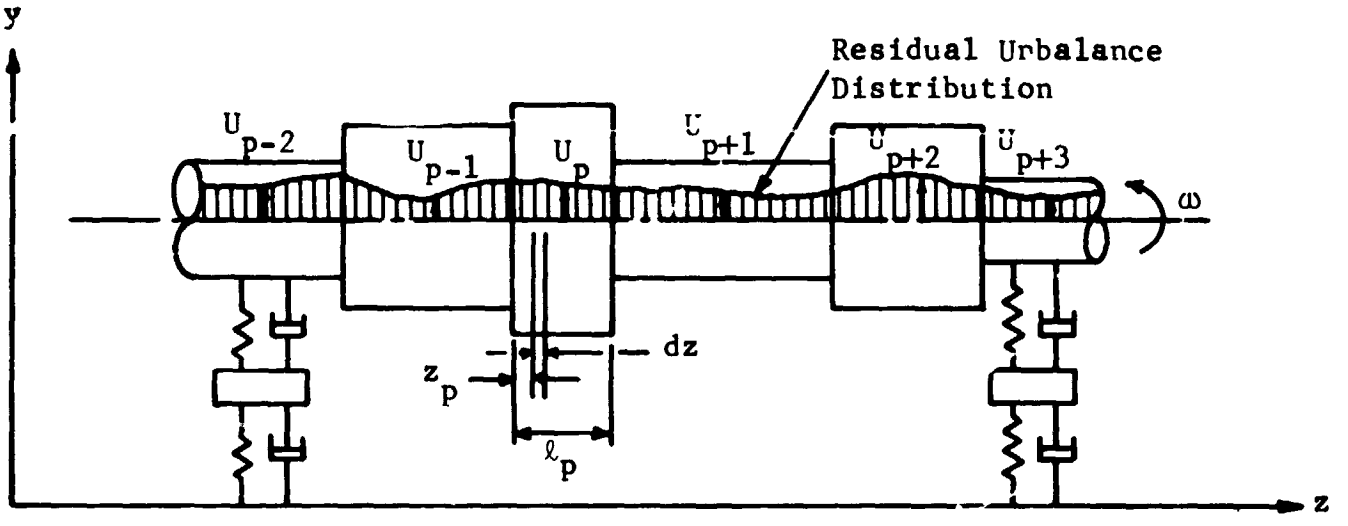

Fig. 1 Distribution of Residual Unbalance in a Generalized Rotor

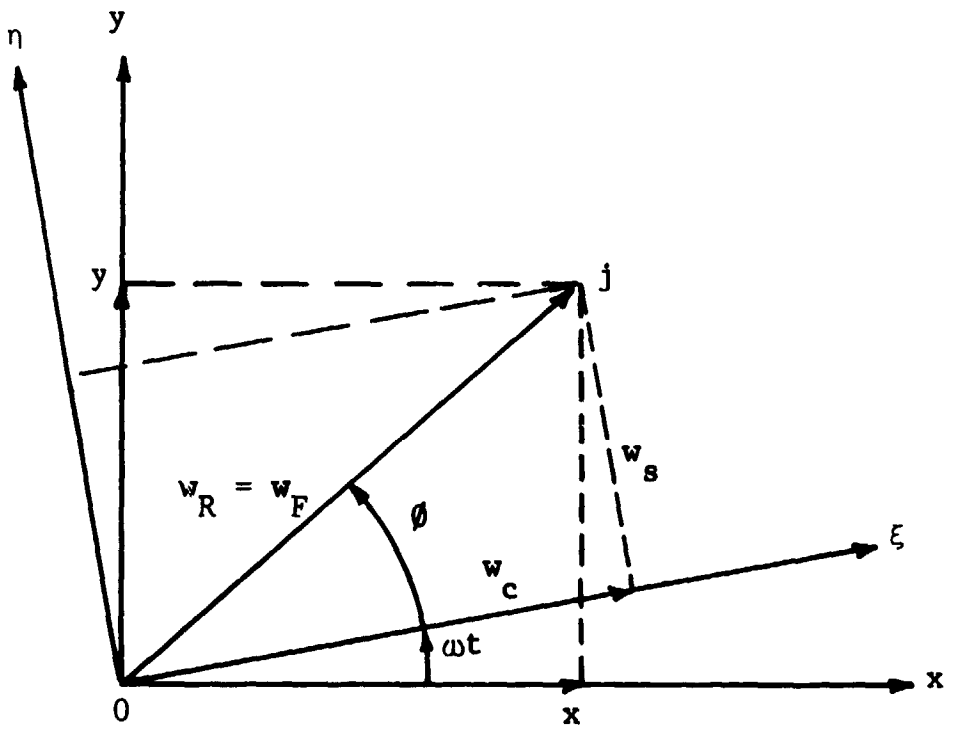

Fig. 2 Fixed (x,y) and Rotating (ξ,η) Coordinate Systems

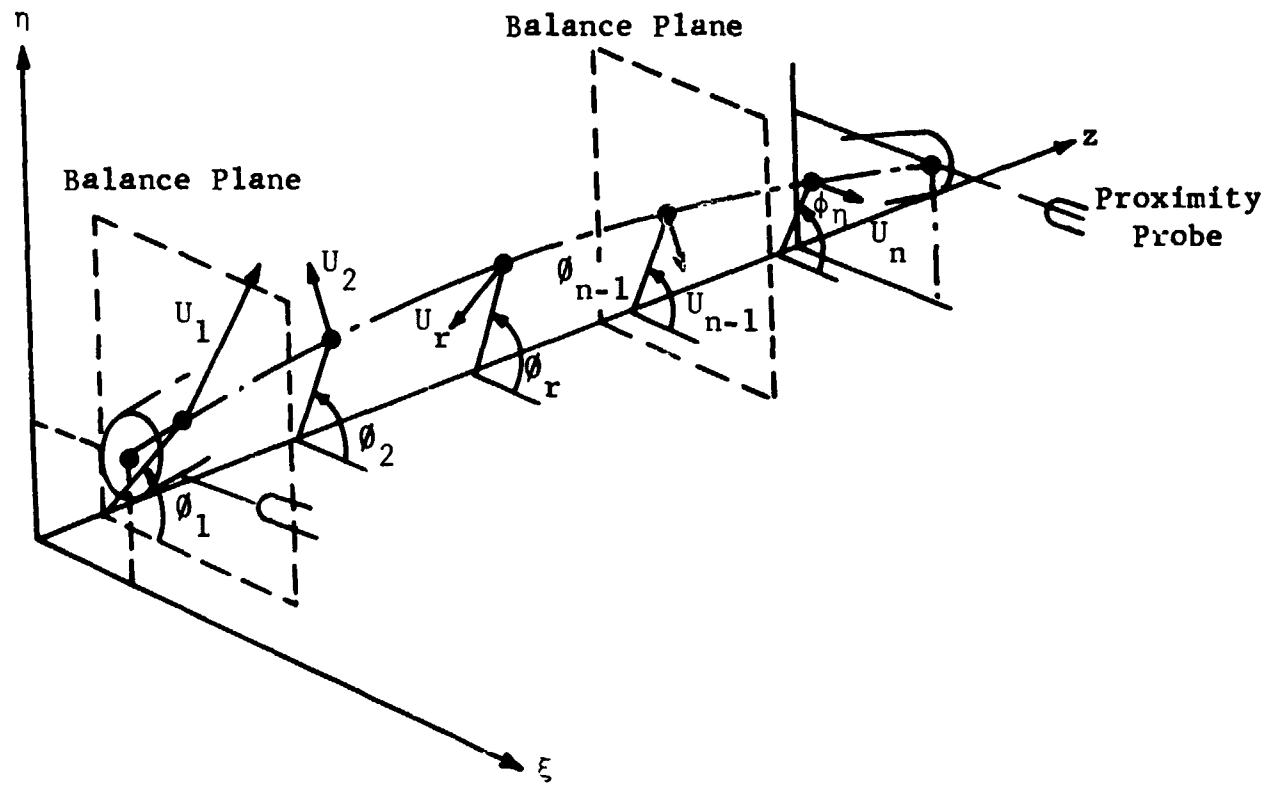

Fig. 3 Approximation of Axially-Distributed Rotor Unbalance by n Discrete Unbalance Moments

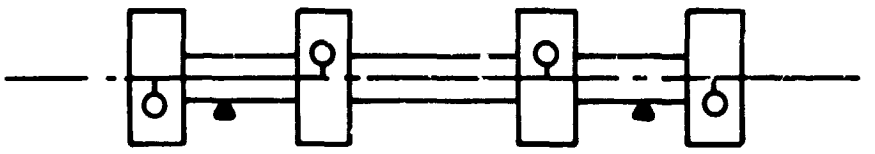

(a) Flexible four-disk rotor

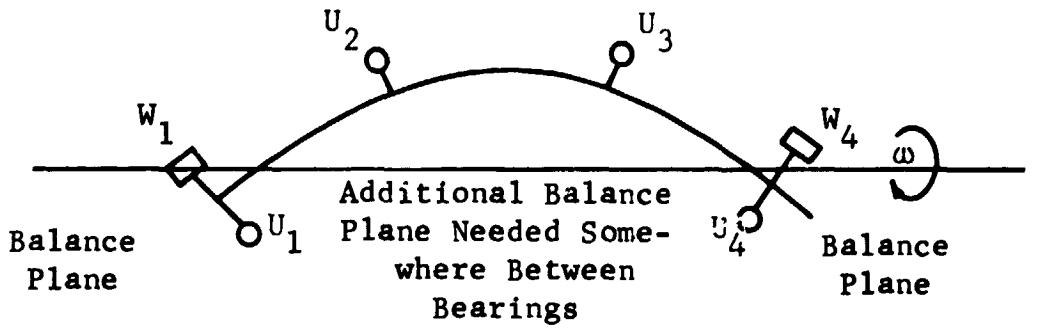

(b) Inadequacy of two balance planes for balancing near the first flexural critical speed

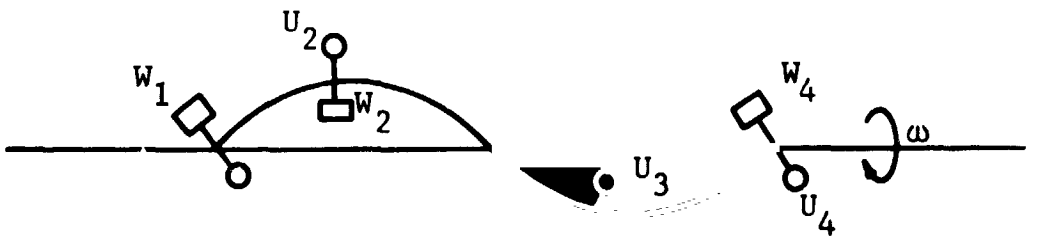

(c) Inadequacy of three balance planes for balancing near the second flexural critical speed

Fig. 4 Dependence of Balancing Effectiveness on the Number of Balancing Planes Used

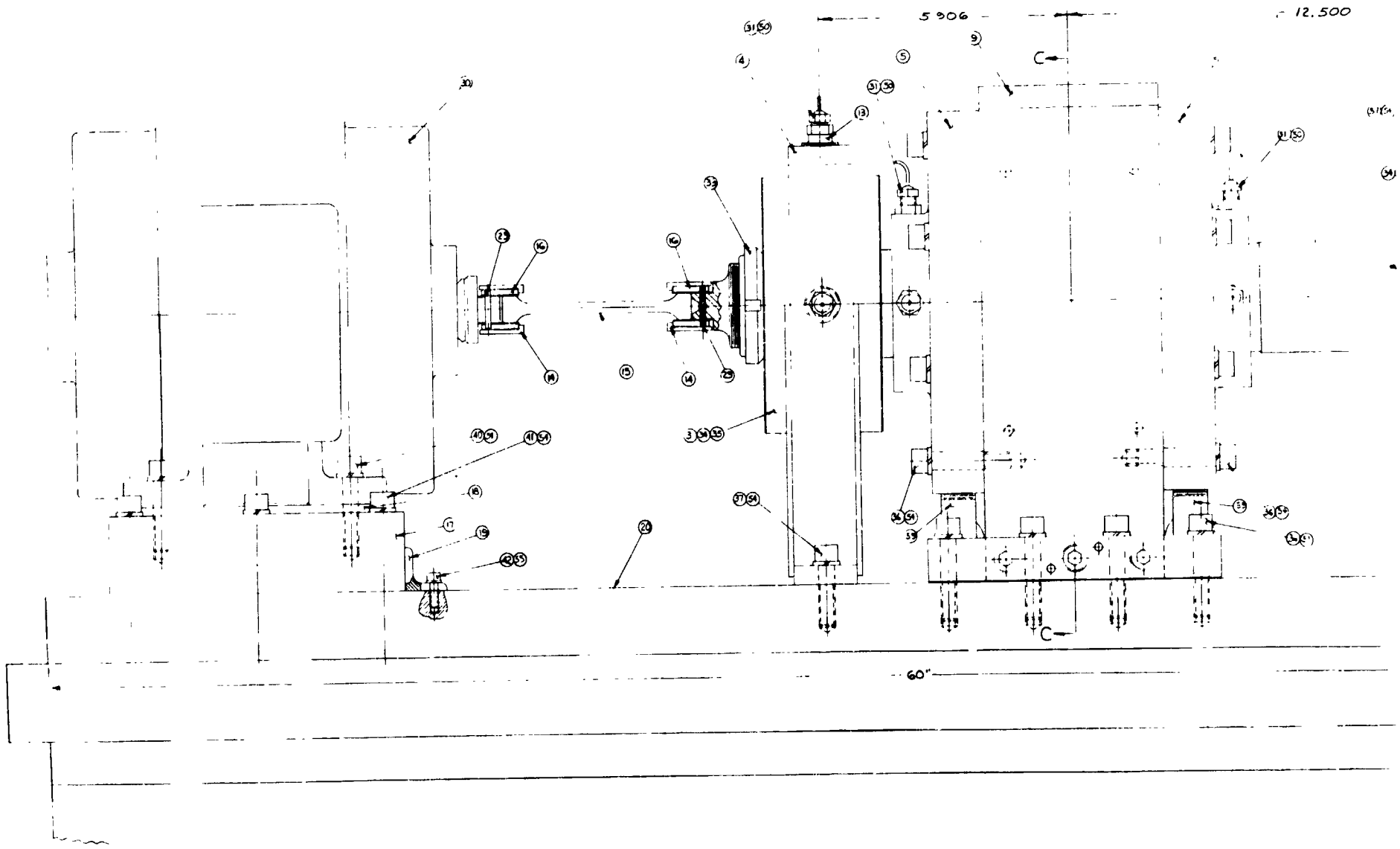

Fig. 5 Assembly Drawing of Flexibl

FOLDOUT FRAME 1

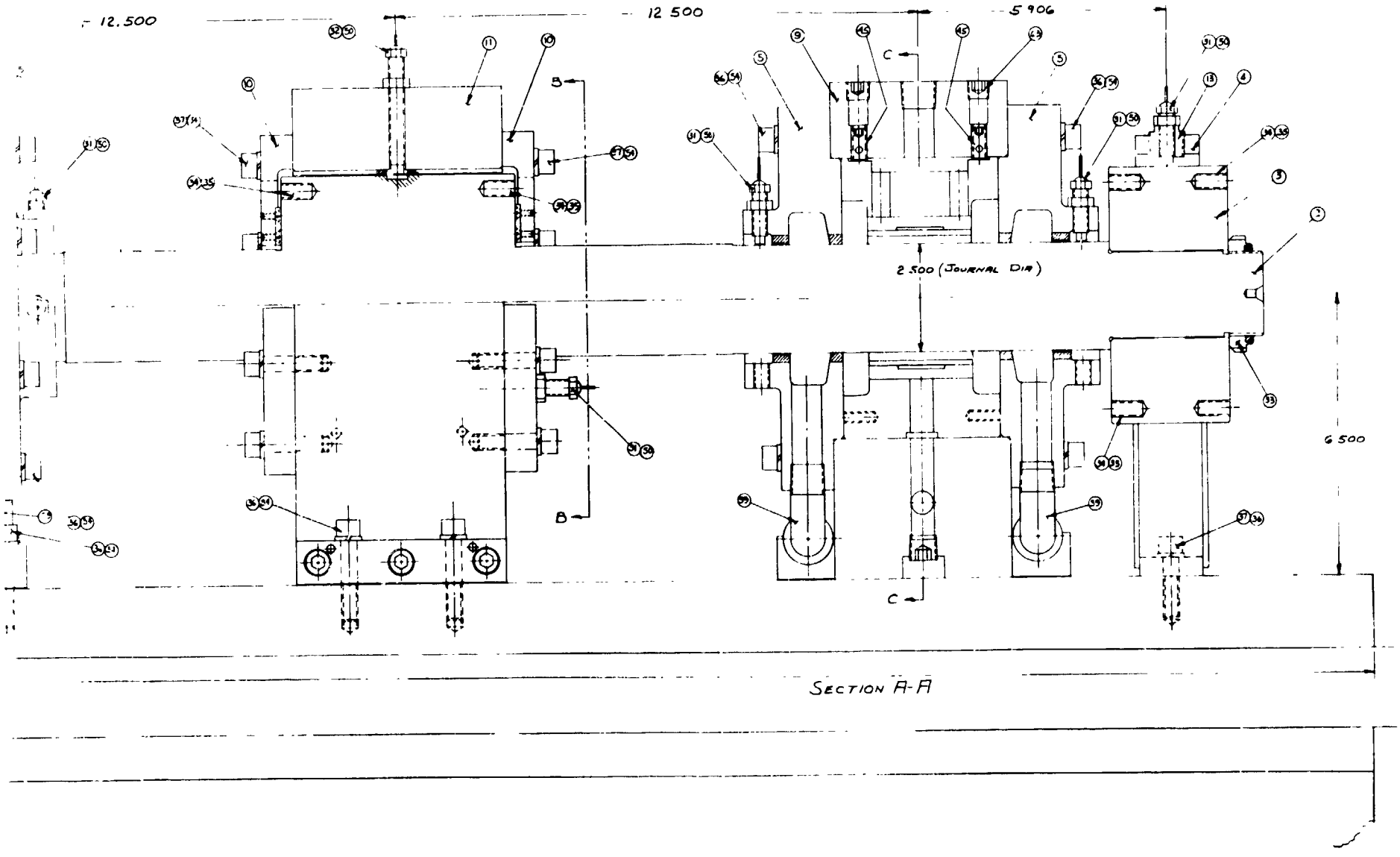

ing of Flexible-Rotor Test Rig

FOLDOUT FRAME 2

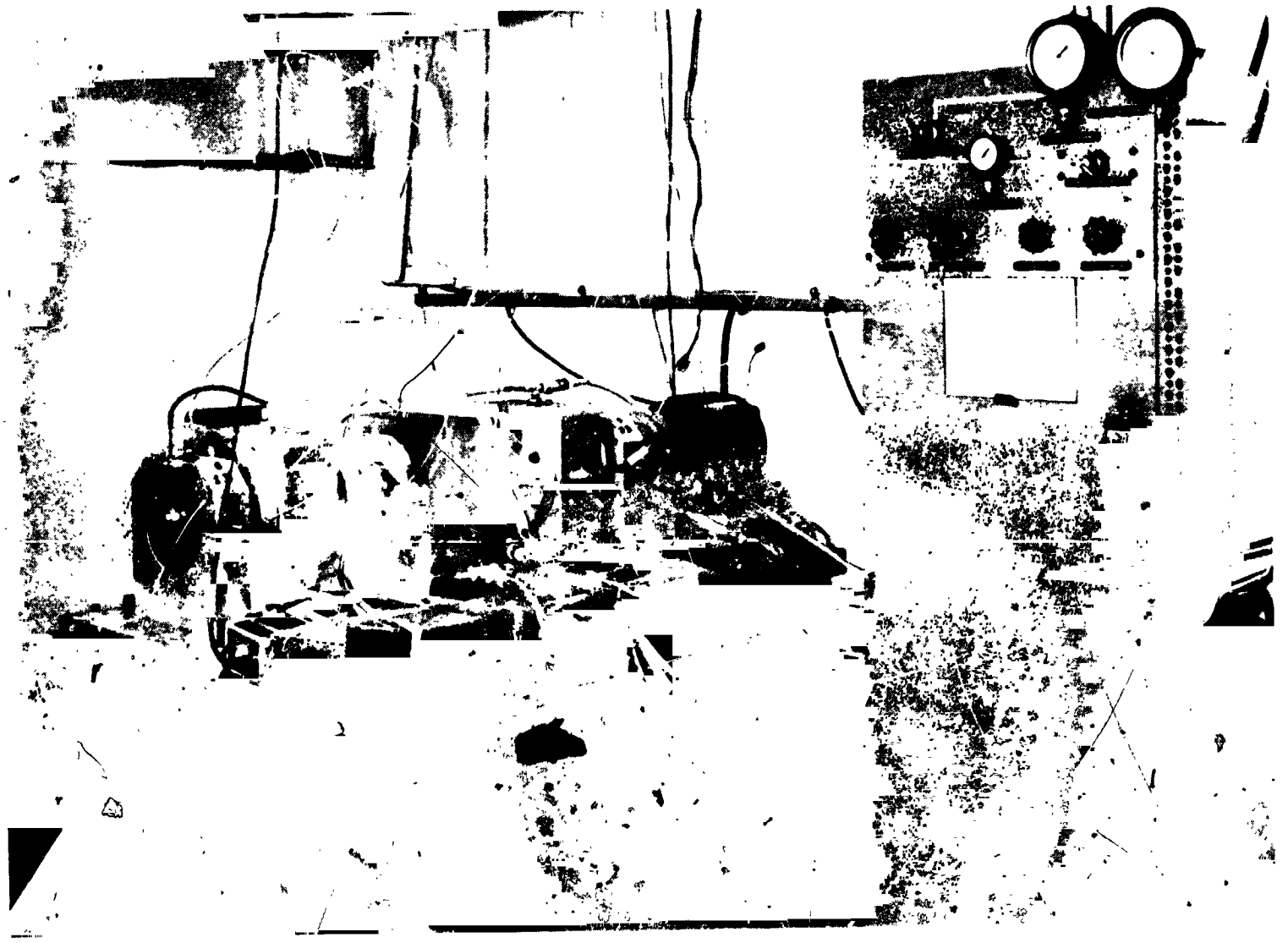

Fig. 6 View of Flexible-Rotor Test Rig

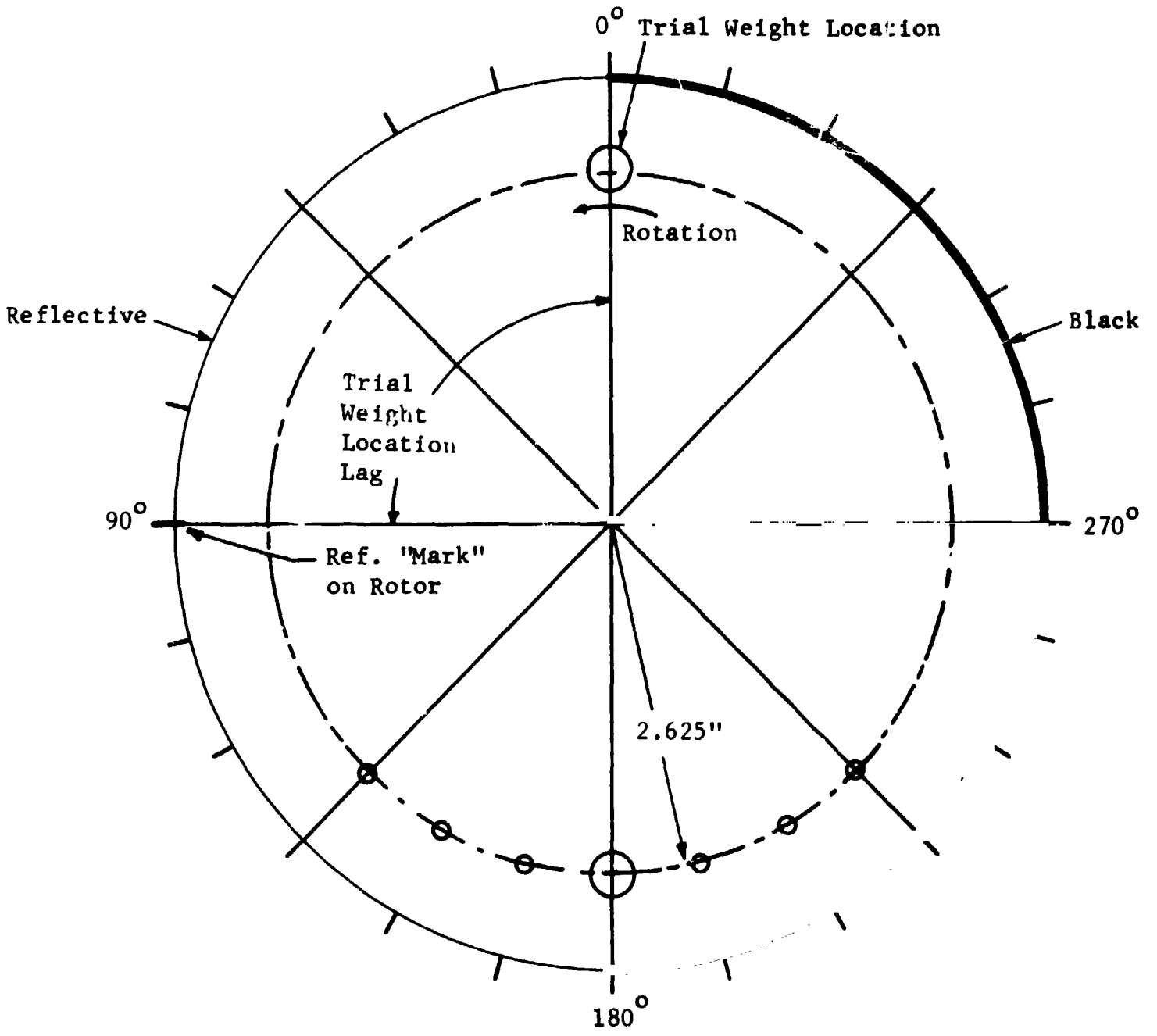

Fig. 7 End View of Rotor End Mass (Opposite Drive End) with Reference Mark and Typical Holes for Balancing Weights

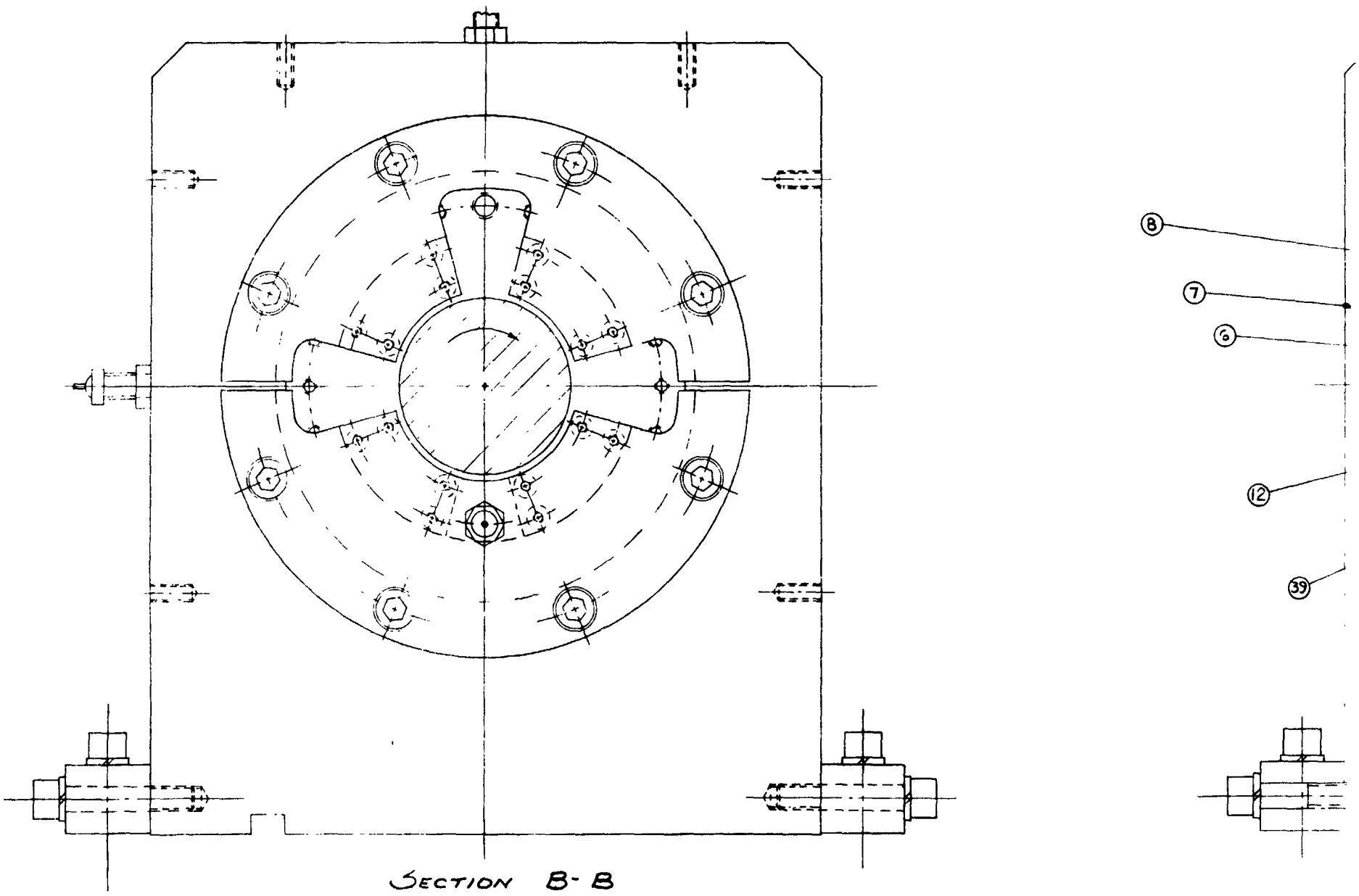

(See Figure 5)

Fig. 8 Bearing Assembly Drawing of Flexible Rotor

FOLDOUT FRAME |

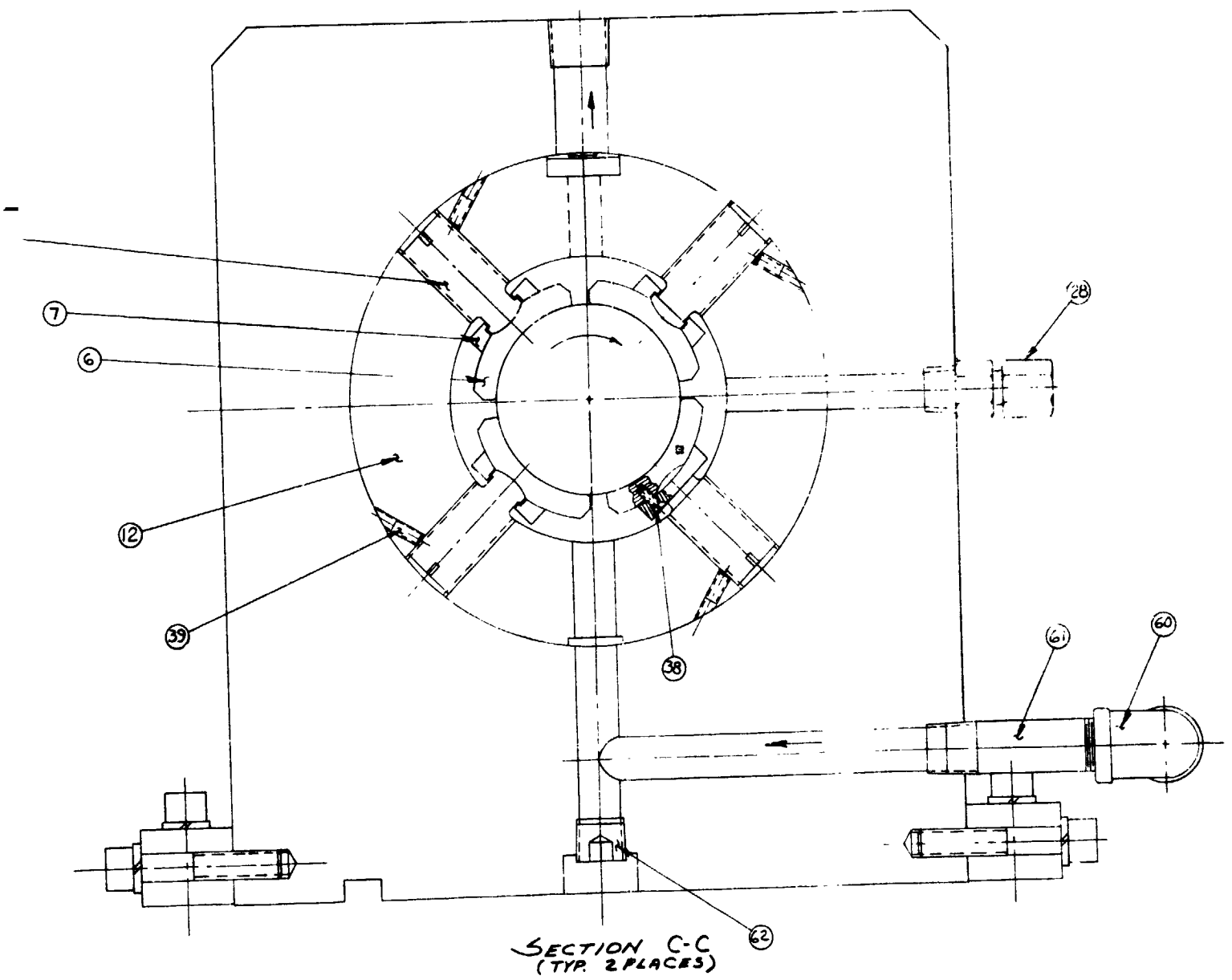

(See Figure 5)

Flexible Rotor Test Rig

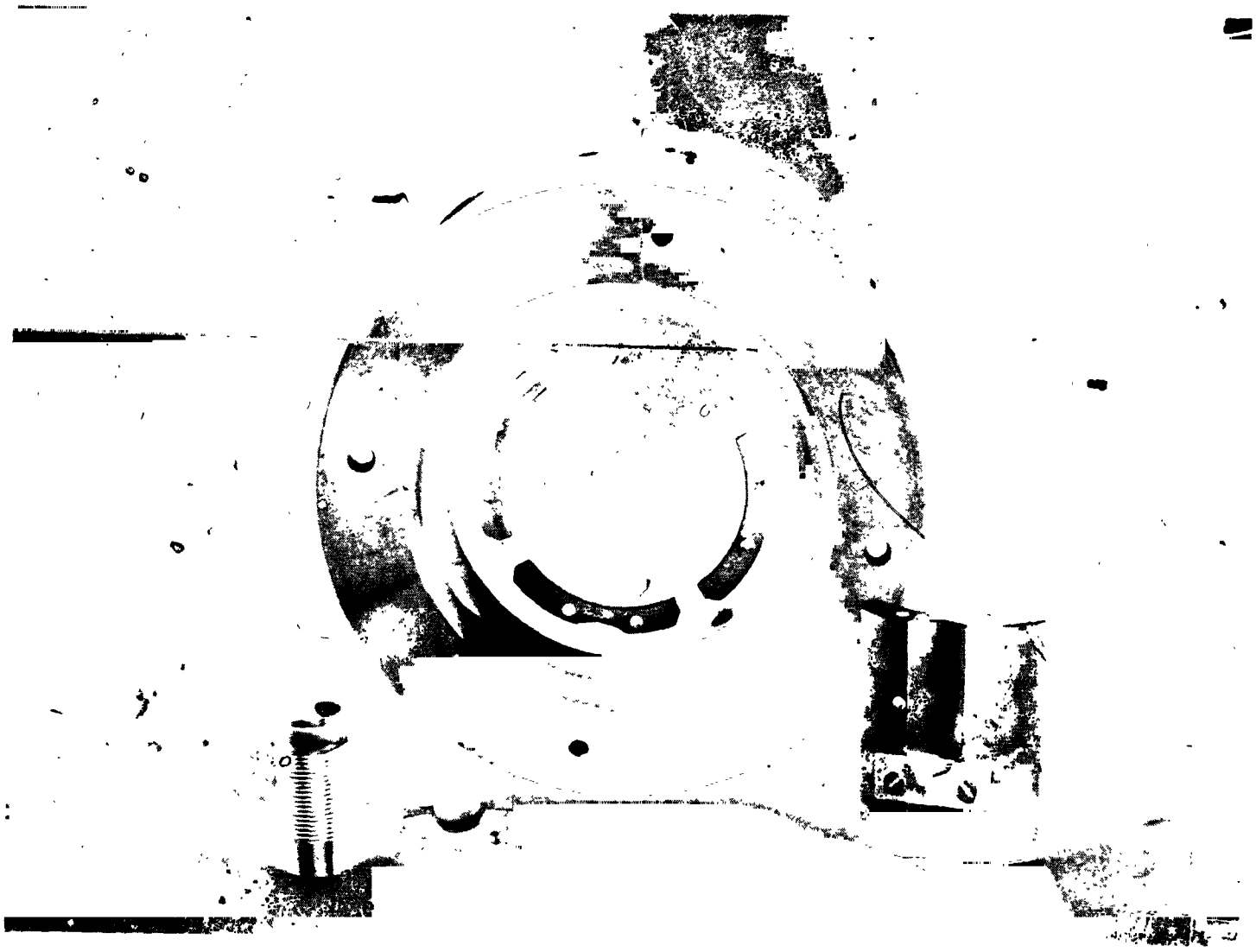

Fig. 9 Tilting Pad Journal Bearing for Test Rig Rotor

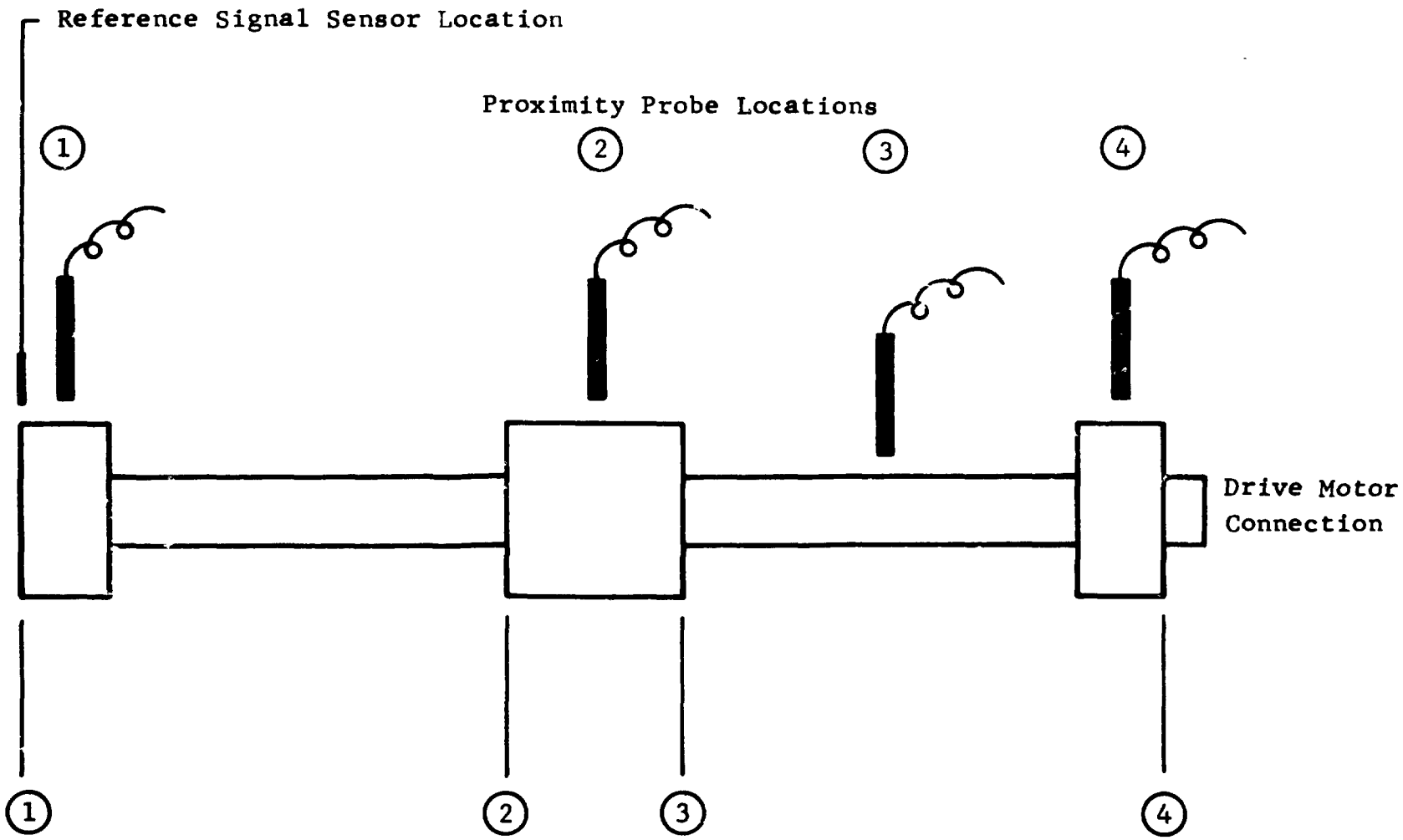

Fig. 10 Probe and Balancing Plane Locations Along Test Rotor

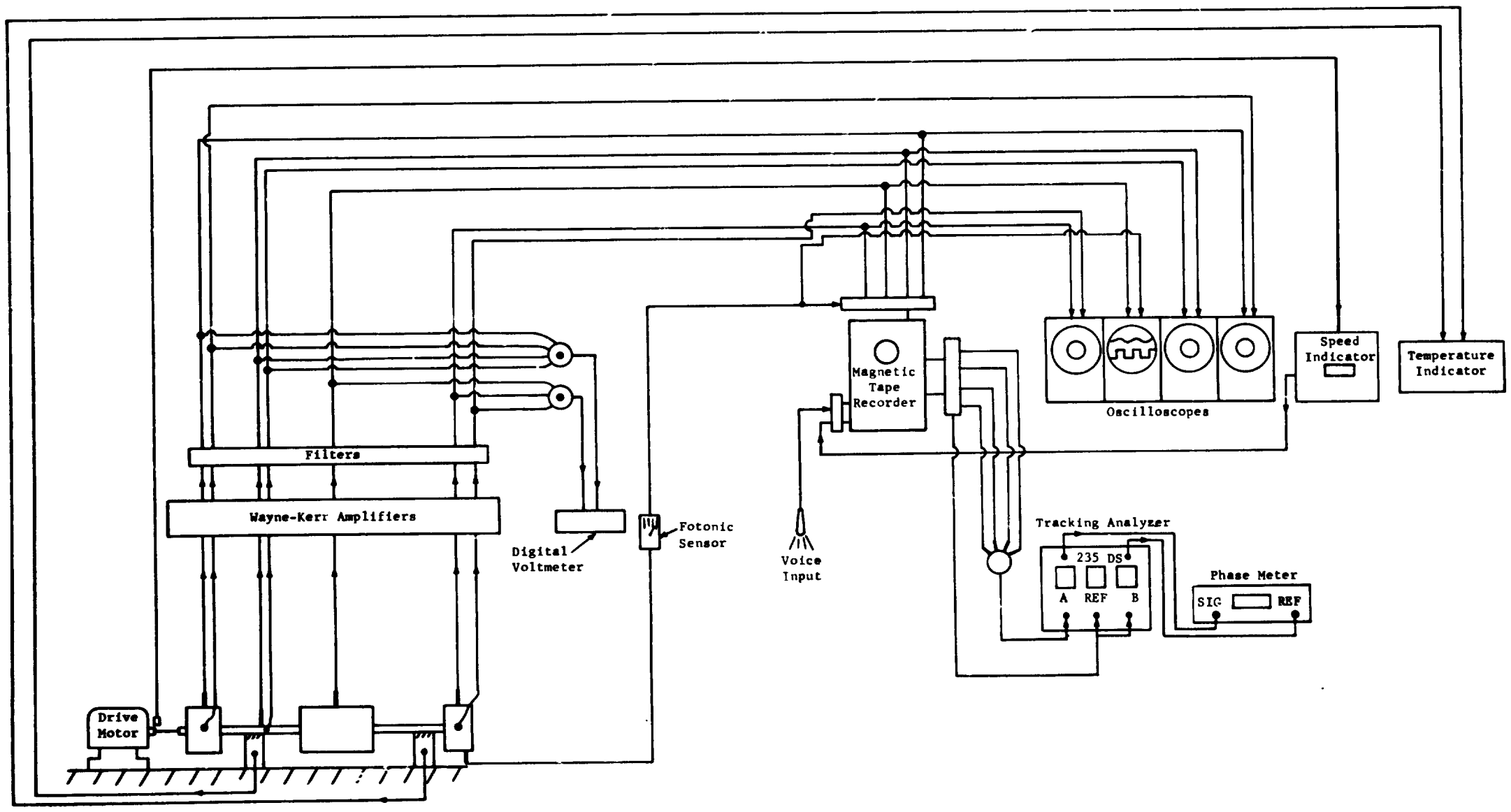

Fig. 11 Schematic of Flexible Rotor Balancing Instrumentation

MTI-9486

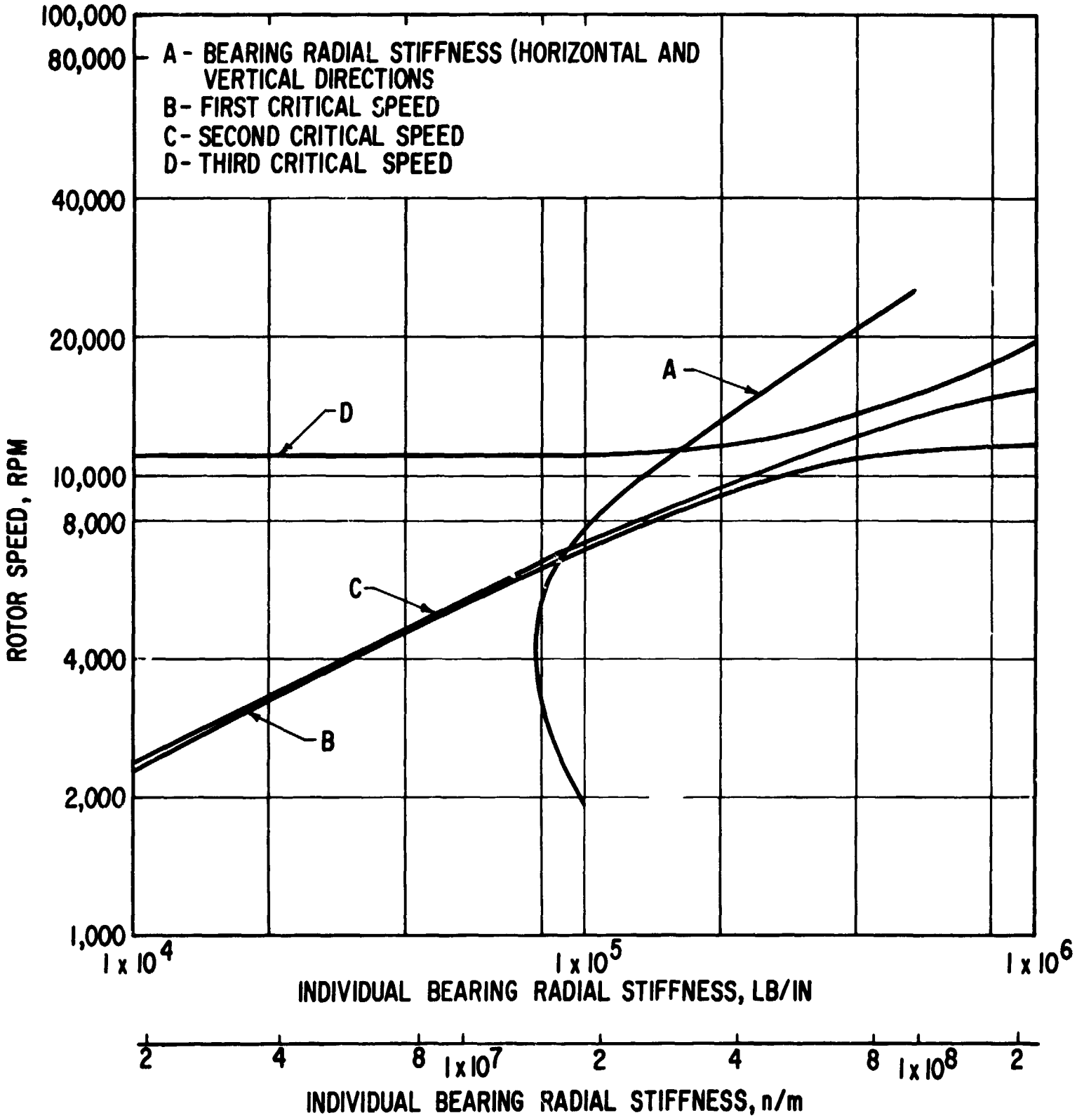

Fig. 12 Critical-Speed Map for Flexible-Rotor Test Rig

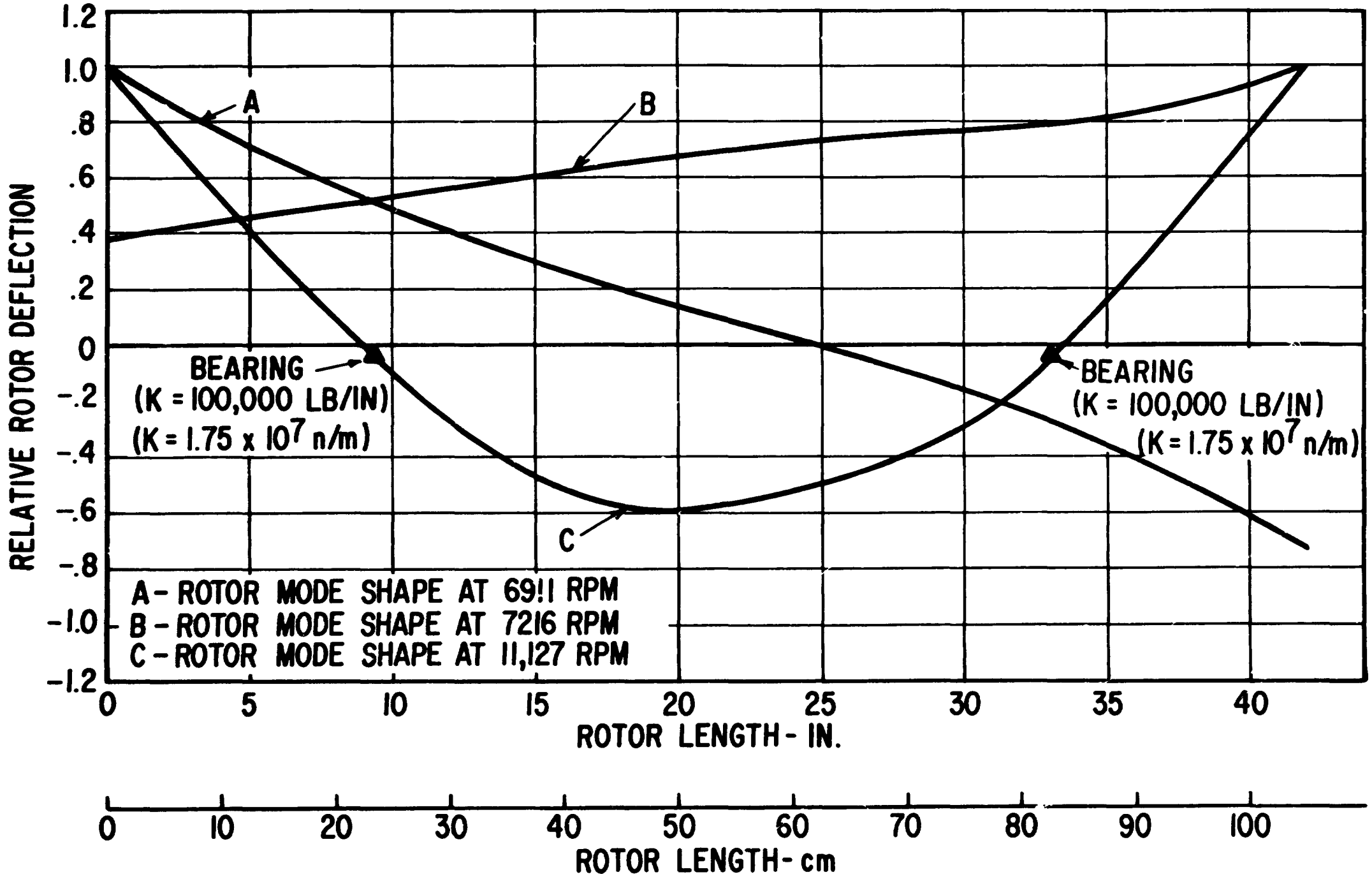

Fig. 13 Undamped Critical-Speed Mode Shapes for Flexible-Rotor Test Rig

MTI-9501

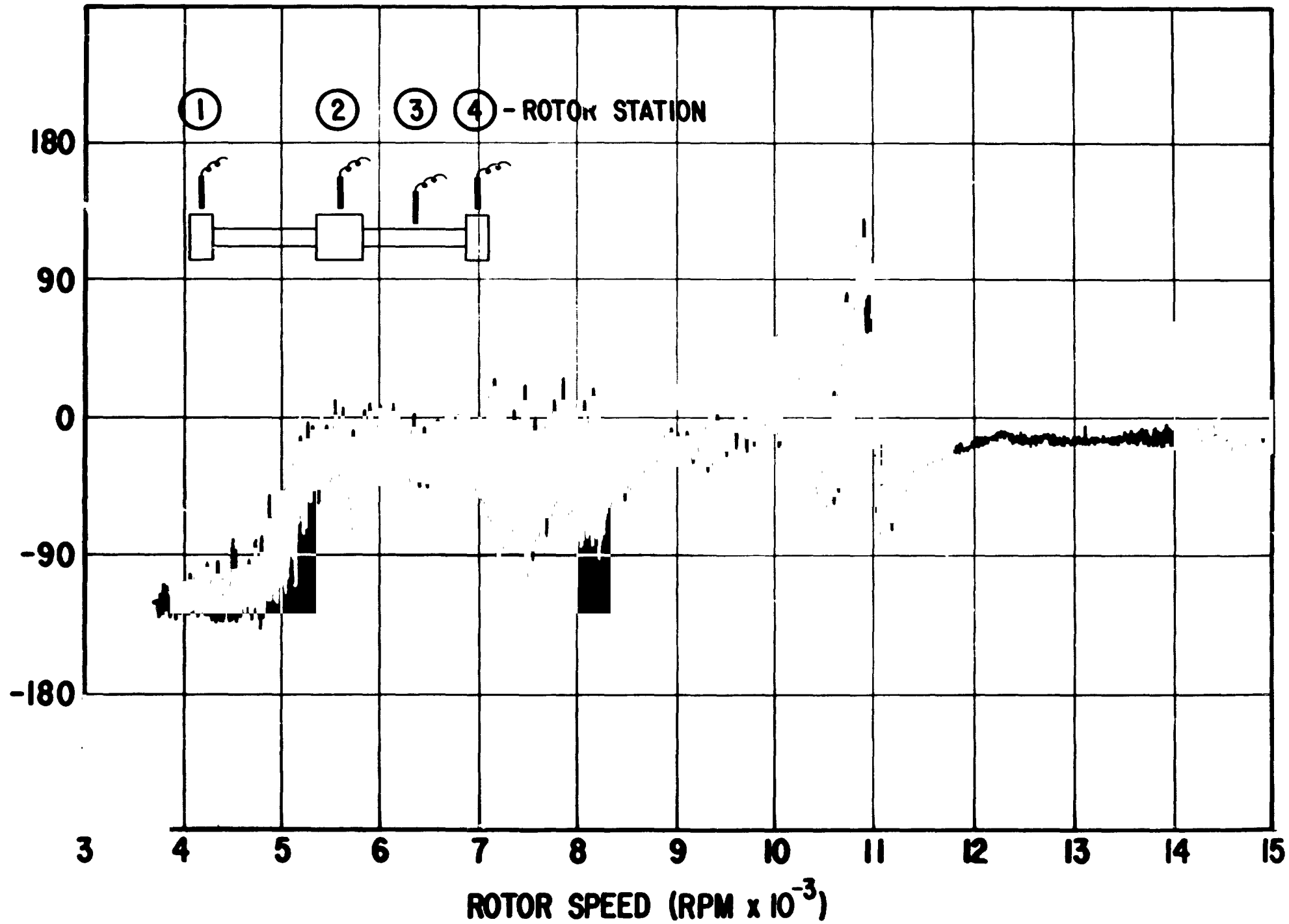

Fig. 14 Phase Angle Between Reference Signal and Maximum Dynamic Displacement at Rotor Station 1

MTI-9551

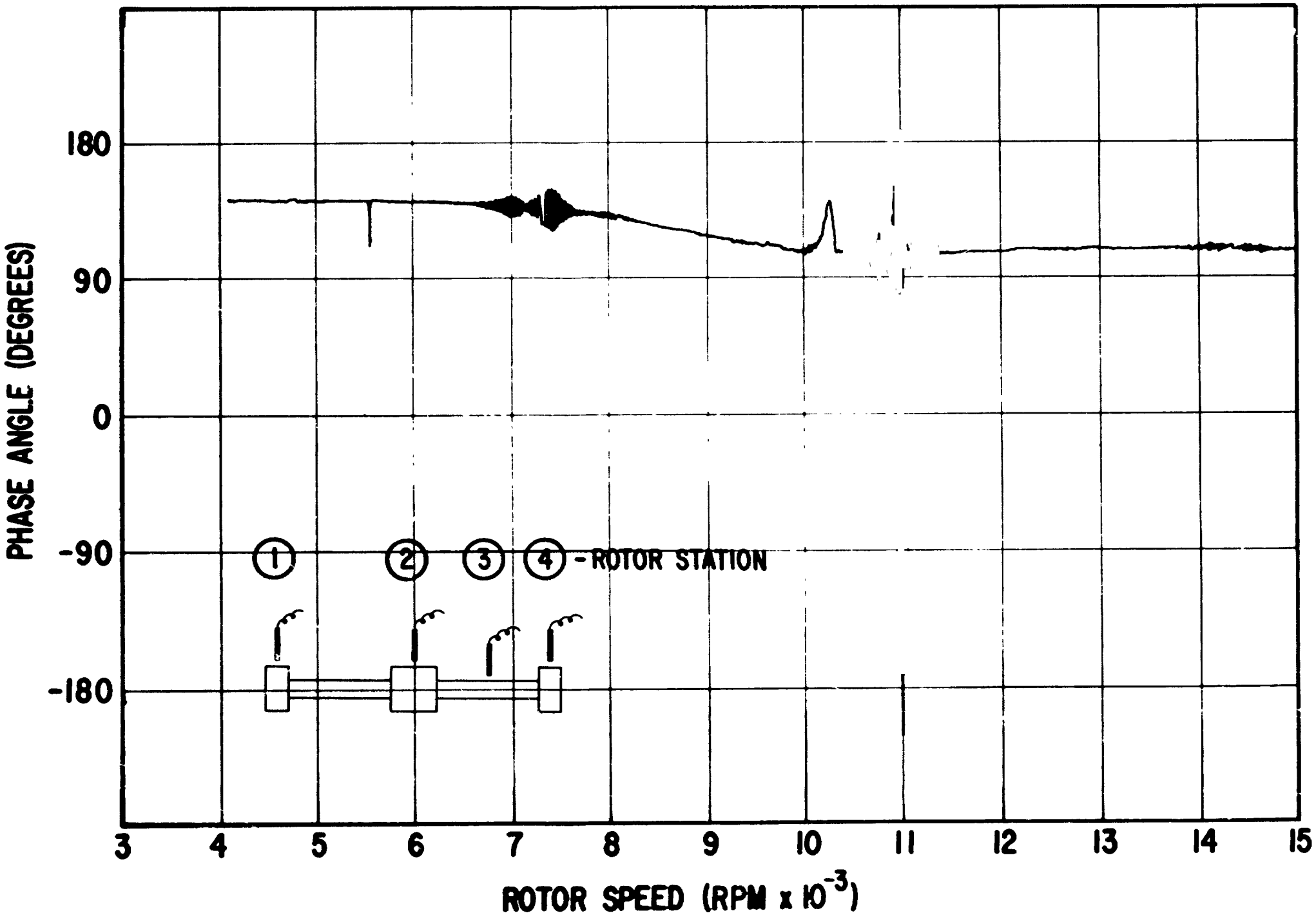

Fig. 15 Phase Angle Between Reference Signal and Maximum Dynamic Displacement at Rotor Station 2

MTI-9552

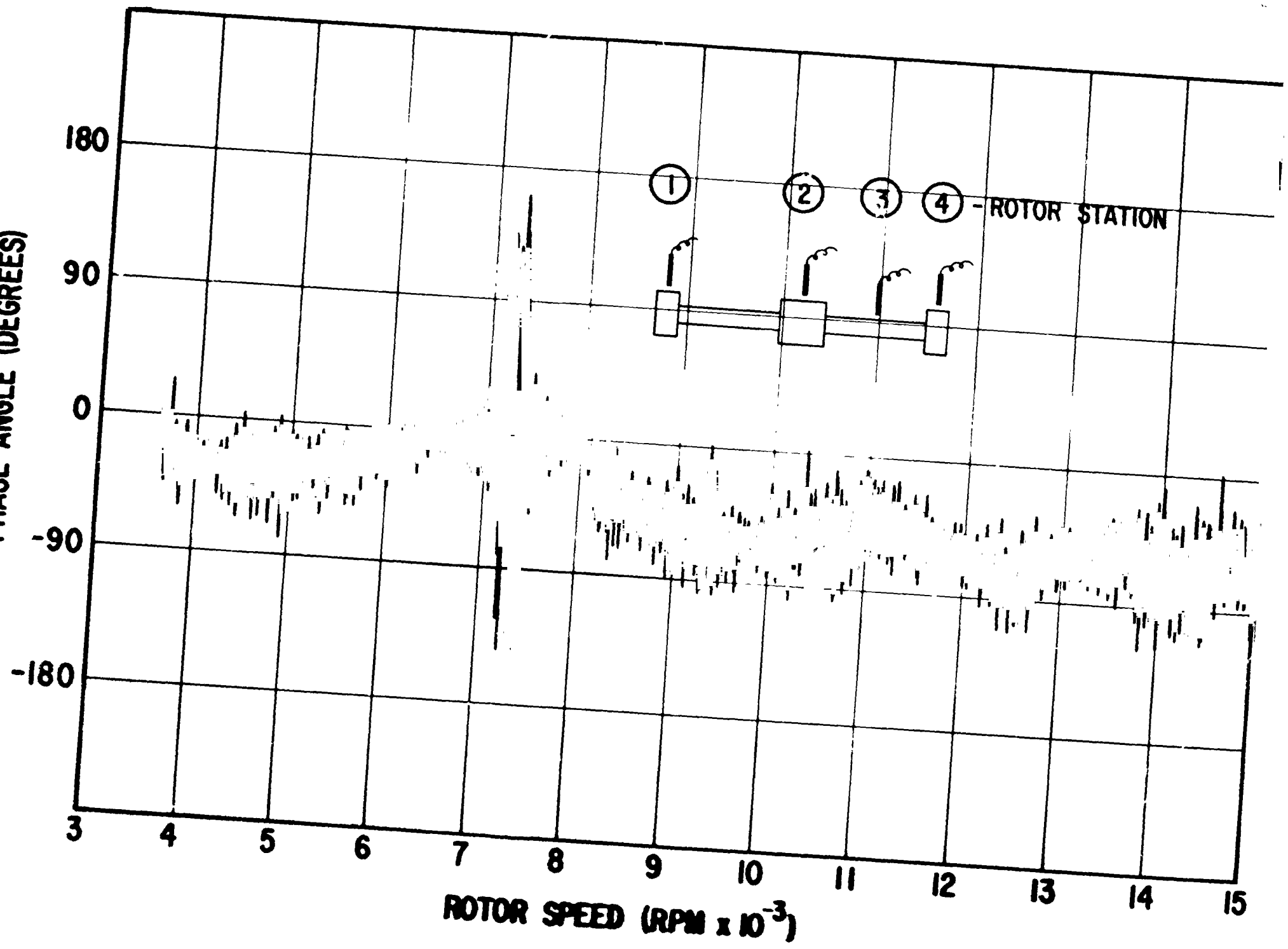

Fig. 16 Phase Angle Between Reference Signal and Maximum Dynamic Displacement at Rotor Station 3

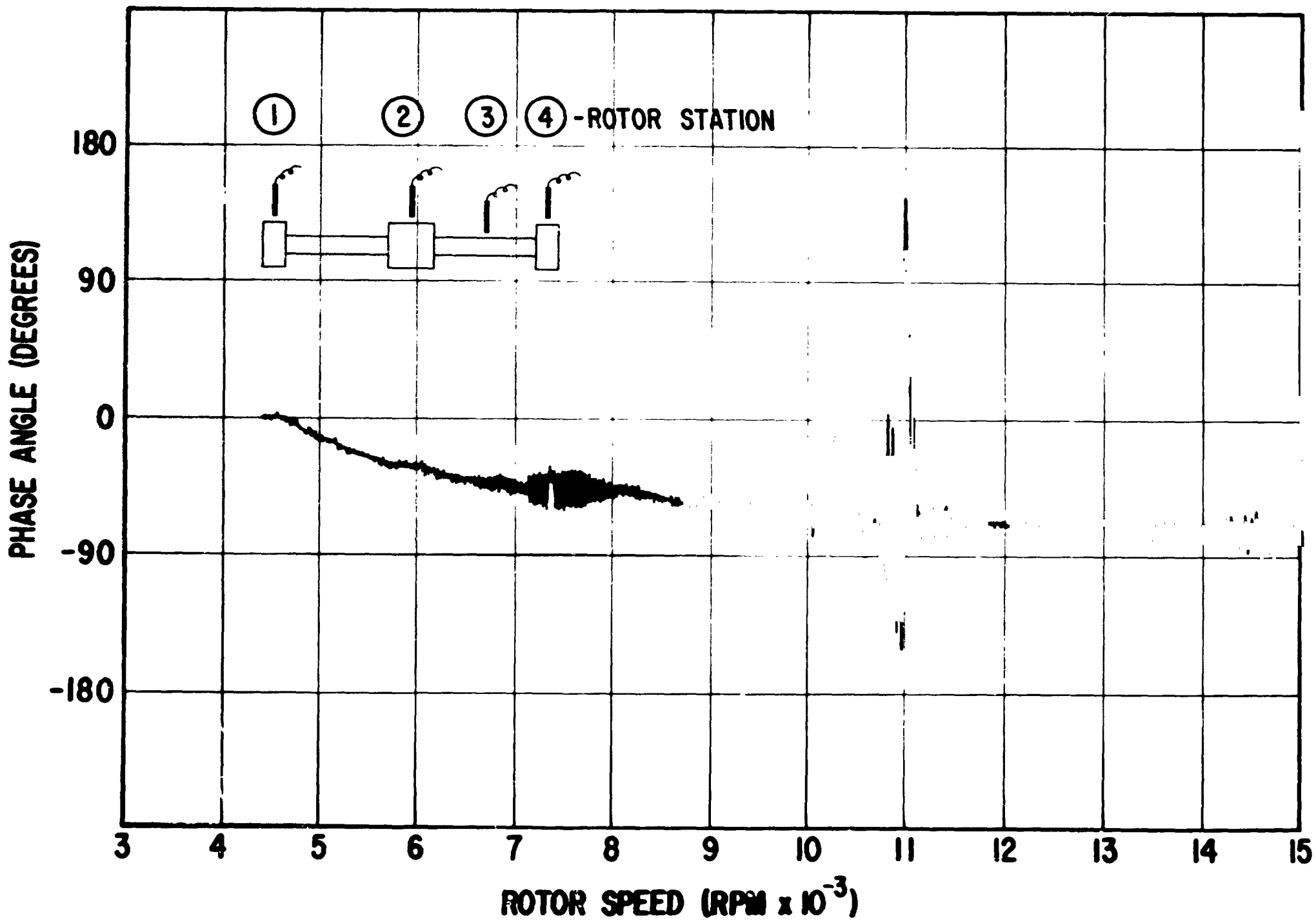

Fig. 17 Phase Angle Between Reference Signal and Maximum Dynamic Displacement at Rotor Station 4

MTI-9502

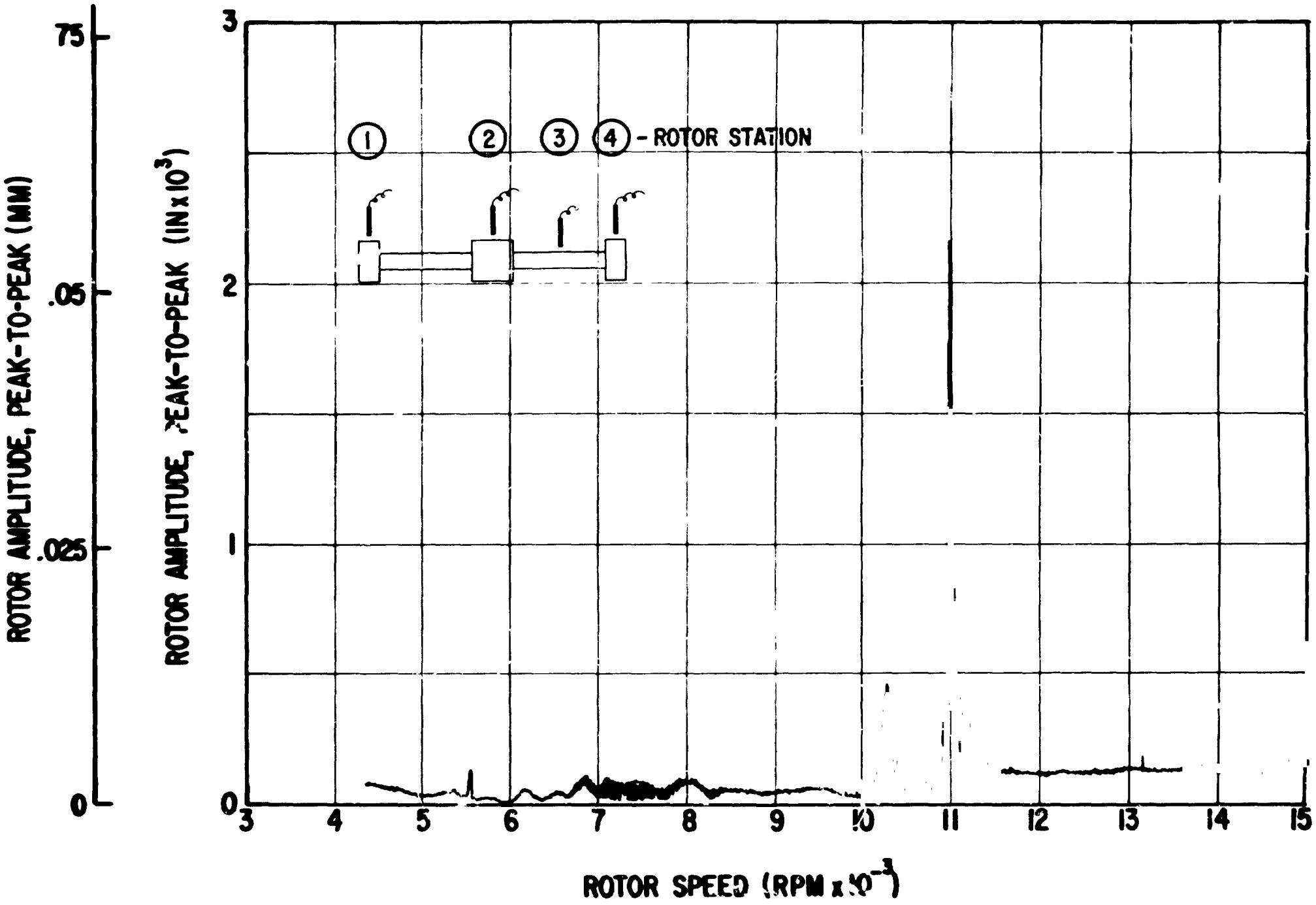

Fig. 18 Rotor Amplitudes at Station 1 at Conclusion of Test Case I

MTI-9549

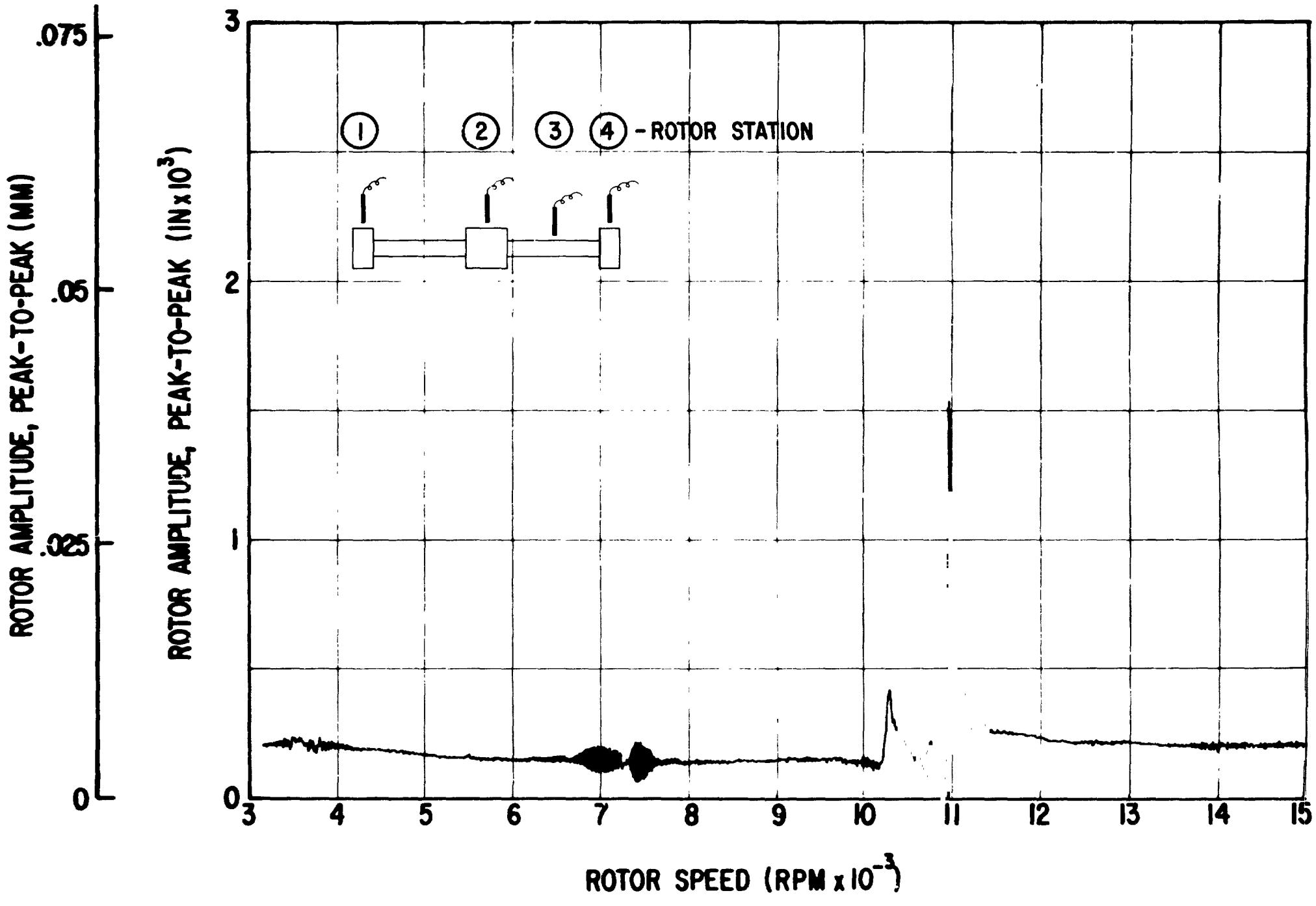

Fig. 19 Rotor Amplitudes at Station 2 at Conclusion of Test Case I

MTI-9548

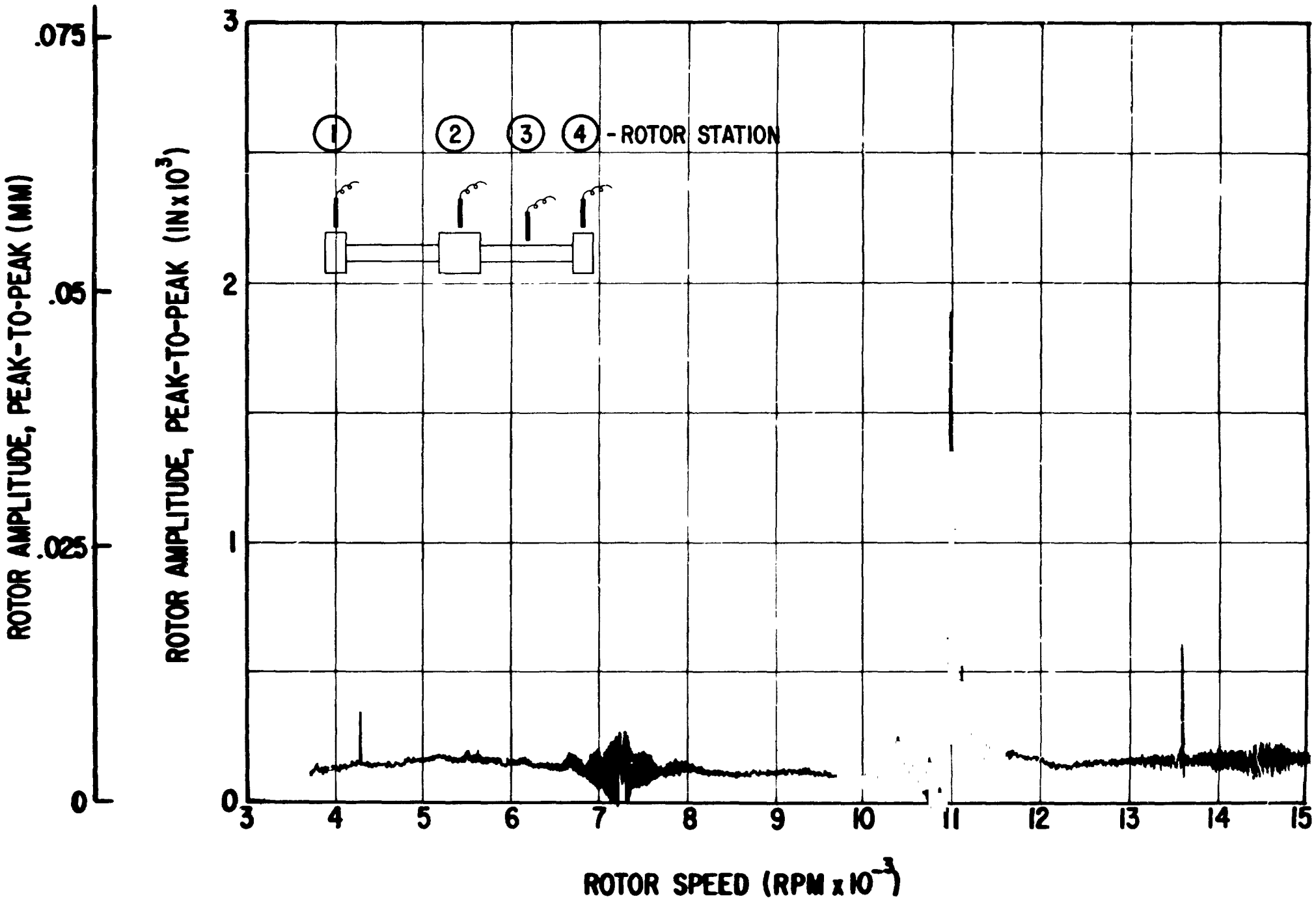

Fig. 20 Rotor Amplitudes at Station 4 at Conclusion of Test Case I

MTI-9547

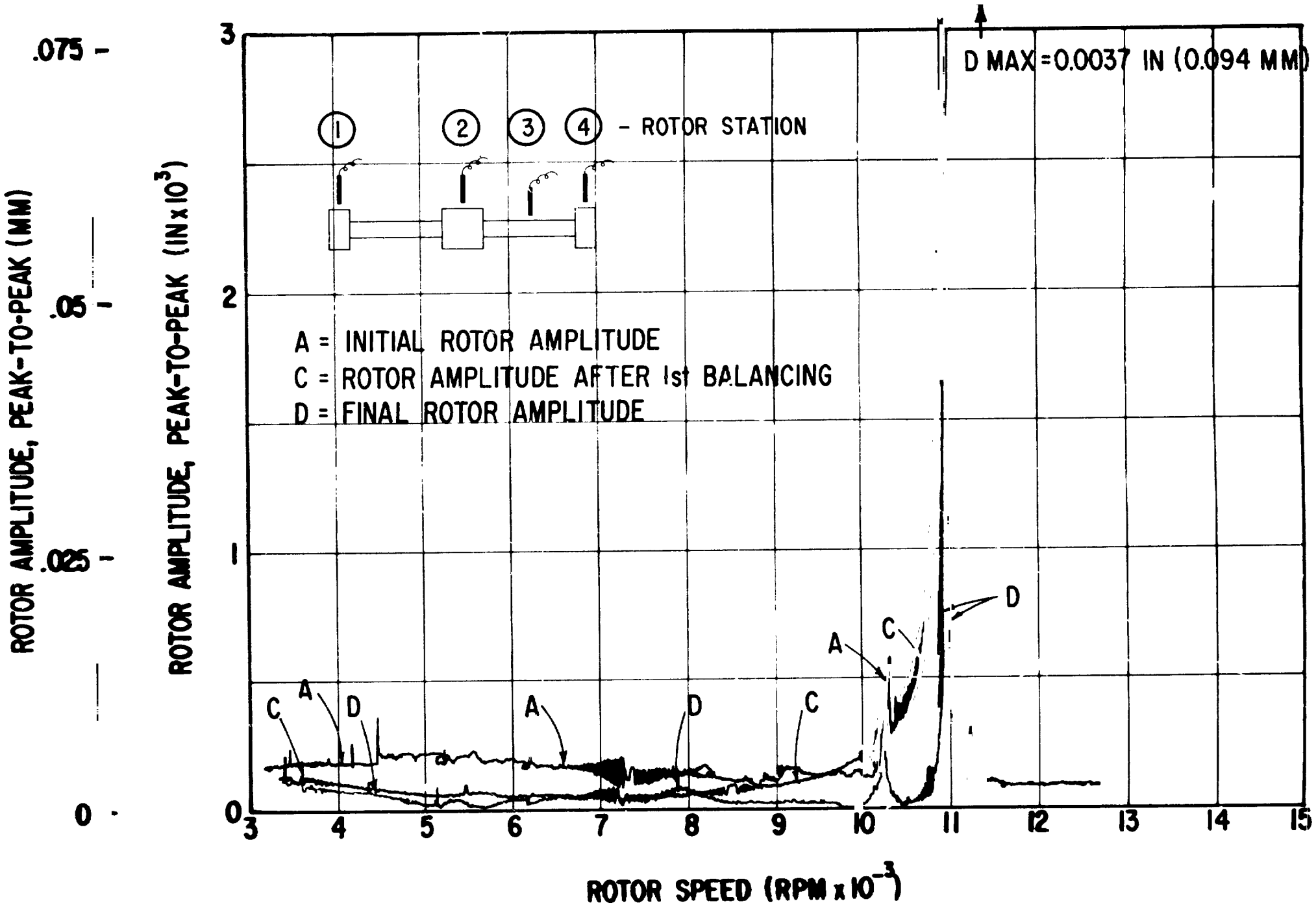

Fig. 21 Rotor Amplitudes at Station 1 - Initial Condition and After Two Consecutive Balancing Runs, Test Case I

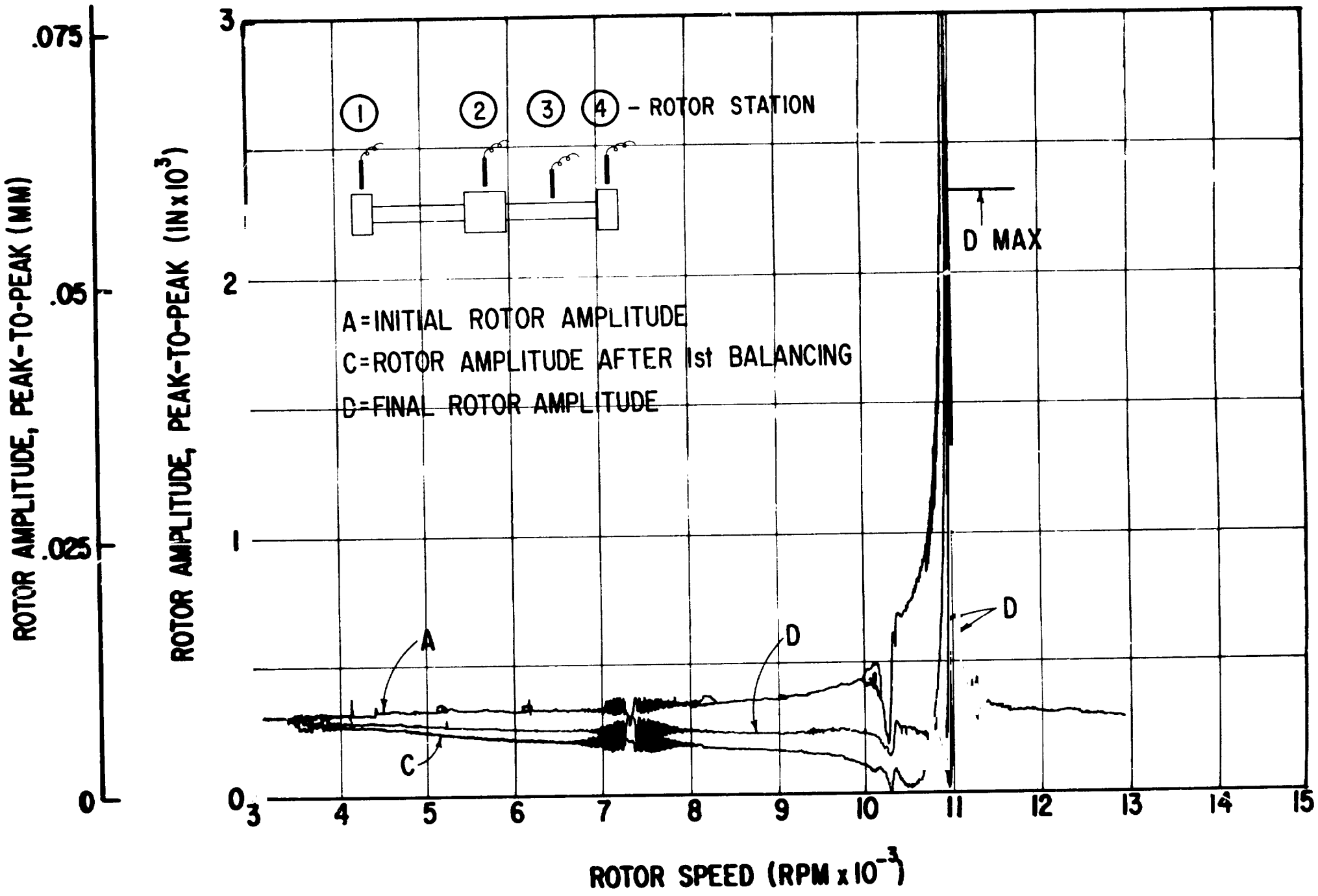

Fig. 22 Rotor Amplitude at Station 2 - Initial Condition and After Two Consecutive Balancing Runs, Test Case I

MTI-9545

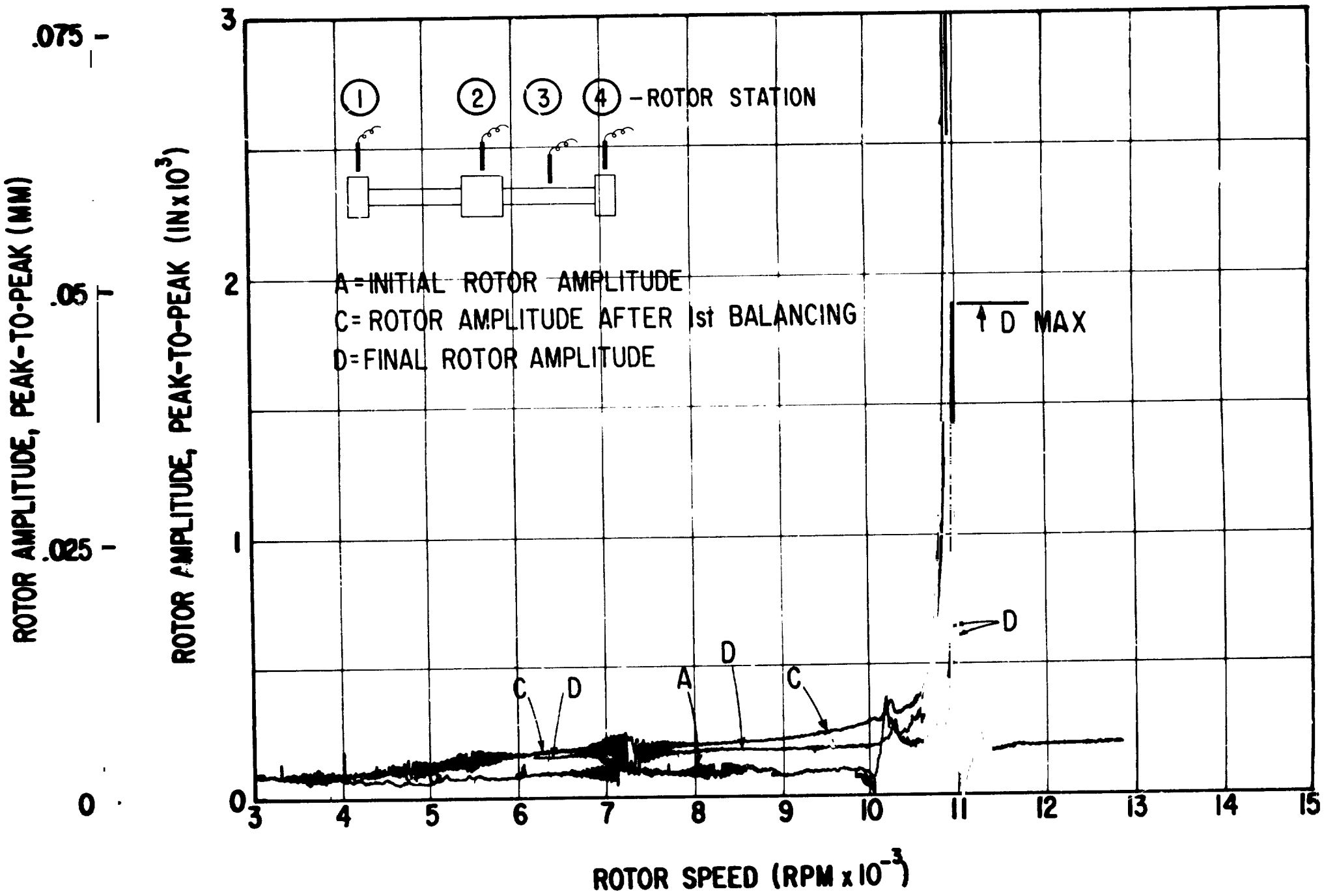

Fig. 23 Rotor Amplitudes at Station 3 - Initial Condition and After Two Consecutive Balancing Runs, Test Case I

MTI-9544

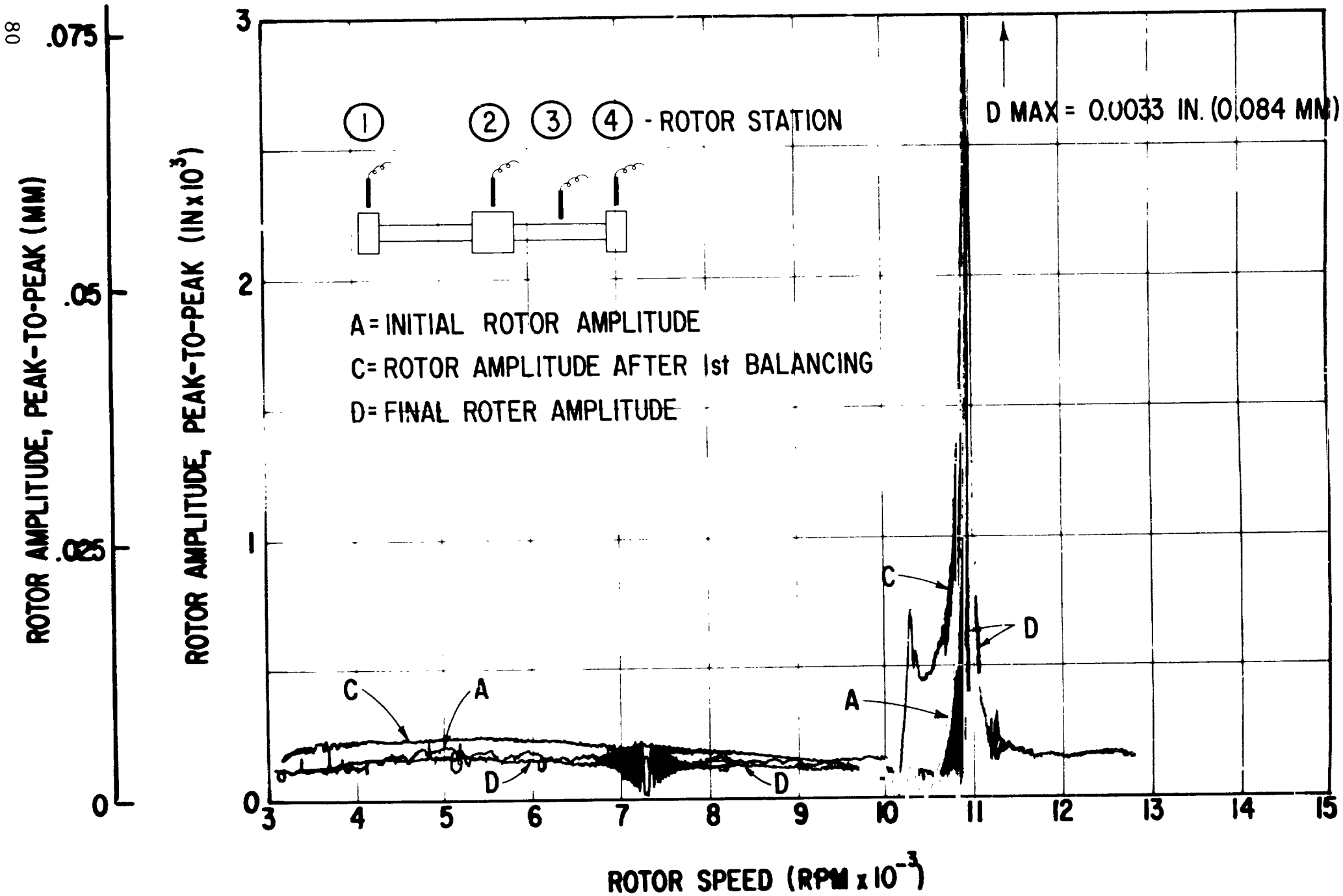

Fig. 24 Rotor Amplitudes at Station 4 - Initial Condition and After Two Consecutive Balancing Runs, Test Case I

MTI-9543

FOLDOUT FRAME

ROTOR IN ORIGINAL CONDITION - A (FIGS. 21-24 AND 26-29)

TRIAL WEIGHT RUN # I-1
TRIAL WEIGHT = 0.073 OZ-IN (5.256 GR-CM)
TRIAL WEIGHT LOCATION: 0°
ROTOR BALANCING SPEEDS: 6060 AND 10,450 RPM

CALCULATION # 1

2 PROBES

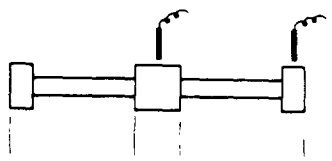

4 PLANES

2 SPEEDS: 6060 AND 10,450 RPM
TRIAL WEIGHT AT 0°

IMPROVED ROTOR B (FIGS. 26-29)

CALCULATION # 2

4 PROBES

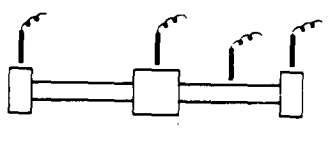

4 PLANES

1 SPEED: 10,450 RPM
TRIAL WEIGHT AT 0°

CALCULATED CORRECTION WEIGHTS TOO LARGE FOR TAPPED HOLES IN CENTER DISK. REVERT TO 3 PLANE BALANCING.

CALCULATION # 3

3 PROBES

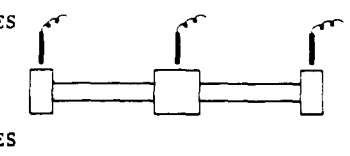

3 PLANES

1 SPEED: 10,450 RPM
TRIAL WEIGHT AT 0°

IMPROVED ROTOR C (FIGS. 21-24)

TRIAL WEIGHT RUN # I-2
TRIAL WEIGHT = 0.073 OZ-IN (5.256 GR-CM)
TRIAL WEIGHT LOCATION 0° AND 180°
ROTOR BALANCING SPEED: 10,700 RPM

CALCULATION # 10

4 PROBES

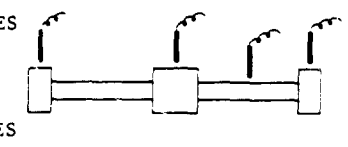

4 PLANES

1 SPEED: 10,700 RPM
TRIAL WEIGHT AT 0° AND 180°

FINAL ROTOR CONDITION

IMPROVED ROTOR D (FIGS. 21-24)
FIRST RUN THROUGH THIRD CRITICAL SPEED

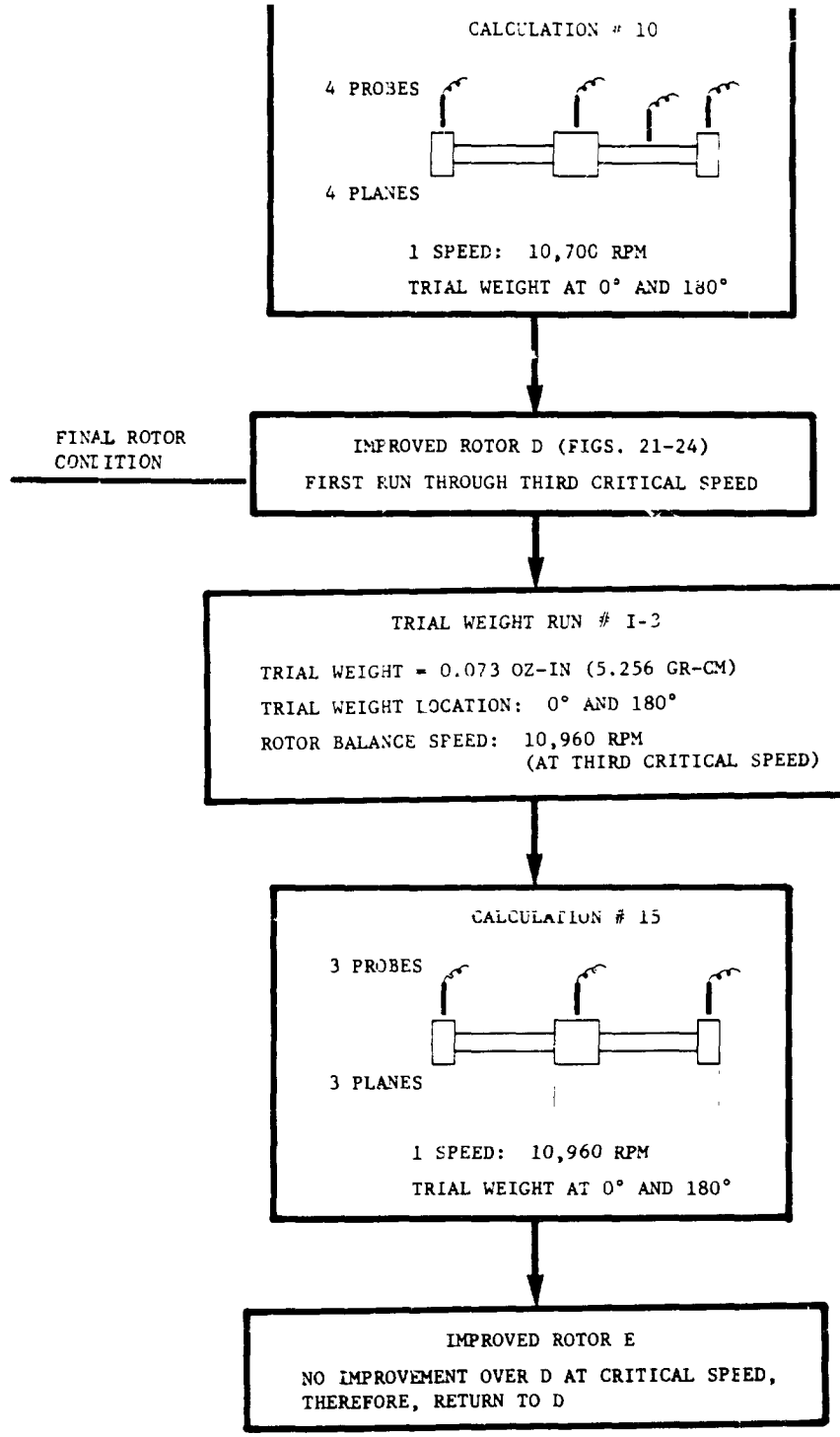

Fig. 25 Test Case I; Residual Rotor Unbalance

FOLDOUT FRAME 2

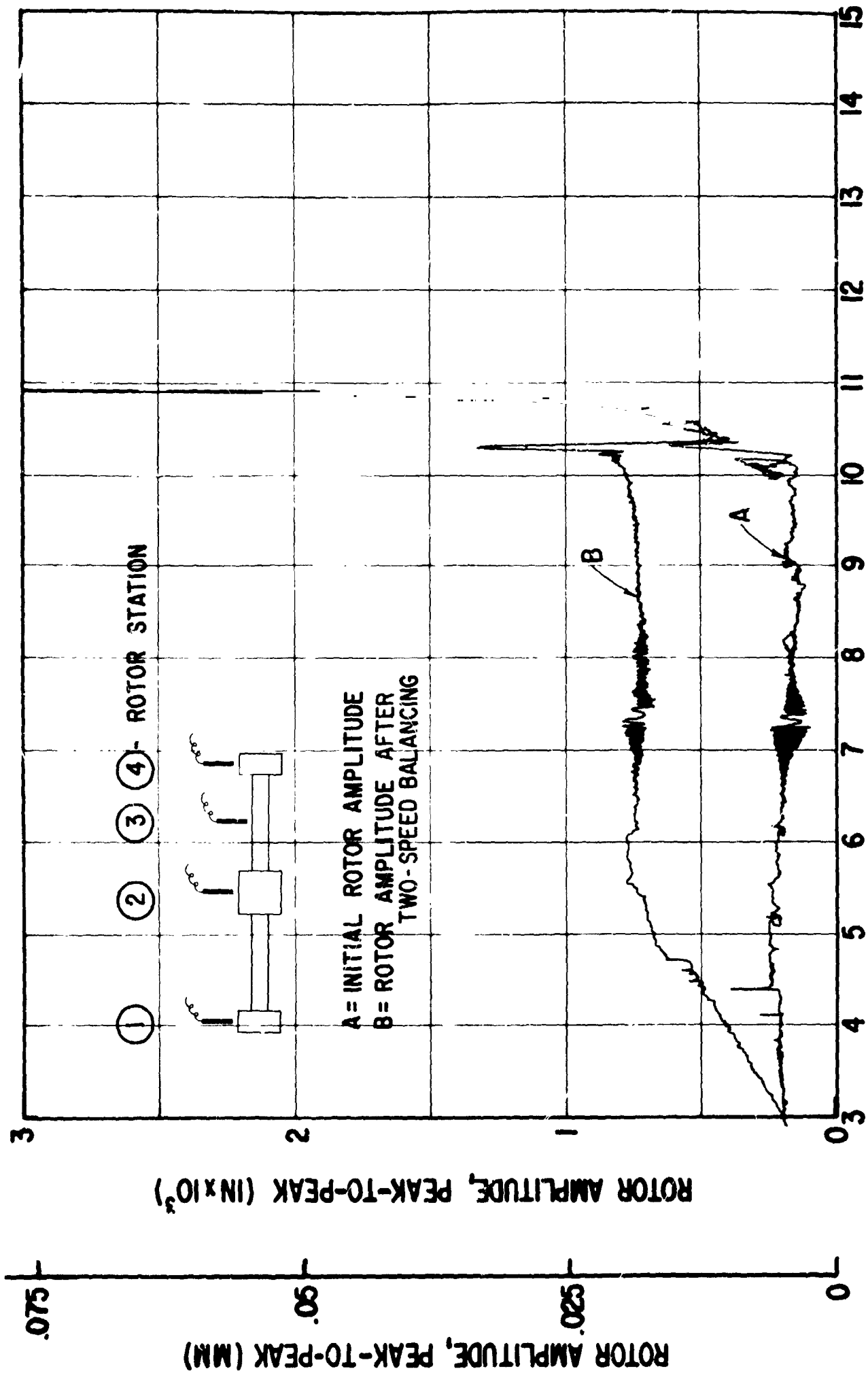

Fig. 26 Rotor Amplitudes at Station 1 - Initial Condition and After Two-Speed Balancing Run, Test Case I

MTI-9542

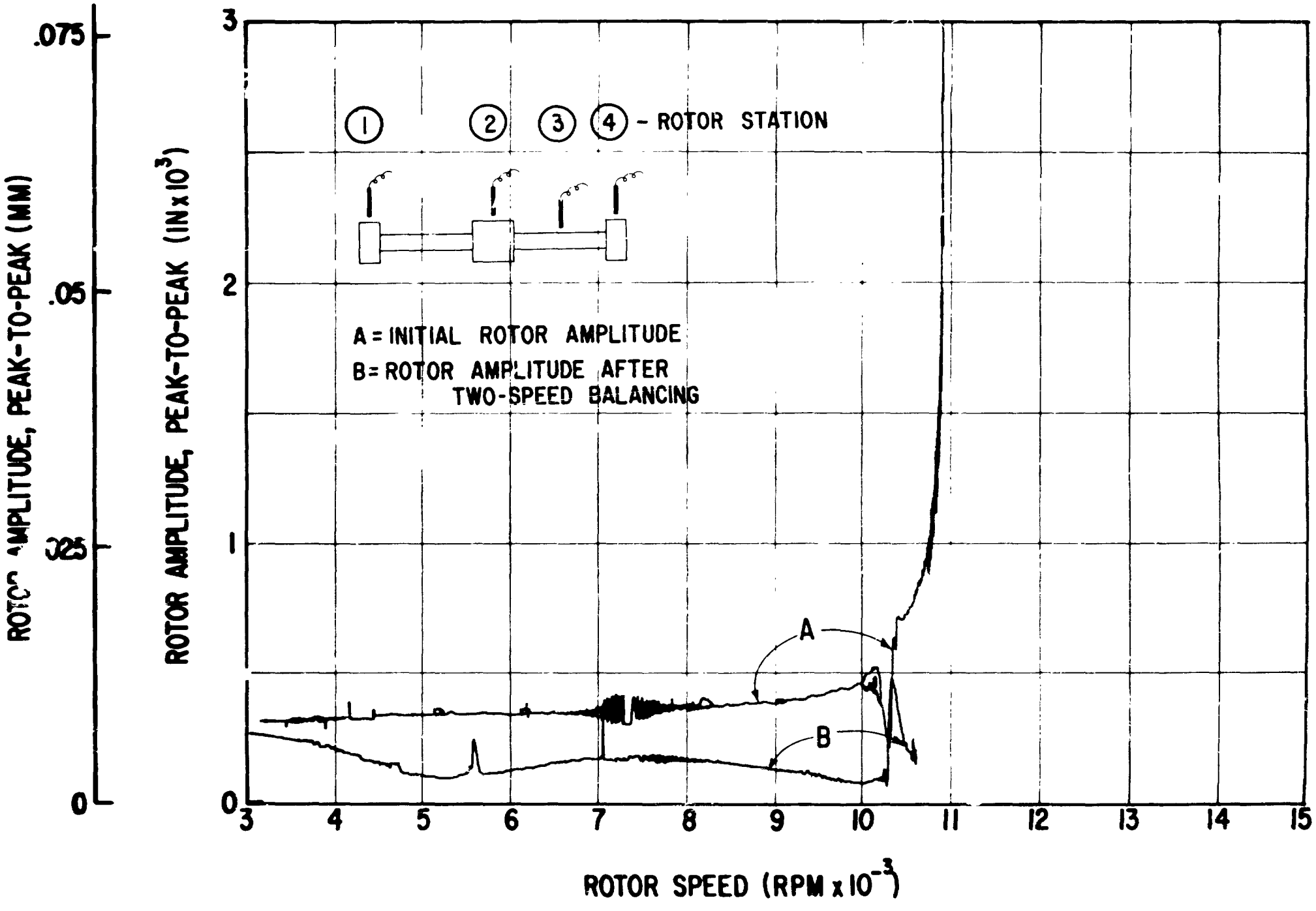

Fig. 27 Rotor Amplitudes at Station 2 - Initial Condition and After Two-Speed Balancing Run, Test Case I

MTI-9541

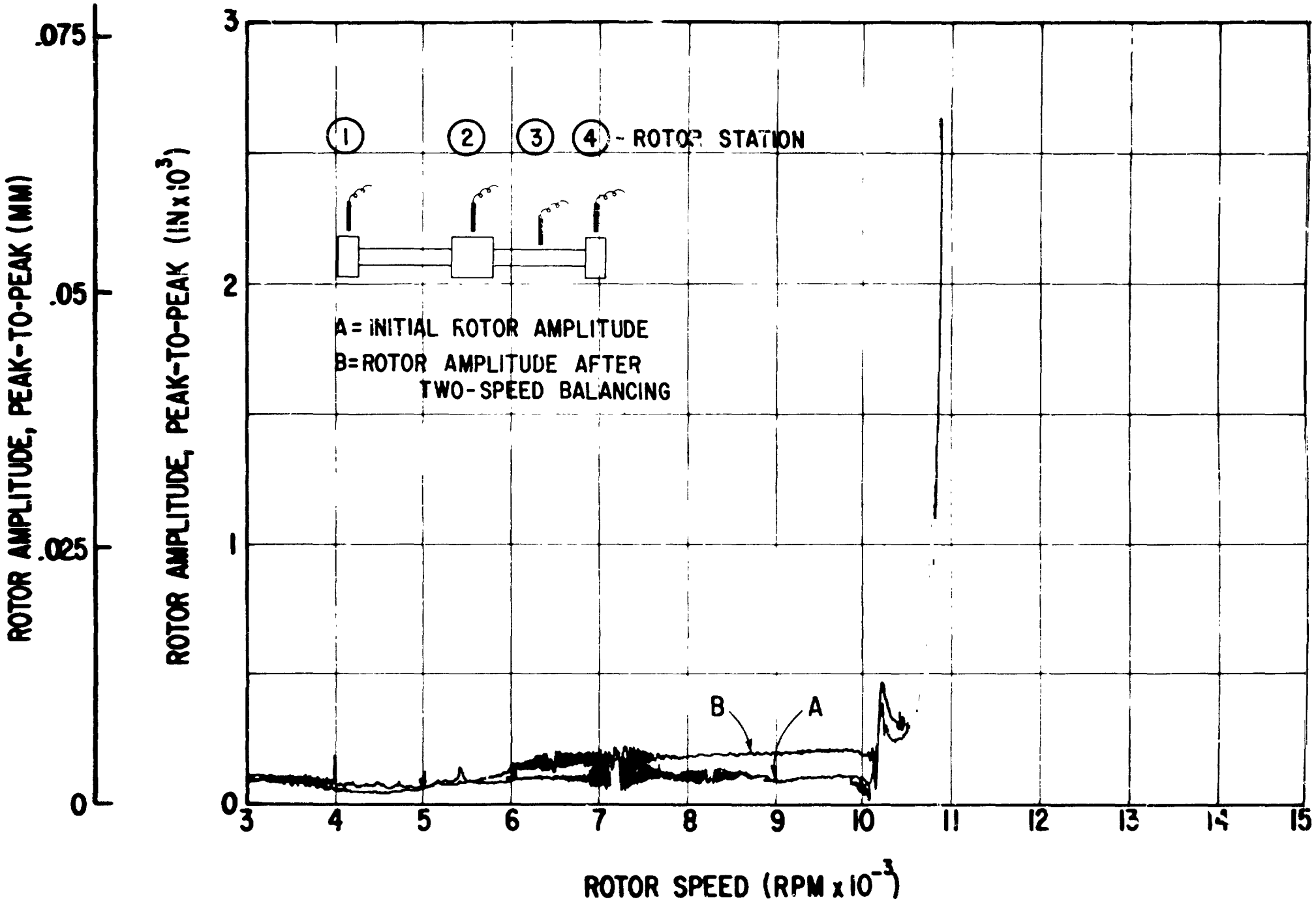

Fig. 28 Rotor Amplitudes at Station 3 - Initial Condition and After Two-Speed Balancing Run, Test Case I

MTI-5340

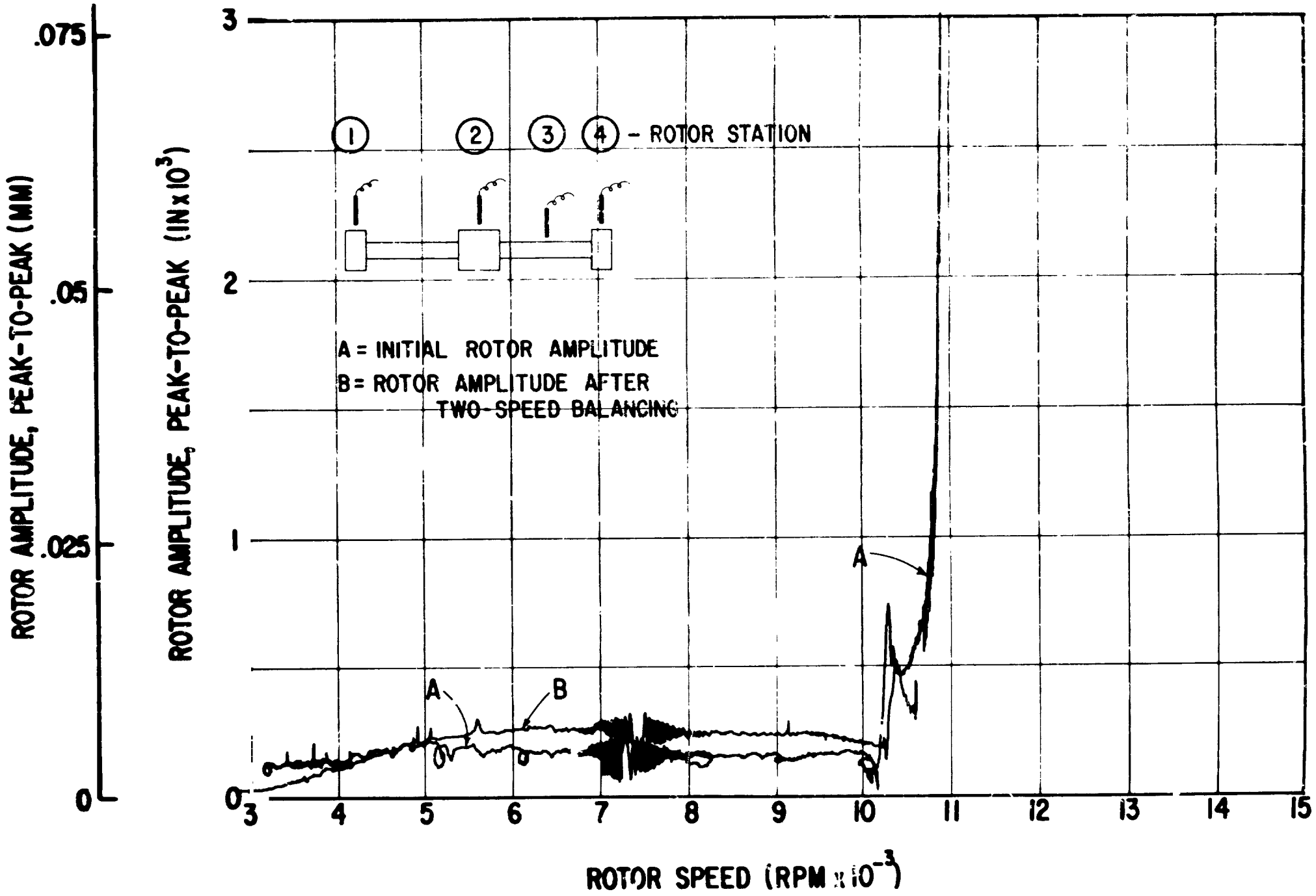

Fig. 29 Rotor Amplitudes at Station 4 - Initial Condition and After Two-Speed Balancing Run, Test Case I

MTI-9553

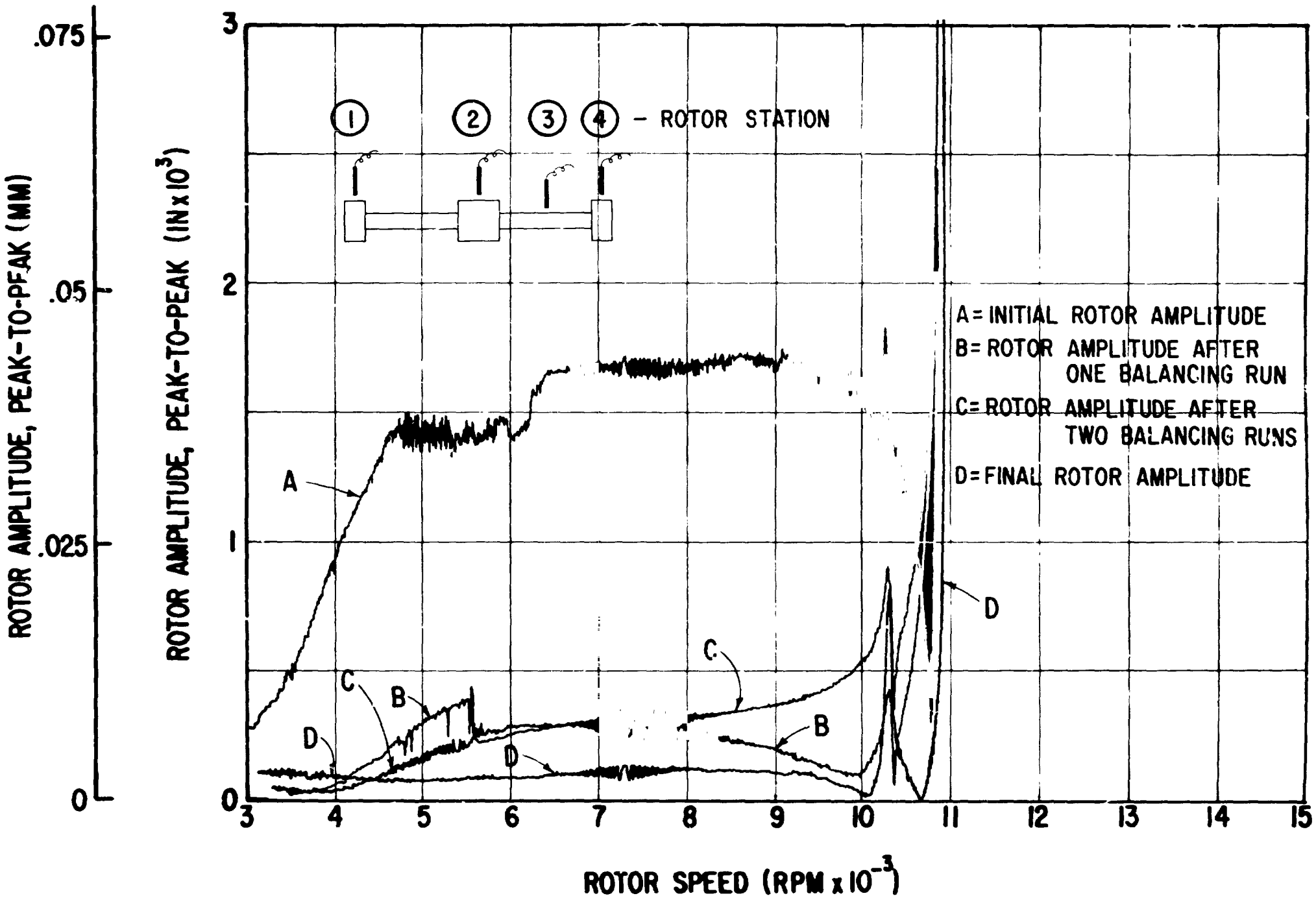

Fig. 30 Rotor Amplitudes at Station 1 - Initial Condition and After Three Consecutive Balancing Runs, Test Case II

MTI-9503

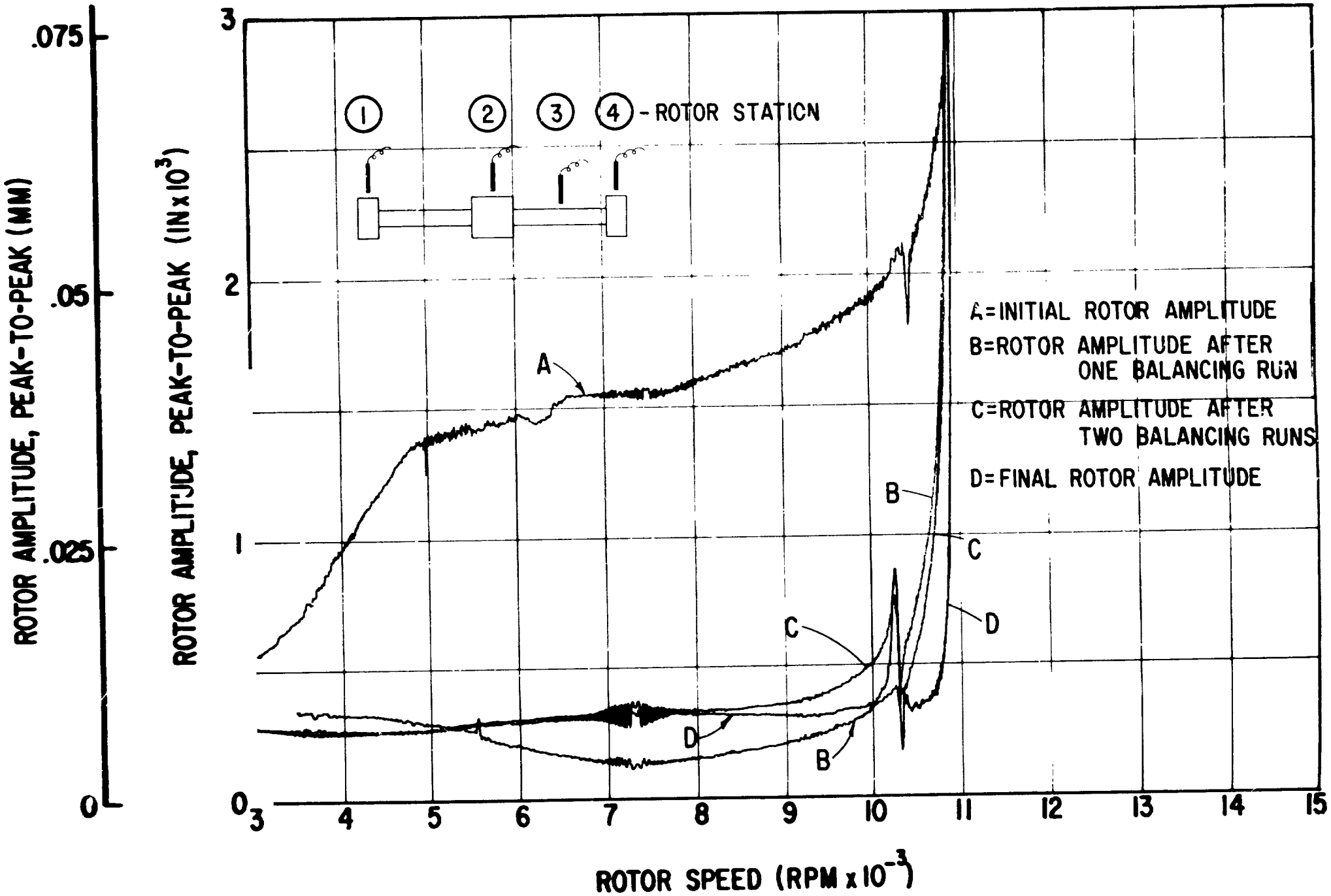

Fig. 31 Rotor Amplitudes at Station 2 - Initial Condition and After Three Consecutive Balancing Runs, Test Case II

MTI-9510

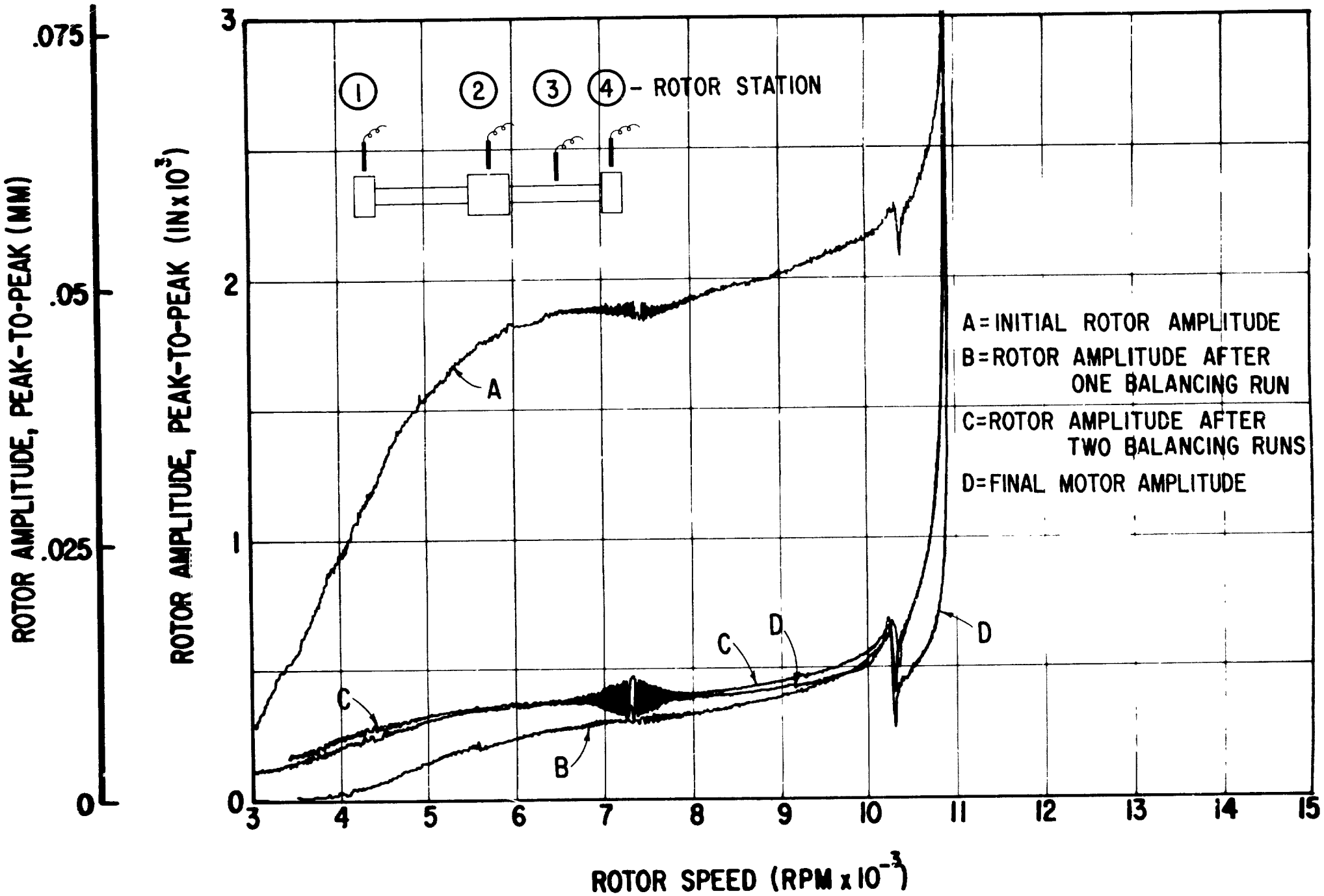

Fig. 32 Rotor Amplitudes at Station 3 - Initial Condition and After Three Consecutive Balancing Runs, Test Case II

MTI-9505

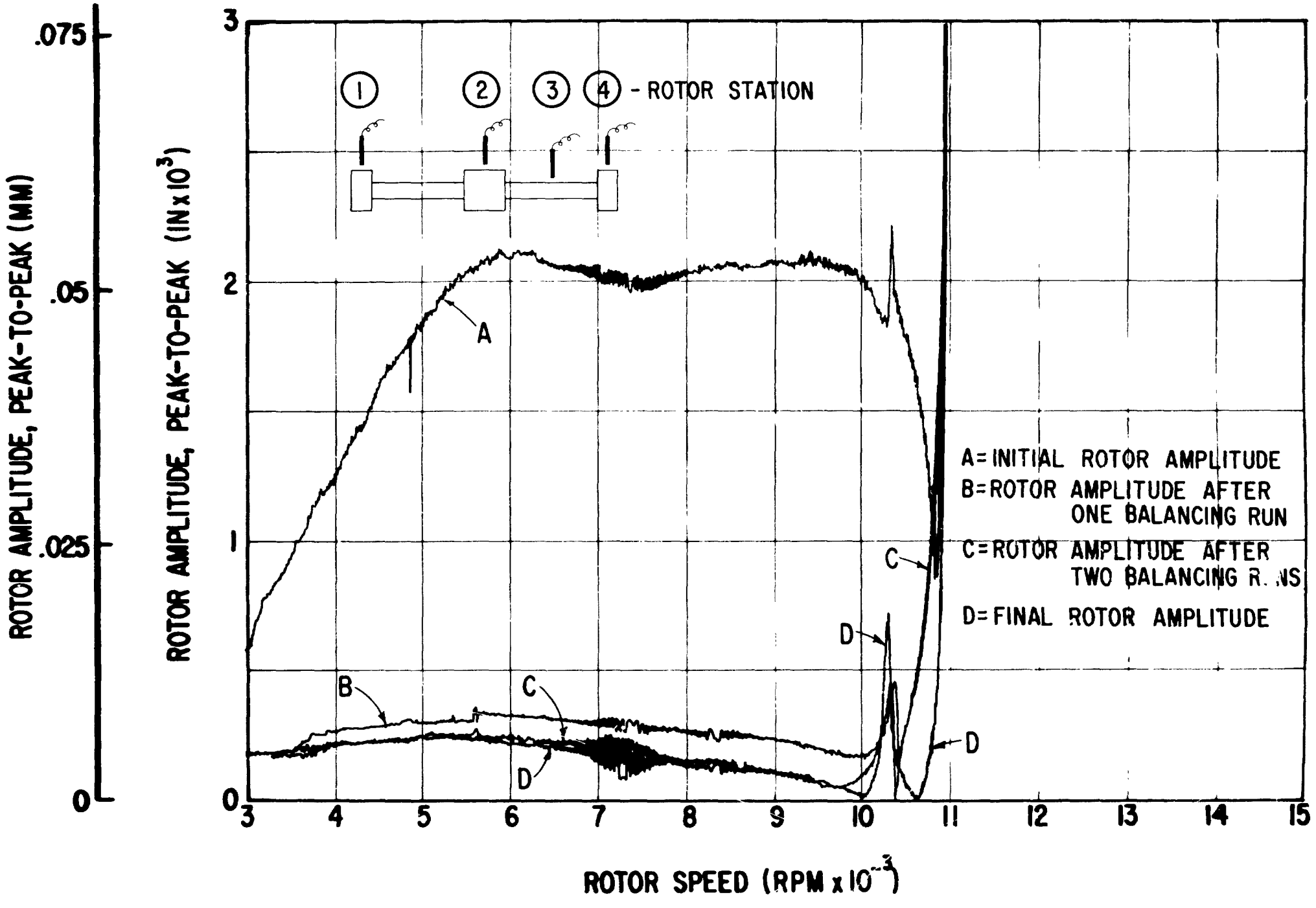

Fig. 33 Rotor Amplitudes at Station 4 - Initial Condition and After Three Consecutive Balancing Runs, Test Case II

MTI-9506

FOLDOUT FRAME 1

ROTOR WITH IN-LINE UNBALANCE OF 1.368 OZ-IN - A (FIGS. 30-33)

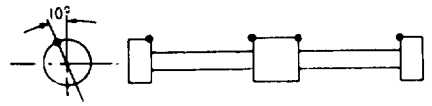

0.342 OZ-IN (24.6 GR-CM) (EACH)

TRIAL WEIGHT RUN # II-1

TRIAL WEIGHT = 0.073 OZ-IN (5.256 GR-CM)
TRIAL WEIGHT LOCATION = 0° AND 180°
ROTOR BALANCING SPEED: 8740 RPM

CALCULATION # 16

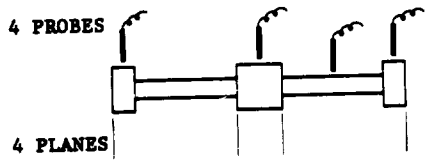

1 SPEED: 8740 RPM
TRIAL WEIGHT AT 0° AND 180°

COMPUTED CORRECTION WEIGHTS TOO LARGE FOR TAPPED HOLES IN CENTER DISK. REVERT TO 3 PLANE BALANCING.

CALCULATION # 18

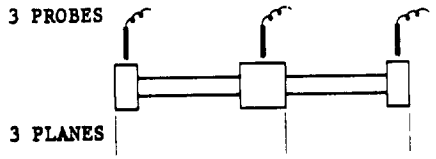

1 SPEED: 8740 RPM
TRIAL WEIGHT AT 0° AND 180°

IMPROVED ROTOR B (FIGS. 30-33)

TRIAL WEIGHT RUN # II-2

TRIAL WEIGHT = 0.073 OZ-IN (5.256 GR-CM)
TRIAL WEIGHT LOCATION = 0° AND 180°
ROTOR BALANCING SPEED: 10,780 RPM

CALCULATION # 20

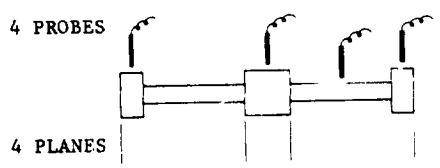

1 SPEED: 10,750 RPM
TRIAL WEIGHT AT 0° AND 180°

IMPROVED ROTOR C (FIGS. 30-33)

FO

FOLDOUT FRAME 2

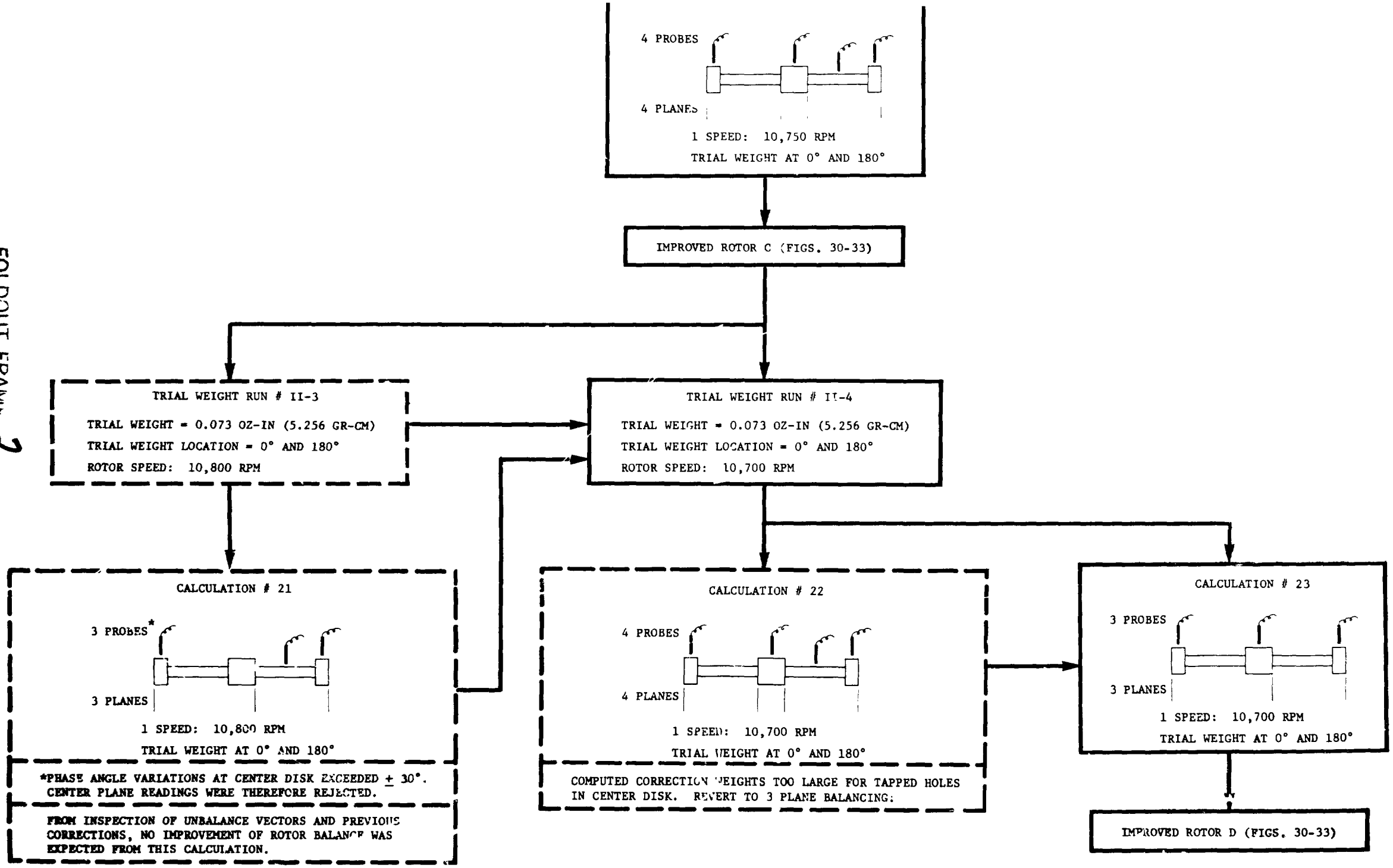

Fig. 34 Test Case II; In-Line, In-Phase Rotor Unbalance

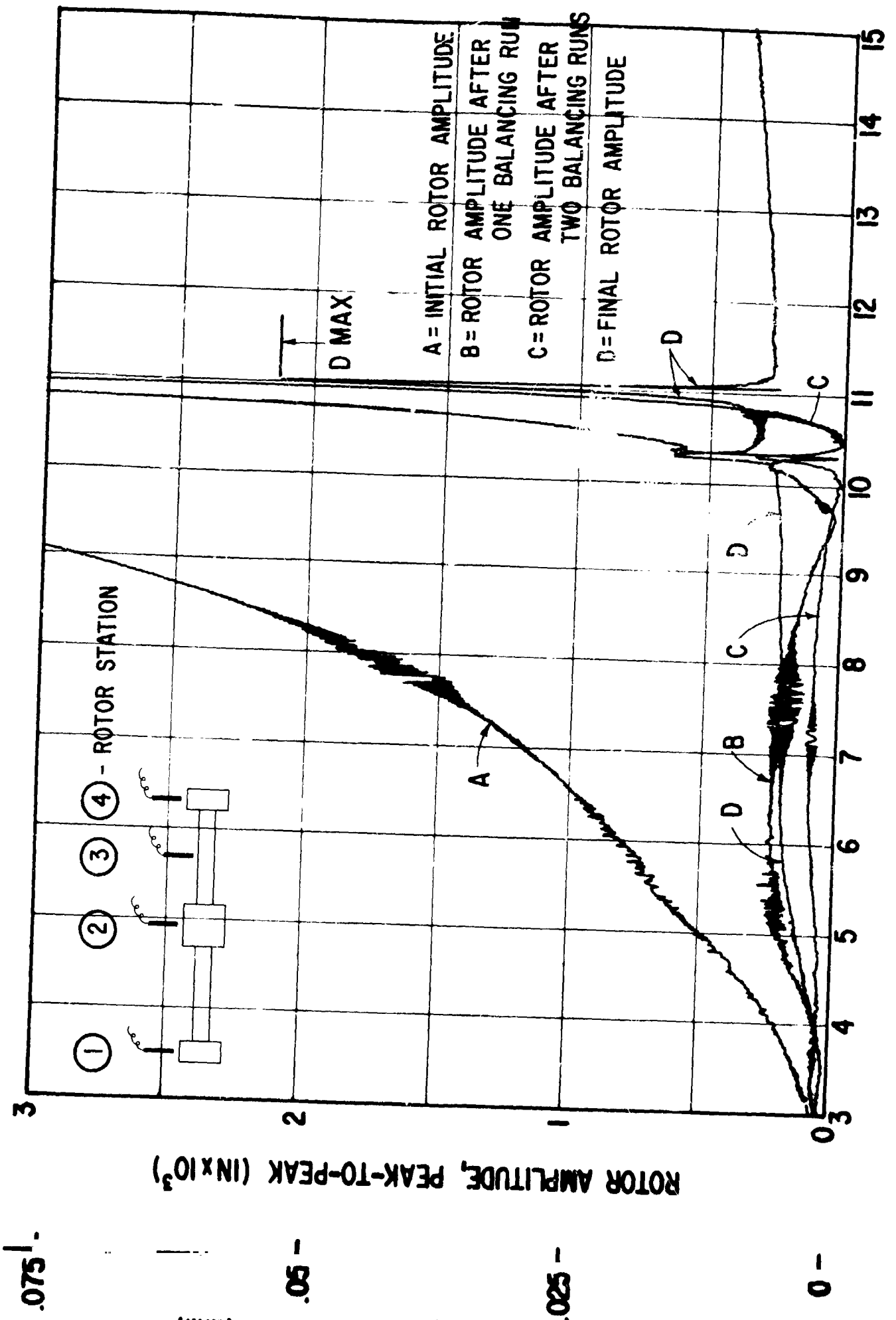

Fig. 35 Rotor Amplitudes at Station 1 - Initial Condition and After Three Consecutive Balancing Runs, Test Case III

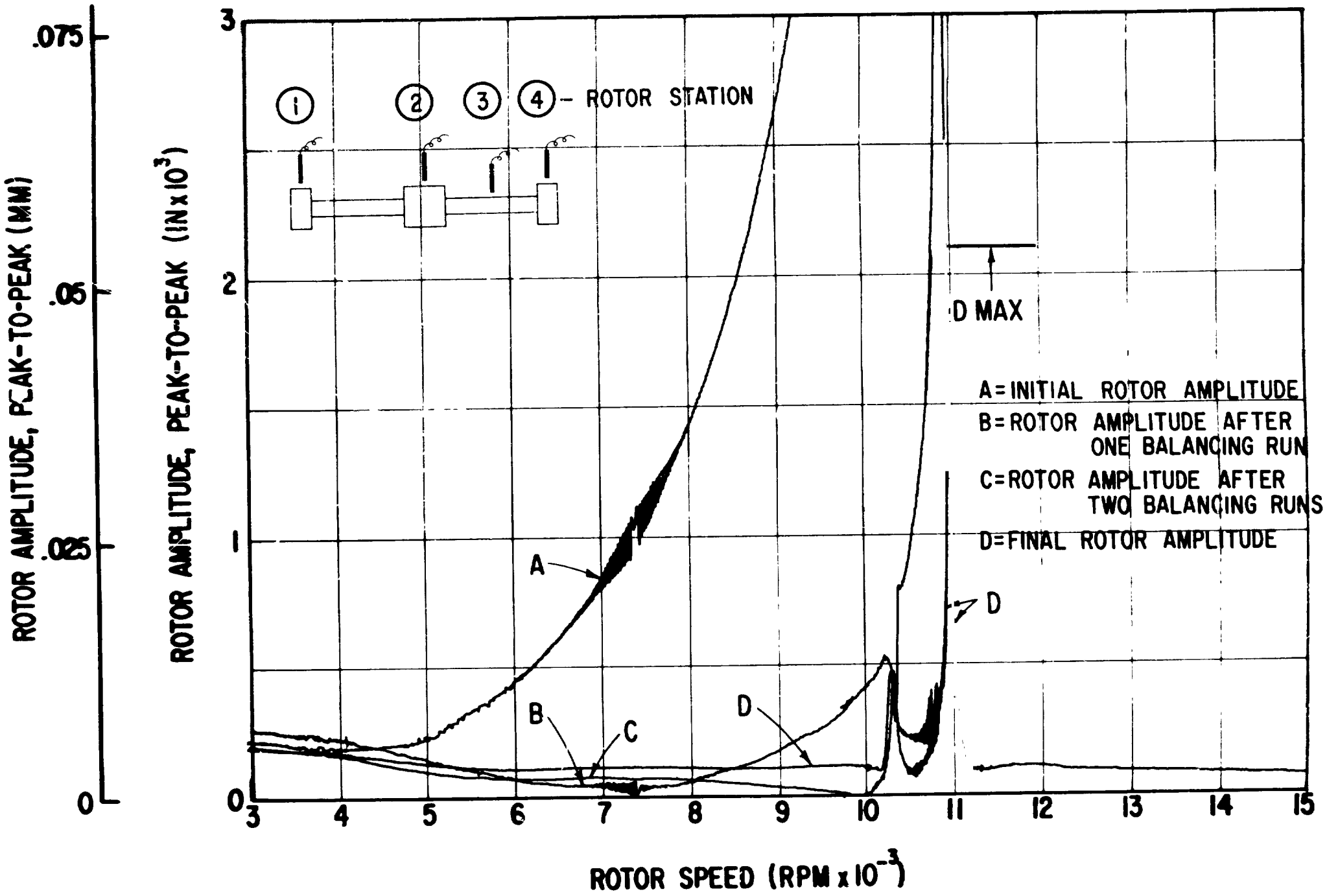

Fig. 36 Rotor Amplitudes at Station 2 - Initial Condition and After Three Consecutive Balancing Runs, Test Case III

MTI-9507

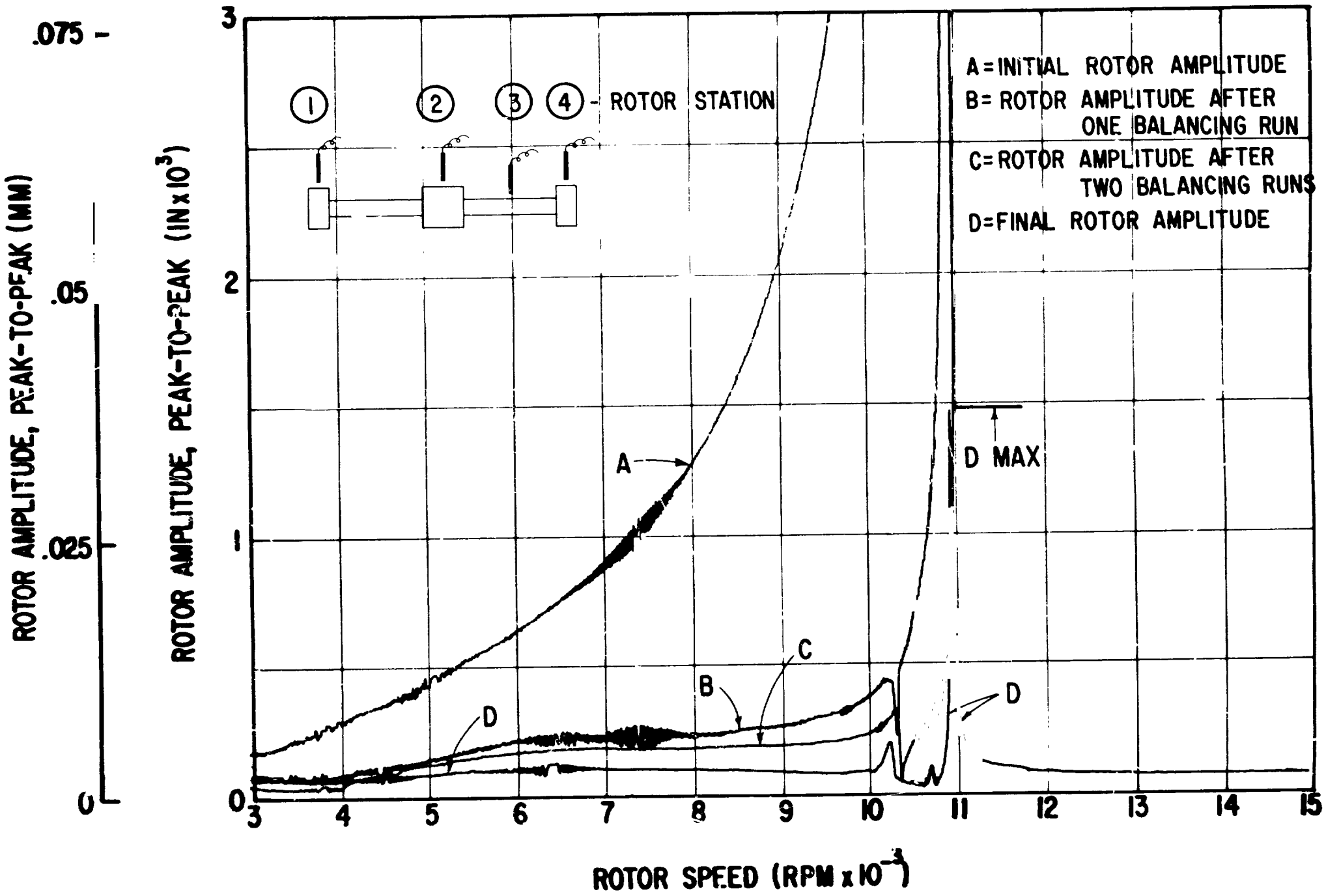

Fig. 37 Rotor Amplitudes at Station 3 - Initial Condition and After Three Consecutive Balancing Runs, Test Case III

MTI-9508

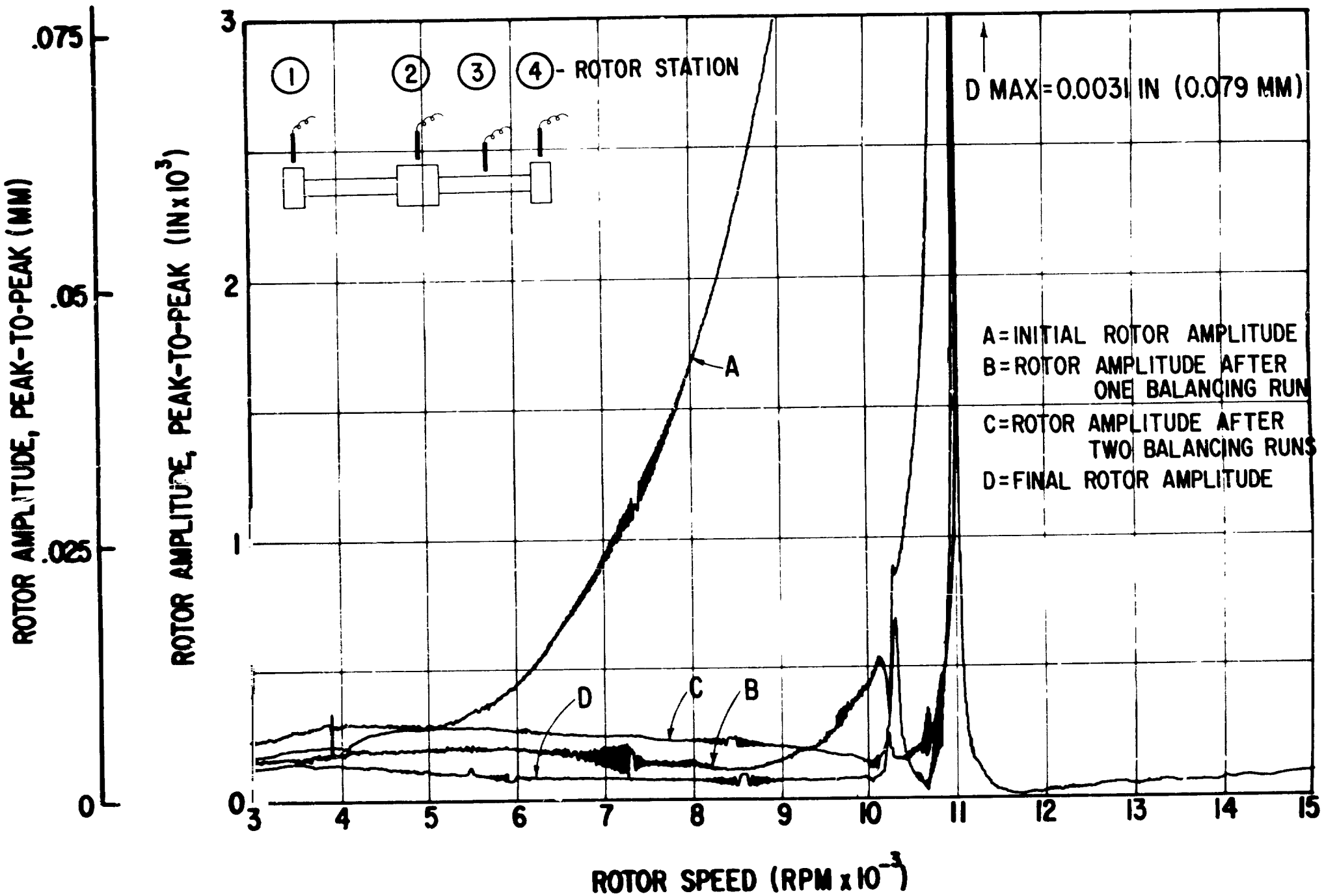

Fig. 38 Rotor Amplitudes at Station 4 - Initial Condition and After Three Consecutive Balancing Runs, Test Case III

MTI-9509

FOLDOUT FRAME

ROTOR WITH IN-LINE, OUT-OF-PHASE UNBALANCE - A (FIGS. 35-38)

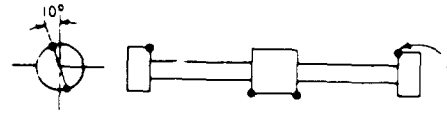

0.342 OZ-IN (24.624 GR-CM) (EACH)

TRIAL WEIGHT RUN # III-1

TRIAL WEIGHT = 0.1709 OZ-IN (12.304 GR-CM)

TRIAL WEIGHT LOCATION AT 0° AND 180°

ROTOR BALANCING SPEED: 8200 RPM

CALCULATION # 24

4 PROBES

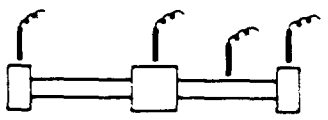

4 PLANES

1 SPEED: 8200 RPM

TRIAL WEIGHT AT 0° AND 180°

COMPUTED CORRECTION WEIGHTS TOO LARGE FOR TAPPED HOLES IN CENTER DISK.

CALCULATION # 25

3 PROBES

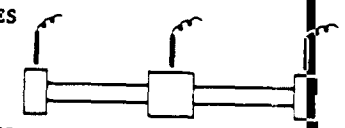

3 PLANES

SPEED: 8200 RPM

WEIGHT AT 0° AND 180°

IMPROVED ROTOR B (FIGS. 35-38)

TRIAL WEIGHT RUN # III-2

TRIAL WEIGHT = 0.1709 OZ-IN (12.304 GR-CM)

TRIAL WEIGHT LOCATION AT 0° AND 180°

ROTOR BALANCING SPEED: 10,500 RPM

CALCULATION # 26

4 PROBES

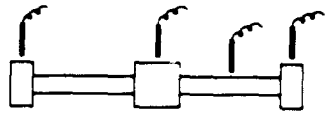

4 PLANES

1 SPEED: 10,500 RPM

TRIAL WEIGHT AT 0° AND 180°

CALCULATION # 27

3 PROBES

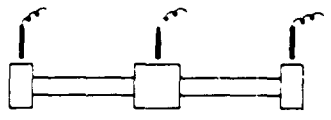

3 PLANES

1 SPEED: 10,500 RPM

TRIAL WEIGHT AT 0° AND 180°

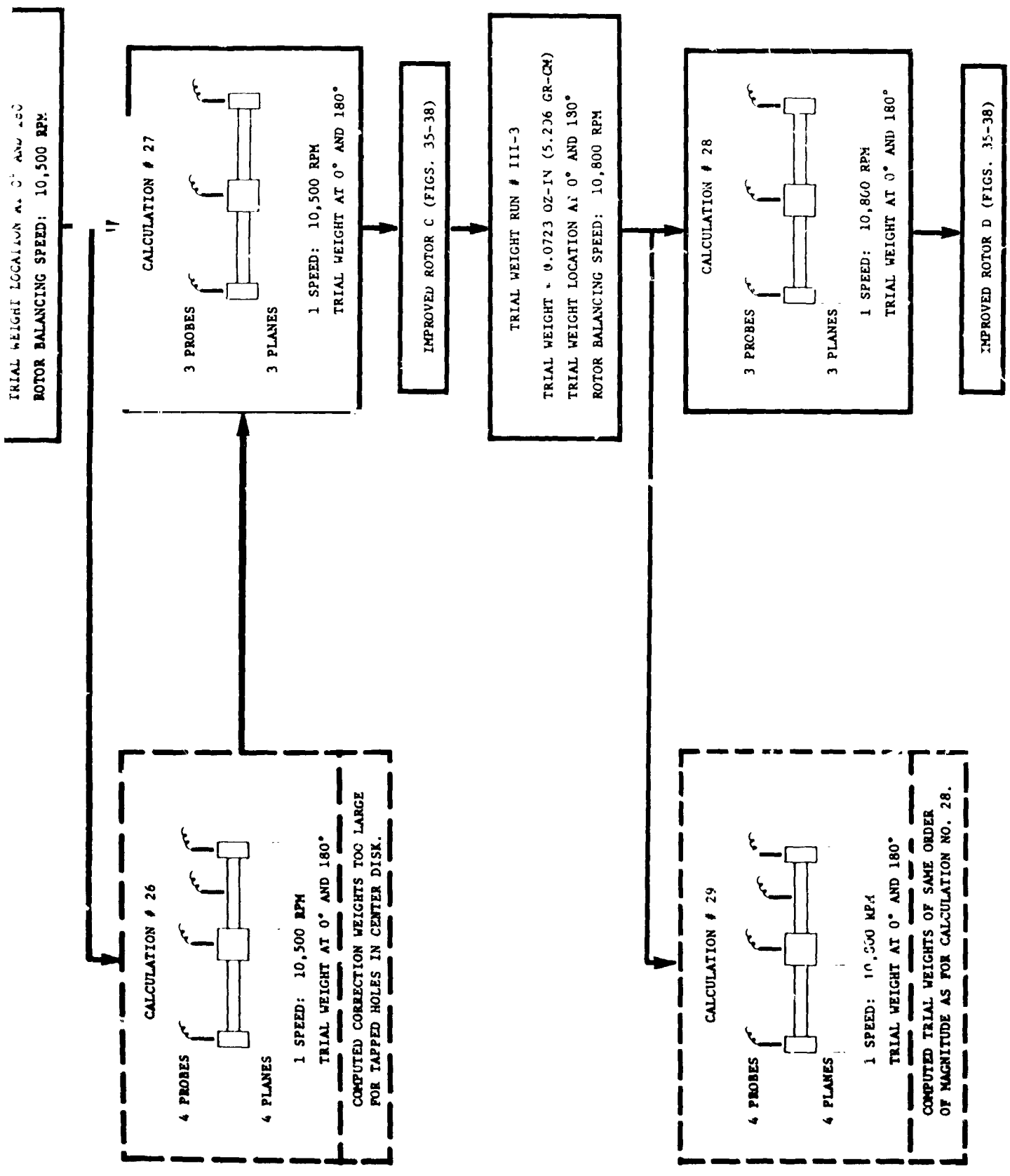

Fig. 39 Test Case III; In-Line, Out-of-Phase Unbalance

FOLDOUT FRAME 2